MCIC Report/June 1974

Properties of Textured Titanium Alloys

Dr. Frank Larson, Chief
Mr. Anthone Zarkades, Metallurgist

Materials Development Laboratory
Army Materials & Mechanics Research Center
Watertown, Massachusetts

MCIC-74-20

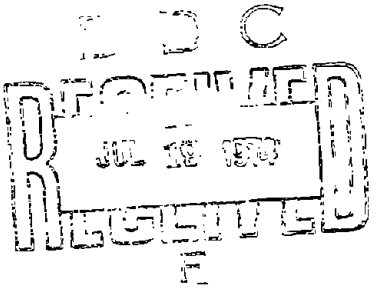

METALS AND CERAMICS INFORMATION CENTER
A Department of Defense Information Analysis Center

ACKNOWLEDGEMENT

This document was prepared by the Metals and Ceramics Information Center (MCIC), Battelle's Columbus Laboratories, 505 King Avenue, Columbus, Ohio 43201. MCIC's objective is to provide a comprehensive current resource of technical information on the development and utilization of advanced metal- or ceramic-base materials.

The Center is operated by Battelle-Columbus under Contract Number DSA900-74-C-0616 for the U.S. Defense Supply Agency; technical aspects of MCIC operations are monitored by the Army Materials and Mechanics Research Center. The support of these sponsor organizations is gratefully acknowledged.

TABLE OF CONTENTS

TABLE OF CONTENTS (Cont.)

PROPERTIES OF TEXTURED TITANIUM ALLOYS

SUMMARY

This report reveals that many important engineering properties of titanium and its alloys are anisotropic and that this anisotropy can be used to achieve improvements in structures and other applications. From this review of textures found in commercial titanium products and the way in which they develop, it can be seen that a wide variety of different types are possible and many others will undoubtedly be developed as the knowledge increases or a specific need arises. The current principal types of textures are simple or compound. A simple texture is one basic type, and a compound texture is a combination of two or more basic types. The eight main basic types are illustrated schematically in Figure 1.

The variation of properties, for a predominately alpha structure, with texture and specimen orientation is summarized and illustrated schematically for certain specific cases in Figures 2 and 3. In the illustrations, α is the angle between the rolling direction and the specimen axis. A longitudinal specimen would coincide with 0 degrees and a transverse specimen with the 90-degree orientation. Evident in Figures 2 and 3 is the large variation on property control possible through a texture/specimen-orientation interrelationship. For example, Young's modulus can range from a minimum of 14.5×10^6 psi to a maximum of 21.0×10^6 psi. The schematics present some of the current significant variation in engineering properties that are affected by texture. It is clear that important improvements are possible through texture control. The application of anisotropic yield theory to the design of pressure vessels (the major effort in this field) has been carried through to the experimental stage, and successful improvement of structural efficiency has been demonstrated up to 1.6 times the uniaxial strength. An obvious extension of anisotropic yield theory is the design of hydraulic tubing. Of the many possibilities that exist, one extremely attractive area is that of improved fatigue properties. Although considerable additional work is needed, the early results are quite promising.

A popular belief is that texture intensity is a minor consideration in most commercial alloys. This is generally not true for wrought titanium mill products, even in fairly large sizes, and it takes very little work in the alpha-plus-beta field to generate intense textures, which cannot be eliminated. They may be minimized or made nearly orthotropic (i.e., longitudinal and transverse properties similar) by beta annealing or heat treatment, but the intense texture will remain although it is of a different type. The important point concerning anisotropic properties is that they cannot be ignored and must be reckoned with.

Even if one is content to accept the anisotropic properties and use isotropic design, the variation in properties in "real" materials must be considered, i.e., the material must be completely characterized. Vastly improved properties through exploitation of anisotropic properties will be difficult, for it will require tailor-made materials applied with anisotropic design principles.

Although many of the characteristics have been known to the research community for years, there is a general lack of appreciation of the magnitude of effects. Several empirical approaches have revealed the nature and extent of anisotropy in titanium alloys. Although there has been a fairly large effort in anisotropic yielding under biaxial loading directed toward pressure vessels, there has not been a widespread application. It appears that a wider appreciation of anisotropy due to texturing is needed among designers or materials-application people, and, greater amounts of information or data on this subject will strengthen and provide a greater awareness of the potential. It has been shown that there is great improvement in certain properties. And, if these improvements can be further documented, this will provide the necessary driving force for industrial application.

Many important problem areas remain to be investigated. Some of the significant ones are listed below.

- Characterization of texture
- Rapid, inexpensive method of texture determination
- Development of industrial methods to produce specific desired textures
- Optimization of properties
- Development of a data base for application to design
- Development of increased awareness by materials-applications personnel and designers of texture effects
- Conduct of research on effects of texture effects on properties other than those discussed in this report
- Development of prototype or model demonstration.

To briefly illustrate some of the above items, the characterization of textures has been receiving increasing attention, and progress in this field has reached the point where accurate and detailed information can be produced by using so-called axis distribution charts. These charts portray the texture in a quantitative manner and will be important in future accurate prediction of properties. For routine texture determination, either for quality control

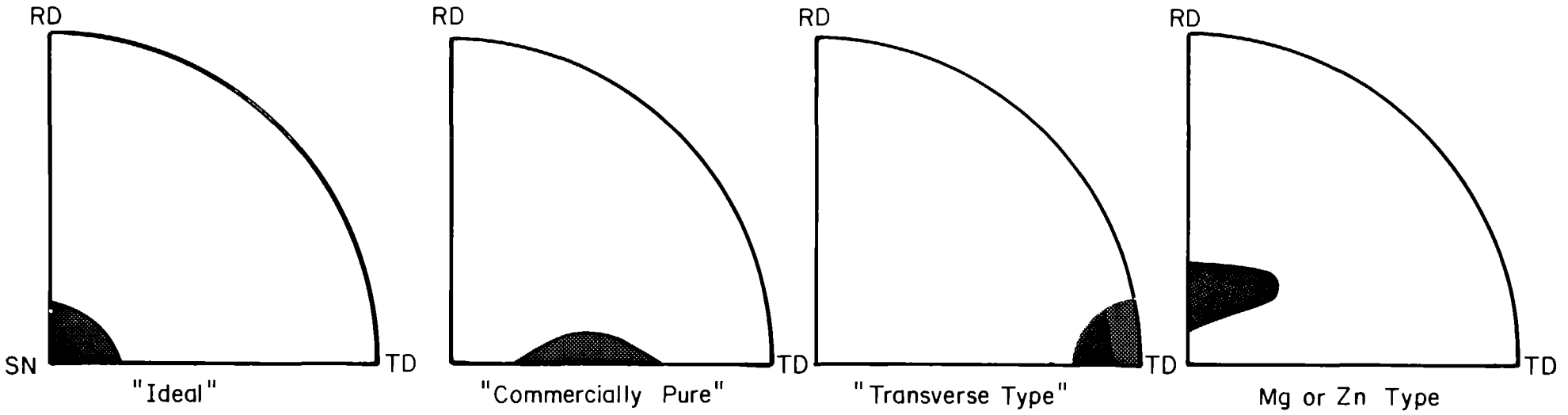

a. (0002) Alpha-Deformation-Type Textures

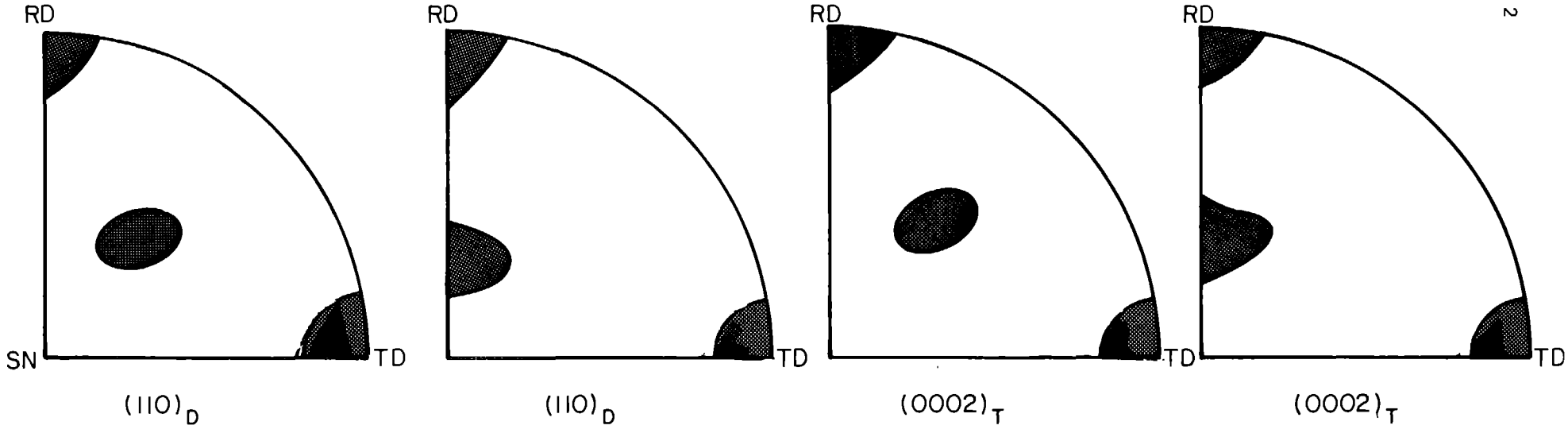

b. Beta-Deformation-Transformation-Type Textures

FIGURE 1. SCHEMATIC OF THE EIGHT BASIC TEXTURES IN TITANIUM MATERIALS

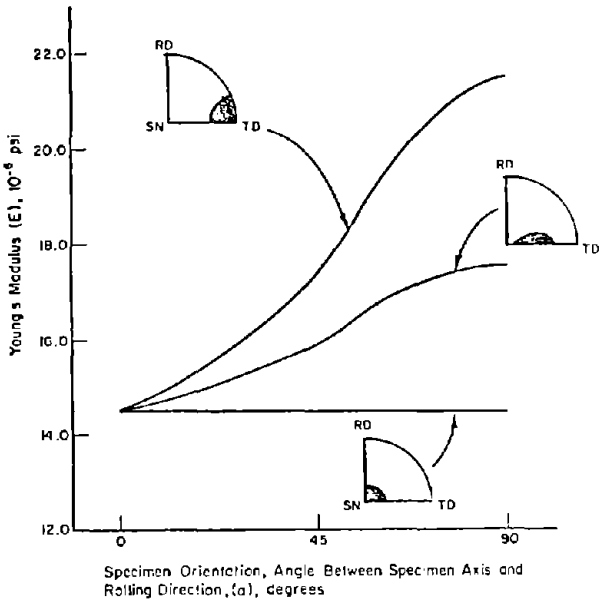

a. Young's Modulus

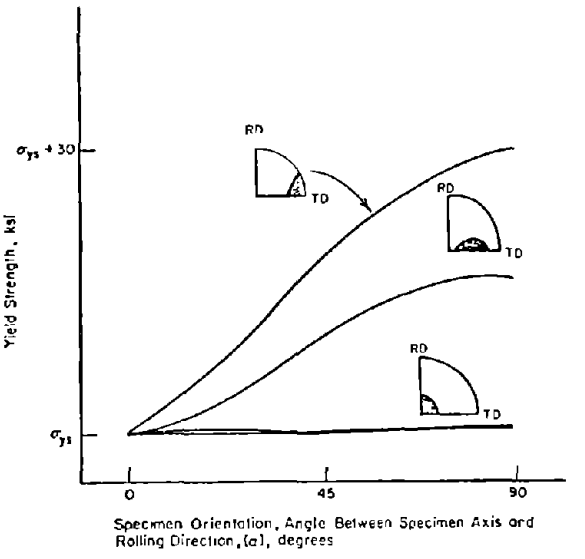

b. Yield Strength

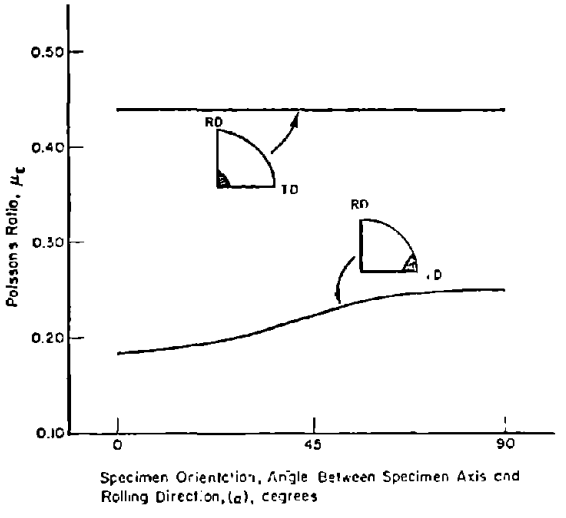

c. Poisson's Ratio

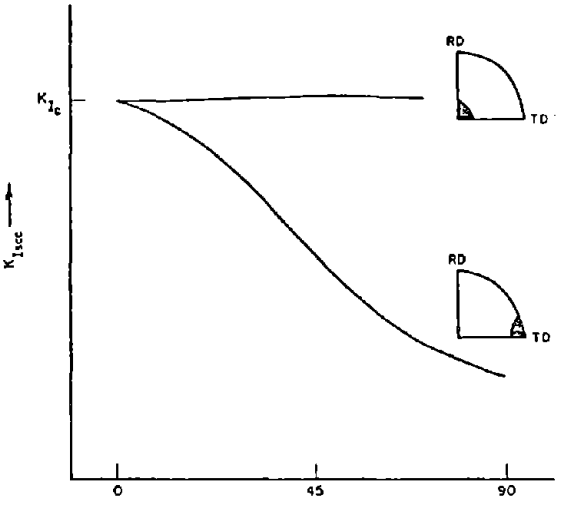

d. Stress Corrosion Cracking

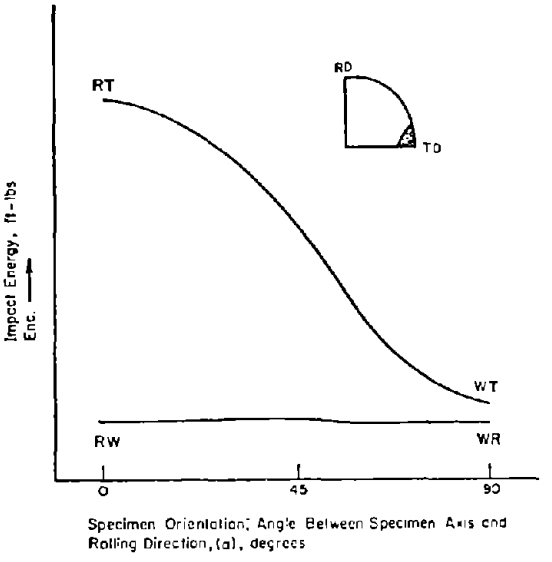

e. Charpy Impact

FIGURE 2. SCHEMATIC REPRESENTATION OF THE VARIATION IN PROPERTIES OF TITANIUM AND IT'S ALLOYS WITH SPECIMEN ORIENTATION AND (0002) TEXTURE

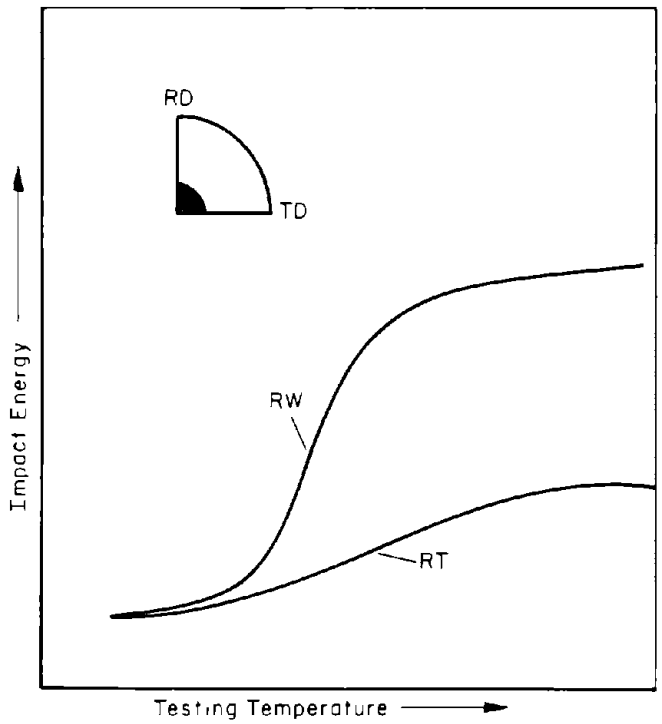

FIGURE 3. SCHEMATIC REPRESENTATION OF THE EFFECT OF (0002) TEXTURE AND SPECIMEN NOTCH ORIENTATION ON THE CHARPY-IMPACT TRANSITION TEMPERATURE

or screening testing purposes the current method of obtaining pole figures will probably offer the best procedure. The main difficulty in this area is that texture determination requires fairly lengthy experimental runs on X-ray equipment which most materials-application personnel and designers do not have. Before this area can move forward, standardized methods or procedures will have to be developed for specifications.

Although some laboratory progress has been made in texture development and control, there is, to date, no off-the-shelf inventory of different guaranteed textures available. Once the industrial availability of textures comes into being, and before industrial applications can be made, a data base must be developed in order to establish design allowables and specification minimums.

Exploitation of the large improvements cannot proceed until the designer or materials application people are aware of potential benefits that are possible. In some cases, this will cause extreme difficulty in design procedures because it will require use of anisotropic design procedures rather than the simplified isotropic methods which designers are most commonly using. In many cases, control of textures will produce a variety of "highs" and "lows" in other secondary properties and in other directions, and this complicates the design procedures. Consideration of the total picture will have to be made.

Considerably more research on the effect of texture upon properties is needed. Although the initial framework has been illustrated, quantitative values do not allow predictions to be made; and the theory in some areas such as fatigue, is considered vague or unknown.

Finally, success is the best cure for inactivity or lack of utilization of textures for improved performance. Thus it appears that selected prototype or successful model demonstration could stimulate the exploitation of texture for improved materials utilization.

INTRODUCTION

During the late 1950's and early 1960's considerable efforts had been directed towards classical alloy development of titanium through basic physical-metallurgy research. As the alloys became more advanced and complex, greater emphasis was placed upon microstructural correlations with properties. Although major improvements in strength, toughness, and other properties have been and will continue to be made, an important underlying variable, crystallographic texture, continues to be neglected. It is the purpose of this report to present the current information on the effects of texture upon properties and to show the untapped potential for improvements that texture control offers. The authors believe that texture control could provide a new generation of materials with greatly improved and more consistent properties, and thus add a third dimension to alloy development along with composition and microstructure. Proper selection of texture would increase structural efficiency because current design allowables reflect low material properties which are obtained in titanium when texturing is not controlled or taken into account.

These material improvements can be demonstrated to varying degrees in the laboratory. Although the research and development efforts have been small, significantly improved properties have been illustrated in several areas. The practical applications of textured titanium recently demonstrated will be difficult to implement because of the newness of the idea. Yet, there is a growing awareness of the gains possible and a rapidly growing interest. In fact, the conclusions reached in the titanium-technology phase of the SST materials[1-8] development program stated that texture is a primary metallurgical factor causing property variation and must be controlled.

Much of the past efforts in texture control have been directed towards randomizing crystal orientations. These efforts have been motivated by the so-called need to eliminate anisotropy because most designs are based upon isotropic theory and do not take into account the vastly improved properties that are possible from anisotropic materials. Since most engineering applications involve a

single critical property in one principal direction, it should be possible to use anisotropic design theory and specify a mill product which will have the optimum property in the desired direction, thus maximizing the potential strength, toughness, or other engineering properties desired in a given application.

BACKGROUND

It is well known that polycrystalline materials can be anisotropic.[9] This anisotropy arises from the directional properties of single crystals and is dependent upon the degree of preferred orientation or texture of the polycrystalline aggregate. Metals of hexagonal-close-packed structure are particularly anisotropic, with titanium being an outstanding example. Many physical and mechanical properties exhibit this anisotropy and it forms the basis for improvement of processing techniques or materials for certain applications. One example of improved processing is the increased drawability for sheet metals.[10,11]

During deformation or metal processing, such as rolling the single crystals which make up the polycrystalline aggregate acquire a crystallographic preferred orientation. The deformation process or subsequent heat treatments may result in a texture with more than one distinct preferred orientation or create a structure that approaches a single crystal, with or without scatter. A schematic representation of the two extremes, "random" orientation and a one-point or pseudo single-crystal preferred orientation, is illustrated in Figure 4. Textures that are developed can be illustrated by pole figures, using data obtained from X-ray diffraction. Sheet textures can be defined by specifying Miller indices of a plane parallel to the rolling plane (hkl) and a direction parallel to the rolling direction [uvw].

A schematic illustrating the relation of a one-quadrant, stereographic representation for two common preferred orientations is shown in Figure 5a. Imagine that the grains making up the material are under a hemisphere and that normals to a family of planes within each of the crystallographic unit cells contained in the grain, basal plane (0002) type in this example, are constructed and intersect the hemisphere at points. When the material is textured, the intensity of pole intersections will be nonuniform, with point concentrations about the theoretical points representing the "ideal" case, and the distribution perhaps somewhat more diffuse at increasing distances from the ideal points, for example 2, 4, 8 (arbitrary scale of numbers proportional to density of pole intersections). For a random orientation of crystallites within the grains, the intensity and concentration of poles will be uniform. For convenient two-dimension representation, the poles on the hemisphere are projected to a plane that is related to some known directions of the material being examined. For rolled material, these can be the rolling and transverse directions and sheet normal. Pole figures can be considered

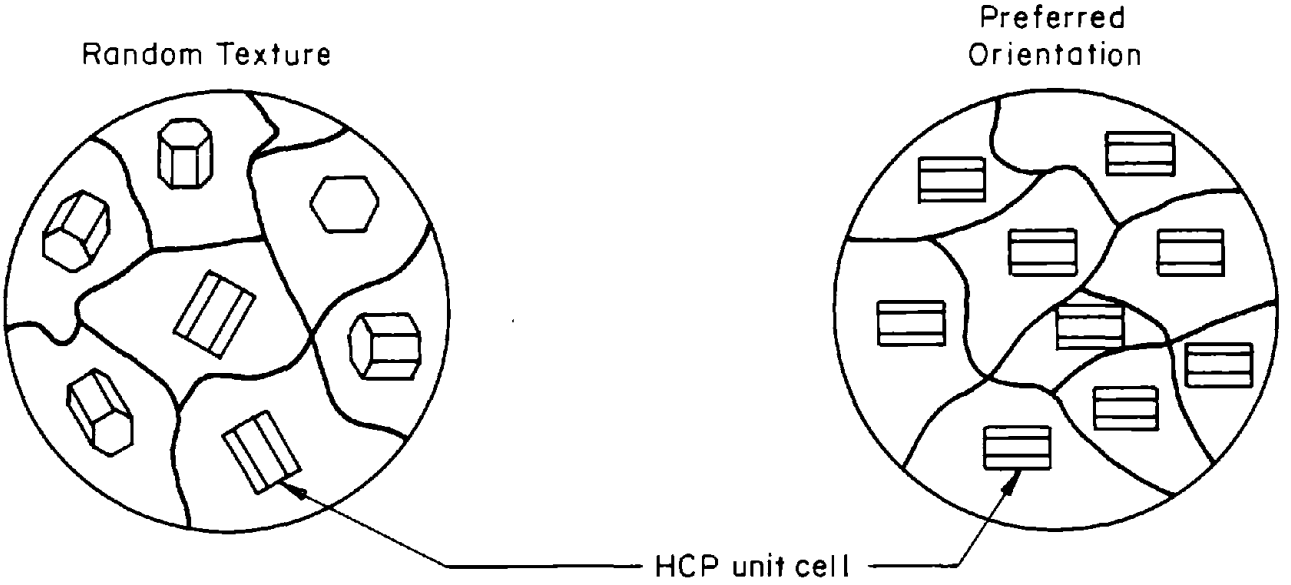

FIGURE 4. SCHEMATIC OF RANDOM AND PREFERRED TEXTURES FOR A PURE METAL OF HCP STRUCTURE

Note: The irregular lines represent grain boundaries.

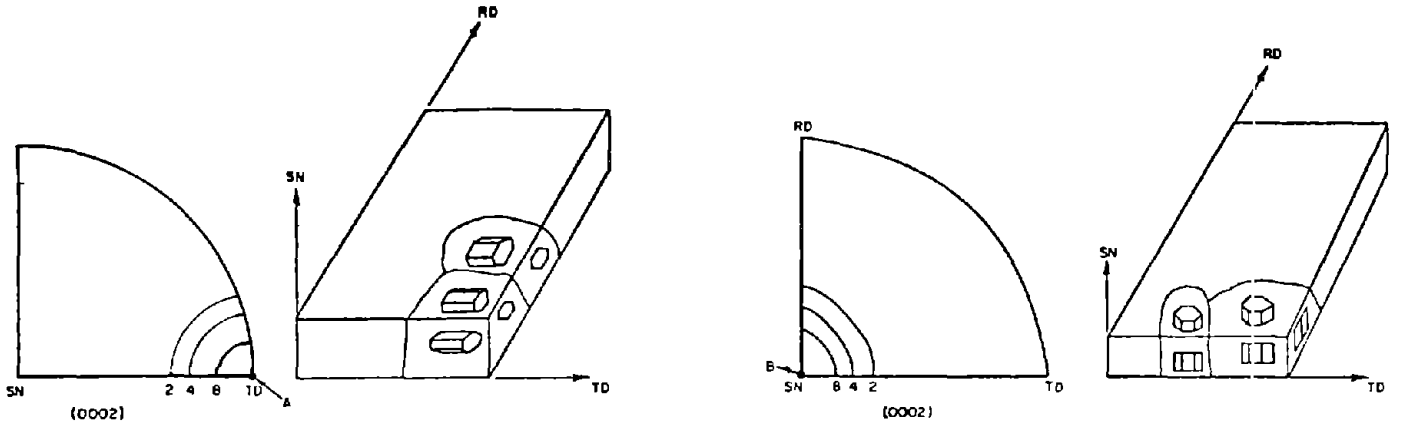

a. Crystallites aligned transverse to the rolling direction

b. Crystallites aligned normal to the rolling direction

FIGURE 5a. BASAL POLE FIGURES FOR TEXTURE OF HCP MATERIAL

Points A and B represent the case of perfect alignment of all crystallites

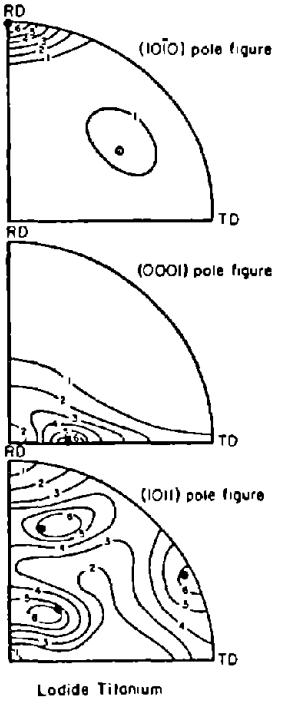

FIGURE 5b. BASAL POLE FIGURES FOR COLD-ROLLED TITANIUM (0001) [10$\bar{1}$0] ROTATED 30 DEGREES TOWARD THE TD ABOUT AN AXIS IN THE RD [37]

as maps for orientation distribution of crystallites within grains with principal directions of the material. The construction of pole figures, utilizing various techniques, is adequately covered by several authors.[12,13]

Because sheet metal normally receives a large amount of reduction from the ingot it is usually considered a potential material for exhibiting intense preferred orientation and much of the understanding of preferred orientation has been developed from research on heavily worked sheets and plate. Therefore, this review will highlight sheet and plate properties. This is not to say that similar results could not be achieved in large forgings[14], because it has been demonstrated that intense textures can be formed in titanium with small reductions, and these textures persist throughout further working[15] and thermal treatments[16,17].

Two principal kinds of anisotropy exist in sheets: normal and planar. In normal anisotropy the properties through the thickness of the sheet are different from those in the plane of the sheet; in planar anisotropy, the properties vary in the plane of the sheet. It has been shown that if the through-thickness strength is greater than that in the plane of the sheet, normal anisotropy, then the material has improved drawability. On the other hand, a large degree of planar anisotropy is detrimental in drawing and causes the formation of "ears".[18]

The anisotropy of strength and plasticity undoubtedly causes other major effects in primary working operations. For example, in sheet metal, when hexagonal close-packed (hcp) metals form a (0001) $[10\bar{1}0]$ "ideal" texture (sheet textures can be defined by specifying the Miller indices of a plane parallel to the rolling plane and a direction parallel to the rolling direction), it becomes very difficult to reduce the sheets further by rolling; higher rolling pressures are needed, and sometimes edge or surface cracking results. The term "ideal" arose from the interest in pressure-vessel applications and the similarity of this texture to the standard projection for a hexagonal metal.

Probably the most successful practical use of anisotropy has been in the field of magnetic properties.[19] Technologically, the control of preferred orientation, or texture control, in iron-silicon sheet is further advanced than that in any other material. In iron single crystals, the cube edge, or [100], direction is known as the easy direction of magnetization, and the [111], or cube diagonal, is the hardest direction of magnetization. Thus, in a polycrystalline magnetic sheet material, control of the texture provides a means for improvement of magnetic properties. Anisotropic magnetic sheet materials have been produced commercially for several years and are used throughout the electrical industry.

The modulus of elasticity may be anisotropic. For most cubic-structure alloys, the [111] direction is the direction of maximum elastic modulus, with the cube edge or [100] direction being the lowest. Thus, a rod or wire with a strong [111] fiber texture would be stiffer than one with a [100] fiber texture. (A fiber texture is one in which a crystallographic direction is specified in relation to the axis of a cylindrical product and other directions are disposed randomly about this axis.) Although there has been no large-scale exploitation of this fact, it has been proposed for making a superior phosphor-bronze spring material[20], and undoubtedly special commercial applications will be forthcoming. The elastic properties in titanium have been shown to be anisotropic and will be discussed in detail later in this review.

Another potential use of anisotropy is for the improvement of yield strength. Although this has received little commercial attention, it has been the subject of recent research.[21-24] "Texture hardening"[21] of titanium has been demonstrated in the laboratory for plane stress loading of sheet materials. It has been shown that, for biaxial loading in tension-tension, the largest improvements in yield strength would probably occur in an hcp metal with creation of an ideal texture, i.e., basal planes oriented parallel to the sheet surface.

Other beneficial effects are possible. For example, a rod in which the c axis is parallel to the rod axis should be 50 to 80 percent stronger than one with a $[11\bar{2}0]$ fiber texture. Texturing of other metals should also produce significant increases in strength. For example, a [111] fiber-textured steel wire should be 20 percent stronger than a randomly oriented material and 50 percent stronger than steel wire with a [100] fiber texture.[25] Similar comments can be applied to textured face-centered cubic (fcc) sheet.[26]

Much interest has been shown in titanium and its alloys because they are highly competitive to high-strength steels on a strength-to-weight basis. Although much of the research on texture strengthening has been directed toward plane-stress applications such as in pressure vessels, other applications might prove to be equally beneficial. Considerable research on anisotropy and preferred orientation in zirconium and its alloys has also been carried out.[27] The findings of this research parallel in many ways those for titanium and its alloys. The information found for zirconium and its alloys probably can be directly translated to titanium, for these two metals have identical crystal structures and similar lattice parameters.

The potential improvements available through texture control seem to have been adequately demonstrated. Why, then, are the practical applications so few? There appear to be many facets to the answer to this question; the most important is that, except for magnetic sheet material and a few cases of deep-drawing sheet, industry is not in a position to supply commercial products controlled to a specified texture. The difficulty in obtaining quantitative preferred-orientation information has probably impeded

progress. However, improved instrumentation for automatically determining pole figures will alleviate this. In some early cases, prototypes or laboratory mockups of end items have not illustrated the predicted improvements, thus failing to convince management of the advantages of texture control. These failures can be directly attributed to the lack of specific intense textures in the material employed for the construction of these prototypes. Recent research and development has been successful and it is felt that commercial practice will be arrived at shortly and controlled textures will be "off the shelf" items. Thus, it is imperative to develop substantial technical information so that the required texture control can be achieved. One purpose of this report is to disseminate knowledge on this subject.

Textures in Titanium

Before a review is set forth describing the influence of texture upon the properties of titanium, a fairly detailed discussion of how textures develop, along with some examples of common types found in commercial alloys, is proper.

There are several mechanisms by which the texture or preferred orientation can be developed. The most important are deformation, recrystallization, grain growth or secondary recrystallization, and phase transformation. In addition, texture development can be affected by alloying and deformation temperature. Several complete reviews[28-31] have been published on this subject. Probably the most complete, at least on titanium, is that by Dillamore and Roberts.[29] To summarize briefly, considerable study has been made of the deformation texture of heavily rolled sheet material of high-purity titanium, somewhat less work on the annealing texture of this material, and some work, but very little reported, on the study of the effects of phase transformation of the same material. A limited amount of work has been reported on the effect of alloying elements on the cold-rolled texture of titanium sheet materials in which large changes of preferred orientation were observed. Therefore, this section will concentrate upon sheet and plate textures.

The first step in texture control would originate with processing at the mill. In most cases, ingot texture is of little significance since the large shape change resulting from subsequent processing is usually sufficient to eliminate ingot texture; thus, the entire history of deformation and heating produces changes in the texture. Therefore, effective texture control can be obtained via precision heating and deformation schedules in the fabrication of titanium mill products. However, because the process control of textures is not well understood, one of the first steps in developing understanding of textures in commercial titanium alloys would be to determine textures in different sheets fabricated from various alloys.

Deformation Mechanisms

A complete knowledge of the basic deformation mechanisms is important in order to understand how preferred orientations occur during the working of a metal. Several workers have studied the plastic deformation of titanium single crystals and have found three important modes of slip and six modes of twinning. The relative contribution of the various modes to the overall deformation varies with temperature[32-35]. These are summarized in Table 1. For more complete discussion on crystallography and deformation of hexagonal metals see the excellent review by Partridge.[36]

Cold-Rolled Textures

The textures that form upon cold rolling of pure titanium sheet have been studied by several investigators[29] and can be described as (0001) $[10\bar{1}0]$ type with the basal pole rotated about 30 degrees toward the transverse direction, as shown in Figure 5b. Williams and Eppelsheimer[37], utilizing the method of Calnan and Clews[38-41], have described the general formation of this texture by a combination of $(11\bar{2}2)$ twinning and (0001) slip. The $(11\bar{2}2)$ twinning is thought to rotate the basal poles toward the transverse direction, and (0001) slip rotates the basal poles toward the sheet normal.

Annealing Textures

Keeler and Geisler[42] have studied the changes in the cold-rolled texture of high-purity titanium occurring upon heating. Their results are shown in Figure 6. Annealing at various temperatures below the beta transus (about 1620 F in pure titanium) has little effect on the basal pole figures, that is, only a sharpening and slight rotation (compare Figures 12 and 13). The main changes can be observed by studying the $(10\bar{1}0)$ pole figures. On heating, the first change noticed may be described as a rotation of about 30 degrees around the c axis so that the $[11\bar{2}0]$ is nearly aligned with the rolling direction. Hu and Cline[43] have also studied recrystallization textures and report that a rotation of 20 degrees about the c axis accompanies recrystallization. Upon heating high into the beta field, a transformation texture results due to alpha-beta transformation relationships.

TABLE 1. TITANIUM DEFORMATION MODES

Slip Modes (all in [11$\bar{2}$0] Direction) [33]

Plane	Designation	Comments
(10$\bar{1}$0)	Prism	Lowest critical resolved shear stress
(10$\bar{1}$1)	Pyramidal	Highest critical resolved shear stress
(0001)	Basal	Intermediate critical resolved shear stress

Twinning Modes[a]

Type[b]	K_1	η_1	K_2	η_2	Shear	Comments	Reference
1	(10$\bar{1}$1)	[10$\bar{1}$2]	($\bar{1}$013)	[30$\bar{3}$2]	0.100	Compression parallel to c axis	34
2	(10$\bar{1}$2)	[$\bar{1}$011]	(10$\bar{1}\bar{2}$)	[10$\bar{1}$1]	0.189	Tension parallel to c axis	32
3	(11$\bar{2}$1)	[$\bar{1}\bar{1}$26]	(0001)	[11$\bar{2}$0]	0.638	Tension parallel to c axis	32
4	(11$\bar{2}\bar{2}$)	[11$\bar{2}\bar{3}$]	(11$\bar{2}\bar{2}$)	[11$\bar{2}$3]	0.957	Compression parallel to c axis	32
5	(11$\bar{2}$3)	[$\bar{1}\bar{1}$22]	(0001)	[11$\bar{2}$0]	0.914	Tension parallel to c axis	32
6	(11$\bar{2}$4)	[$\bar{2}\bar{2}$43]	(11$\bar{2}\bar{4}$)	[22$\bar{4}$3]	0.468	Compression parallel to c axis	32

(a) Here K_1 is the composition or twinning plane, η_1 is the direction of shear in the twin plane, K_2 is the second undistorted plane in the twin, and η_2 is the direction of intersection of the plane of shear with K_2.

(b) Type 1 observed only at high temperature; Types 4, 5, and 6 increase with decreasing temperature.

Effect of Interstitial Alloying Elements on Cold-Rolled Texture

The effects of various interstitial alloying elements have been studied, to a limited degree, by several investigators. It has been established that the interstitial elements up to the amounts sometimes found in commercially pure titanium can give rise to secondary peaks in the basal-plane pole figures at about 20 degrees toward the rolling direction[37,44] as illustrated in Figure 7.

Effect of Solid-Solution Alloying Elements on Cold-Rolled Texture

The effect of solid-solution alloying elements has been studied by McHargue et al.,[45,46] and it has been found that columbium (<3.6 wt %), tantalum (<15,4 wt %), and zirconium (<14.7 wt %) have very little effect upon the cold-rolled texture of titanium.[47] On the other hand, aluminum (≈4.0 wt %) reduces the tilt of the basal planes toward the transverse direction and produces a texture which may be described as ideal, or (0001) [10$\bar{1}$0] [46] (see Figure 8).

More recent extensive studies by Larson et al[48] on the influence of solid-solution alloying elements have corroborated the studies of McHargue.[45] Textures obtained during these studies are similar in many features to those reported by previous investigations.

Effect of Beta-Eutectoid Stabilizer

Beta-eutectoid-type elements alloyed with titanium, with the exception of copper, produced similar changes in the titanium texture patterns. It was not possible to determine the behavior for cobalt and nickel additions to titanium because the higher composition alloys cracked up during rolling and thus were not available for texture determination. However, manganese, iron, and chromium showed similar patterns. With zero-to-intermediate alloy additions, the basal pole moves slowly from the unalloyed position toward the transverse direction. Sometimes two components in the texture are observed, one near the unalloyed position and one in the transverse direction. As will be shown later, the peak in the transverse direction, a (11$\bar{2}$0) [10$\bar{1}$0] texture, is a stable end orientation. With a further increase in alloying addition the beta phase becomes stable, and at approximately 16 to 20 percent beta phase an abrupt change in the texture is observed. This behavior is best seen by examining the manganese series, illustrated in Figure 9. The new basal pole texture is similar to that of zinc or magnesium[28,29] sheet material. However, the titanium alloy still has the [10$\bar{1}$0] parallel to the rolling direction, whereas in zinc and magnesium, the [11$\bar{2}$0] is parallel to the rolling direction.

An exception to the above general behavior was found with the 0.55 wt % copper additions which formed nearly an ideal (0001) [10$\bar{1}$0] type texture. The ideal

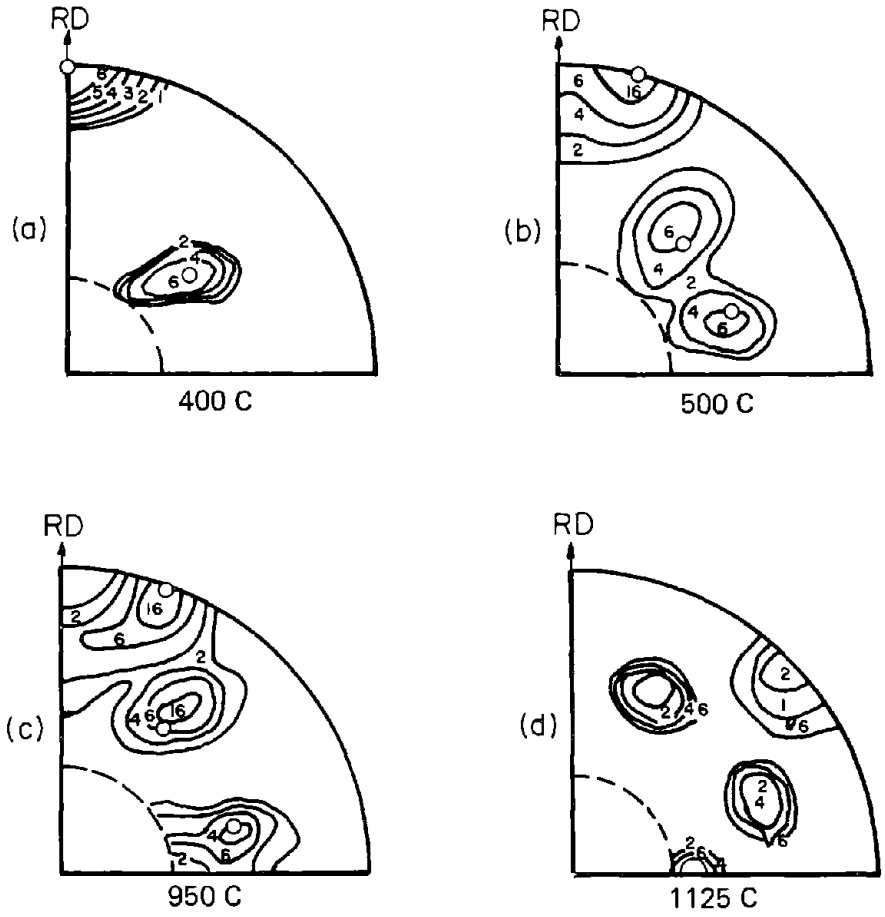

FIGURE 6. (10$\bar{1}$0) POLE FIGURES FOR TITANIUM COLD-ROLLED 99.7 PERCENT AND ANNEALED FOR 1 HOUR AT VARIOUS TEMPERATURES[42]

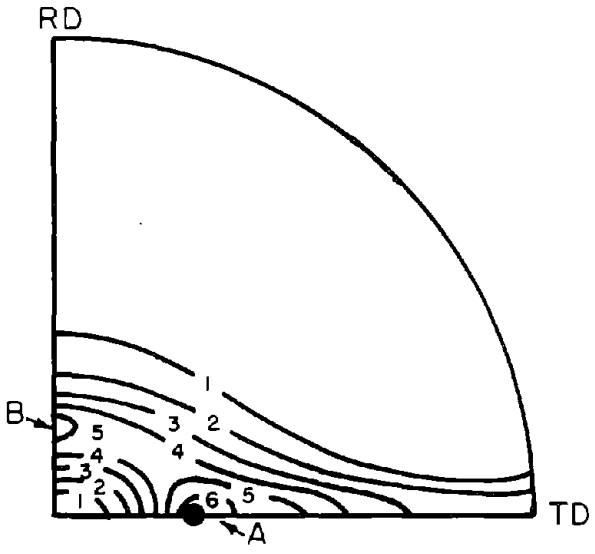

FIGURE 7. (0001) POLE FIGURE FOR COLD-ROLLED COMMERCIAL TITANIUM[37]

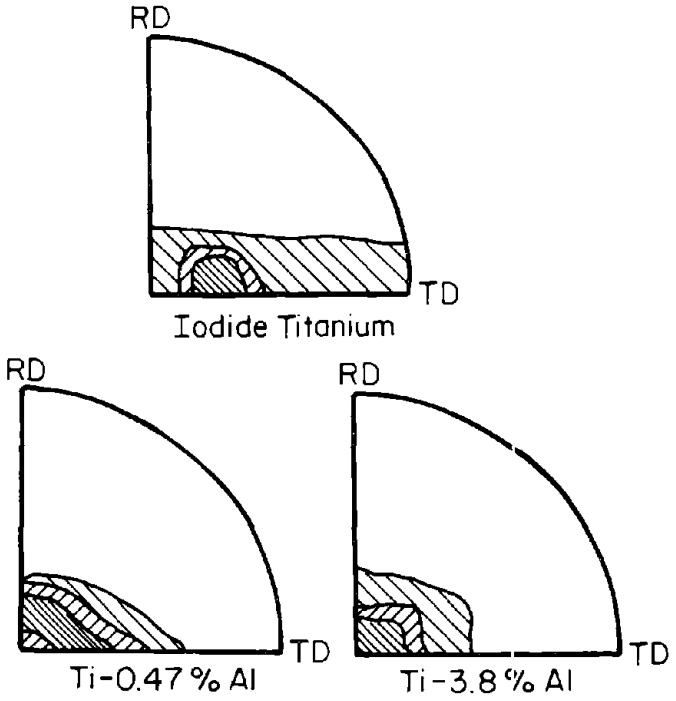

FIGURE 8. BASAL FIGURES (0002) SHOWING EFFECT OF ALUMINUM ON TITANIUM[46]

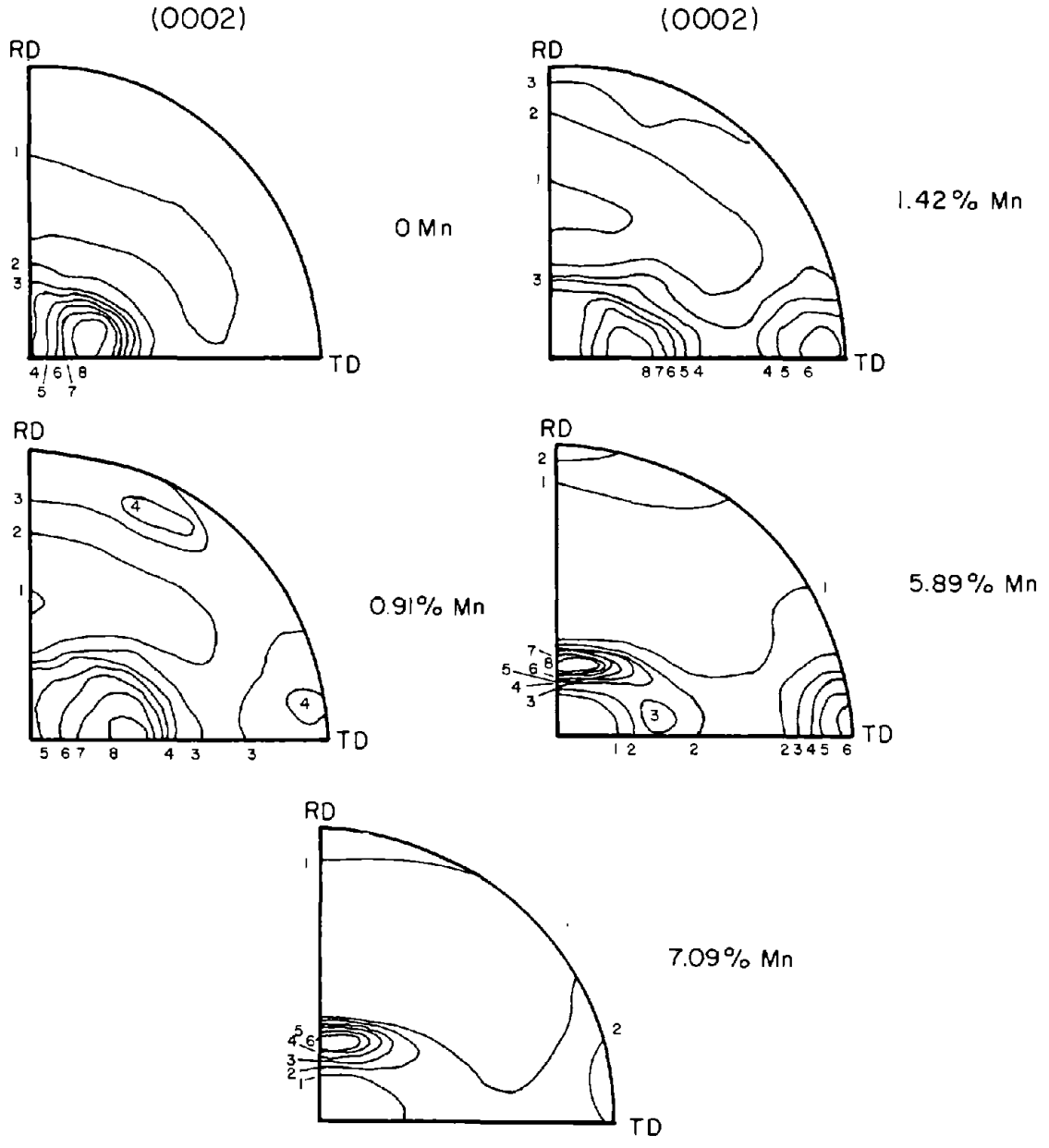

FIGURE 9. TEXTURES OF Ti-Mn BINARYS[48]

texture produced in copper alloys at and above 0.55 wt % may be due to the finely dispersed second phase which is clearly visible in the microstructures. This finely dispersed second phase occurs because of the high solubility of copper in alpha titanium near the eutectoid temperature and the decreasing solubility with decreasing temperature. One of the important factors in influencing twinning tendency is the grain size.[28] The presence of a finely dispersed second phase within a grain has the effect of reducing the "effective" grain size and probably would be influential in the suppression of [11$\dot{2}$2] twinning.

Effect of Beta-Isomorphous Stabilizers

For alloy additions of molybdenum, vanadium, and columbium, the beta-isomorphous stabilizers, texture changes that occurred were similar to those in the beta-stabilized eutectoid alloys described in the previous section.[46]

Effect of Alpha Stabilizers

Additions of aluminum, an alpha stabilizer, caused the basal pole to move toward the sheet normal, producing

an ideal or (0001) [10$\bar{1}$0] type texture similar to that observed by Sparks et al. (Figure 8)[46] Thornburg[49,50] also studied the influence of aluminum additions and found essentially the same results. He found that the texture typical of commercially pure titanium changed to an ideal or basal texture suddenly at a given percent reduction and an aluminum concentration of >2.0 percent. It was also found that split TD textures (low aluminum concentrations, Figure 8) had microstructures which contained large amounts of twinning, which suggests that twinning was required for the formation of split TD textures. Ideal or basal texture microstructures did not show twins. Thornburg developed an isostrain model for texture formation, counterpart to the Calnan and Clews[40] isostress model, and used it to predict texture. This model is not capable of handling twin formation easily. Thornburg indicates that (c + a) slip may be important in the formation of basal textures.

Effect of Neutral Elements

Additions of tin and zirconium had only minor effects upon the unalloyed texture. The changes noted were primarily that of intensifying the unalloyed texture.[46]

THE FORMATION OF DEFORMATION TEXTURES

The Calnan-Clews Method

Theories of the development of deformation textures are not well advanced. This is probably due to the complex nature of polycrystalline deformation. The most complete treatment of the formation of deformation textures is that advanced by Calnan and Clews.[39-41] Williams and Eppelsheimer have applied the Calnan-Clews method to titanium and conclude, after several assumptions, that by suitable choice of slip and twinning modes and their relative critical shear stresses, it is possible to develop a satisfactory explanation of deformation textures in tension, compression, and cold rolling. The weakness of this method is the lack of information about critical shear stresses for different slip planes and the assumption that twinning is achieved by a critical shear stress. In spite of all these difficulties, this method does have value because it allows qualitative discussion of how textures develop.

The main feature of the Calnan-Clews method is the determination of slip rotation and twinning reorientation caused by an applied stress system. To determine the general grain-rotation behavior, a resolved-shear-stress contour diagram for each slip and twinning system having the highest resolved-shear-stress ratio is plotted in a unit triangle. It is then assumed that only the slip or twinning system having the highest resolved-shear-stress ratio will be active. The resolved-shear-stress ratio is defined as the ratio of the resolved shear stress to the critical shear stress. The grain-rotation tendencies for various slip and twinning systems are as follows:

1. Simple slip
   a) Tension – slip direction rotates toward stress axis
   b) Compression – slip plane normal rotates toward stress axis.

2. Duplex slip
   a) Tension – the great circle joining two active slip directions rotates toward the stress axis
   b) Compression – the great circle joining two slip plane normals rotates toward the stress axis.

3. Multiple slip
   a) Rotation occurs until stress axis is located symmetrically.

4. Twinning
   a) Stress direction does not coincide with shear direction – no predictable direction
   b) Stress direction coincides with shear direction – rotations obtained from analysis of twin mode.

Thus, it can be seen that in order to determine the grain rotations, it is necessary to know the stress system that is causing the deformation.

Roll-Gap Stresses and Deformation

One of the main problems in applying any method of determining rolling textures is the tremendous variation in deformation and stresses throughout the roll gap.[51,52] This makes computation of grain rotations an almost impossible task. This complexity can be overcome to some degree by making the gross assumption that sheet rolling can be described as a deformation caused by tension in the rolling direction and compression perpendicular to the rolling plane.[51-53] This simple model of roll-gap stresses has been used by Calnan and Clews[38-40], Williams and Eppelsheimer[37], and Hobson[54]. From this model it is possible to calculate the resolved shear stresses on grains of any orientation within a sheet and to determine which slip or twinning mode has the highest stress. It is then assumed that when this stress exceeds a critical value yielding will occur along with the grain rotation associated with that mode of deformation. Hobson[54], studying cold rolling of zirconium single crystals, reported a computerized program for carrying out the above calculations. Figure 10 shows the results of one such calculation, assuming that all slip and twinning modes yield at the same critical stress and that the tensile stress is equal to the compressive stress.

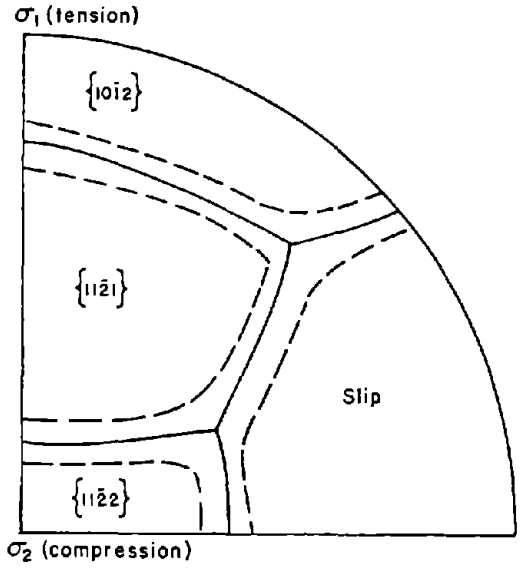

FIGURE 10. STEREOGRAM SHOWING THE DEFORMATION SYSTEMS WITH THE LARGEST SCHMID FACTOR IN A ZIRCONIUM SINGLE CRYSTAL AS A FUNCTION OF BASAL POLE ORIENTATION [54]

Calculations based on loading with $\sigma_1 = \sigma_2$ and the assumption that each mode has the same critical stress for activation. Between dashed boundaries, more than one mode may operate, depending on rotation of the basal pole.

Grain Restraints

Hobson's work [54] was performed on zirconium, which has similar slip and twinning modes to titanium, and it is implied that polycrystalline material behavior is similar to that of single crystals. It is known that this is not entirely true, for Taylor [55] pointed out that in order to maintain grain-to-grain continuity it was necessary that five independent deformation modes occur simultaneously. This continuity requirement and other local grain-grain interactions will undoubtedly cause major effects upon the stresses and deformation modes. Thus it is convenient to accept from the work of Calnan and Clews, of Williams and Eppelsheimer, and of Hobson that the main deformation mode is that which has the highest resolved-shear-stress ratio. Furthermore, this main deformation mode produces the principal changes which occur in the texture, even though other accommodation modes are also active.

Application to Unalloyed Titanium

Starting with a random initial orientation and considering that rolling textures are a combination of tension and compression textures, it is now possible to develop a description of how titanium textures form. First, it can clearly be seen that $\{10\bar{1}2\}$ and $\{11\bar{2}1\}$ twinning reorients all the grains which have their basal poles in those areas labeled in Figure 10. The $\{10\bar{1}2\}$ twinning rotation (about 85 degrees) is such that the new basal-pole orientation would be in or near the area labeled $\{11\bar{2}2\}$. The $\{11\bar{2}1\}$ twinning rotation would be such that the basal poles move along a great circle toward the transverse direction, about 35 degrees. This is illustrated in Figure 11. The absence of basal poles near the rolling direction in real pole figures for titanium supports the twinning theory. Since it is well established that titanium pole figures have a strong $[10\bar{1}0]$ component in the rolling direction, it is evident that tension in the rolling direction causes $\langle 11\bar{2}0\rangle$ duplex slip on either $\{10\bar{1}0\}$ or $\{10\bar{1}1\}$, or on both. From the compression stresses, $\{11\bar{2}2\}$ twinning causes a rotation of the grains which have their basal poles near the sheet normal. This rotation, about 64 degrees, occurs about the rolling direction toward the transverse direction. However, real textures of unalloyed titanium do not have basal pole peaks in the transverse direction; thus an additional rotation back toward the sheet normal is required. The most likely mechanism, considering basic principles, would be basal slip. There is a possibility that $\{11\bar{2}1\}$ twinning could also cause the rotation back toward the sheet normal, since the stress direction would be correct for second-order $\{11\bar{2}1\}$ twinning within the $\{11\bar{2}2\}$ twins. The rotation for this second-order twinning would be about 35 degrees from the transverse direction toward the sheet normal; further rotation by slip would be required in order to orient the basal poles properly. In any event, the position of the

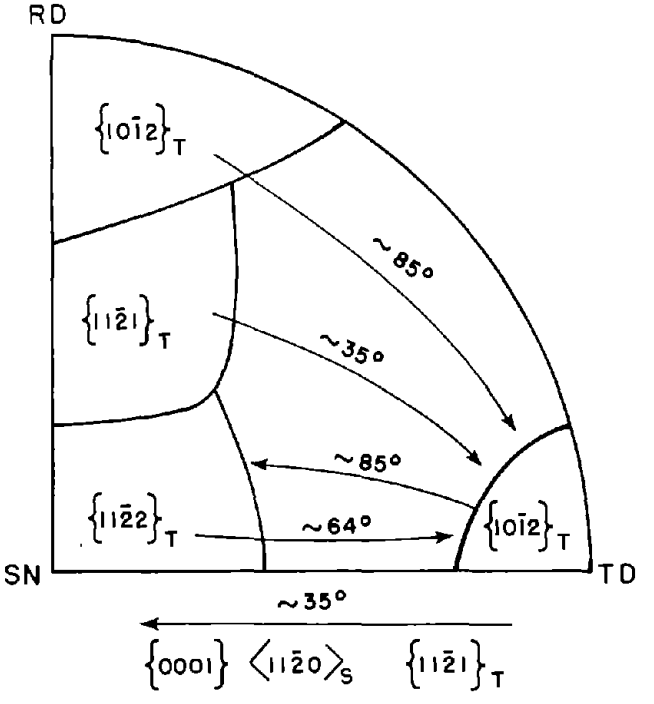

FIGURE 11. ROTATIONS OF THE (0001) POLE IN TITANIUM DUE TO VARIOUS TWIN (T) AND SLIP (S) MODES [48]

The T subscript refers to the twinning modes.

basal poles along the transverse direction—sheet normal great circle may be considered as the end result of a dynamic process of $\{11\bar{2}2\}$ twinning, possible $\{11\bar{2}1\}$ twinning, and basal slip. Therefore, the observed cold-rolled texture of unalloyed titanium of (0001) $[10\bar{1}0]$ rotated about 27 degrees toward the transverse direction can be thought of as a combination of $[10\bar{1}0]$ tension textures and a rotated [0001] compression texture. Since rotation occurs about the $\langle 10\bar{1}0 \rangle$ axis, both are compatible. Some of the principal twinning reorientations are shown in Figure 11.

Modification of Texture by Alloying

Changes in texture caused by alloy additions or variations in processing procedures can be explained by modification of the above mechanism. For the aluminum and copper alloy series, the change is quite clear. The ideal (0001) $[10\bar{1}0]$ texture produced in these alloys seems to be a result of the suppression of $\{11\bar{2}2\}$ twinning. A decrease in the critical resolved shear stress for basal slip could also be effective in producing this texture. For the alloys where a strong $(11\bar{2}0)$ $[10\bar{1}0]$ component shows in the texture, that is in high-molybdenum and intermediate-manganese alloys, it is similarly clear that this is caused by an increased $\{11\bar{2}2\}$ twinning tendency and/or a low critical resolved shear stress for $(10\bar{1}0)$ $[11\bar{2}0]$ slip which produces a stable end texture of this type.

The transformation from a titanium- to a magnesium-type texture is through the introduction of an additional second-order twinning mode. The texture transition is not a true one, for although the basal-pole figures for highly beta-alloyed titanium are similar to those for magnesium, zinc, and cobalt, the titanium has a strong $[10\bar{1}0]$ in the rolling direction, whereas magnesium has a strong $[11\bar{2}0]$ in the rolling direction. Thus the main features of the tension texture in titanium still remain after the texture transition.

The texture formed by highly beta-alloyed titanium can be produced by a second-order twinning of $\{10\bar{1}2\}$ type occurring within the $\{11\bar{2}2\}$ twin. The stress axis is in the favorable direction for this mode of twinning. It is interesting to note that the texture transition occurs only when there is a two-phase structure and the amount of the beta phase is greater than approximately 16 to 20 volume percent. It appears that the deformation of the beta phase, which is softer than the alpha, is producing a strain field which is conducive to this twinning mode. The twinning rotation would be about 85 degrees along a great circle, 30 degrees from the sheet normal and passing through the transverse direction.

TEXTURES IN COMMERCIAL UNALLOYED AND ALLOYED TITANIUM SHEET

The textures found in commercial titanium sheet materials are reviewed in this section. The most prominent of several basic types of titanium-sheet textures is found in cold-rolled sheet.[42] A similar type is also found if the sheet is warm rolled between room temperature and about 1400 F. This texture is characterized by having a basal (0002) pole intensity on the sheet normal (SN), transverse direction (TD), and a great circle at about 27 to 30 degrees from the SN. This texture is further defined by stating that the $(10\bar{1}0)$ poles lie near, or in, the rolling direction (RD). This texture, shown in Figure 12, is called an alpha-deformation texture.

Annealing of cold- or warm-rolled sheets has only a slight sharpening effect upon the (0002) poles. However, the $(10\bar{1}0)$ poles rotate through an arbitrary angle of approximately 30 degrees about the c axis, resulting in the texture shown in Figure 13. This is called an annealed alpha-deformation texture.

In most cases, it is not necessary to distinguish between an annealed and a cold-worked texture since many properties are symmetrical about the c axis. Thus, a basal-pole figure is sufficient to define the crystallographic influence, and the above texture can be modified by either hot rolling[56] (above 1400 F but not above beta transus) and/or alloying. Important observations in relation to texture strengthening were that additions of approximately 4 percent aluminum[45,46] (an early discovery) and approximately 0.5 percent copper (the most recent disclosure) produce the "ideal" texture.[48] It has also been established that the ideal texture can be produced by round rolling.[57] In fact, it seems possible to change the angle at which the basal pole lies from the sheet normal by combinations of alloying and hot rolling.[48] Figure 14 illustrates this for several cases.

A sufficient amount of beta stabilizers (more than 15 volume percent retained beta at room temperature) or hot rolling in the alpha-beta field will cause a texture transition, and the new texture will have a basal-pole figure which looks like the magnesium or zinc type, as shown in Figure 15.

The final important texture found in titanium is that which develops from a beta-worked material and is a result of the Burgers transformation relationship $\{0001\}_\alpha \parallel \{110\}_\beta, \langle 11\bar{2}0\rangle_\alpha \parallel \langle 111\rangle_\beta$.[58] It can be seen that since the basal plane in the alpha is parallel to (110) in the beta, a determination of the (110) pole figure will give the basal-pole figure after transformation. As in most bcc metals, hot or warm sheet rolling produces a texture which has a strong (100) [011] texture component.[59]

Other minor orientation peak components are not usually found in titanium. If the composition has sufficient alloying to retain the beta at room temperature, textures like those in Figure 16 will usually be found. On the other hand, if the beta deformation texture is developed

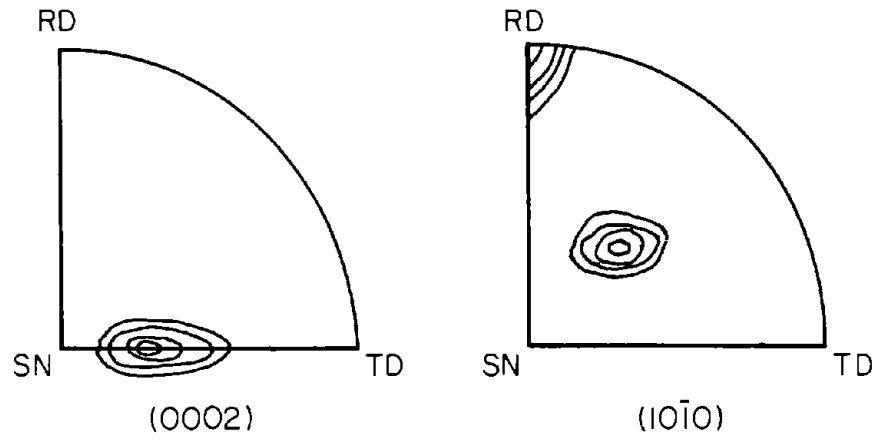

FIGURE 12. ALPHA-DEFORMATION TEXTURE

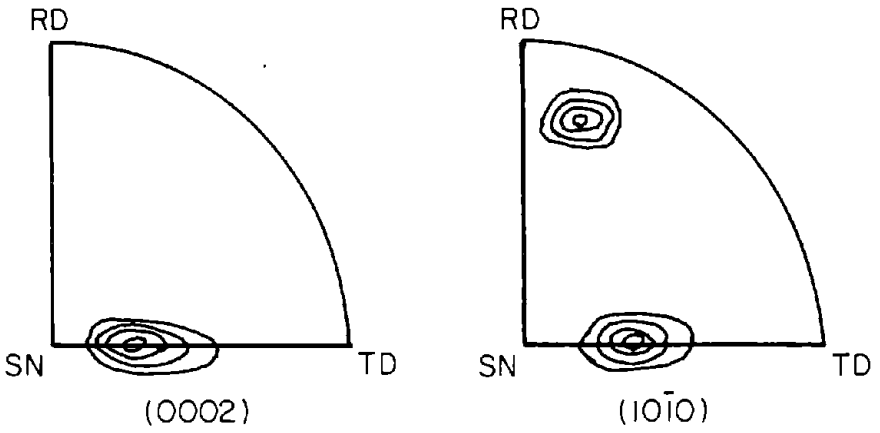

FIGURE 13. ANNEALED ALPHA-DEFORMATION TEXTURE

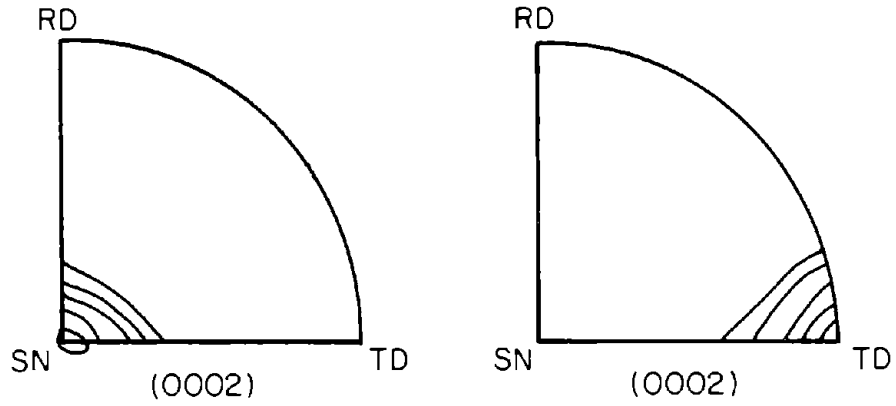

a. "Ideal" Texture Cold Rolled Ti-4Al, Ti-0.55Cu, Cross and Round Rolled Ti-6Al-4V

b. Hot-Rolled Texture Ti-6Al-4V Cold-Rolled Ti-8Mn

FIGURE 14. EXTREMES OF BASAL POLE ROTATION

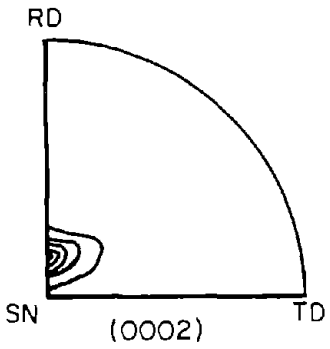

FIGURE 15. MAGNESIUM- OR ZINC-TYPE TEXTURE FORMED IN TITANIUM ALPHA BETA ALLOYS HAVING MORE THAN 15 VOLUME PERCENT RETAINED BETA

by hot working in the beta field and transformation occurs on cooling or on aging as part of the heat treatment, the alpha (0002) basal-pole figure will bear a simple relationship to the beta texture, and may look just like one of the textures shown for the (110) pole figures in Figure 16. However, there are some other textures that can be formed, but, these are of less commercial importance because they are infrequent and are a result of special processing or heat treatments. For example, a cube or (100) [001] texture can be formed by heating very high in the beta field, but this rarely happens in production because of the excessively large grain growth. For the most part, the textures found in commercial sheet are either single type, as described above, or a simple combination of two basic types. Koh[60] reported cold-rolled and annealed textures in thin foils and found that they are also composed of multiple texture components. These were illustrated in a previous report[61] for many unalloyed and alloyed titanium sheets.

Commercially Pure Titanium

For the most part, commercially pure sheets show classical alpha-deformation textures. However, notable exceptions were found in two lots of unalloyed titanium, RC55 and Ti75A, each having remnants of a transformed-beta-deformation texture.[61] Examples of texture types found in several unalloyed titanium sheets are shown in Table 2a. In titanium RC55 heat, heated between 1400 and 1700 F, there is no change of the alpha-deformation texture with increasing temperature.

Titanium-6Al-4V

The most actively studied of the commercial alloys is Ti-6Al-4V.[22,62-65] A great deal of the research effort has been directed toward development of procedures designed to produce "ideal textures" for pressure-vessel applications. In these programs it has been shown that cross rolling at temperatures below 1500 F will produce such textures, and that once developed they are very persistant.

The Ti-6Al-4V alloy sheet examined had several different texture types as shown in Table 2b. One common texture observed for this alloy was a two-component texture where one component was in the TD and the other was near the SN (Heat 1). In some cases, the peak near the SN was very small and that near the TD very intense, Heat 3 (0.070 in.). However, there was a unique case where the texture was nearly random, Heat 4. Heats 3 (0.030 in.) and 2 had a transformed-beta-deformation texture. The effect of heat treatment (Heat 3, 0.070 in.) is also shown, with the material undergoing a texture change from an alpha deformation type to a transformed-beta-deformation type as it was heated higher through the alpha-plus-beta field toward the beta field.

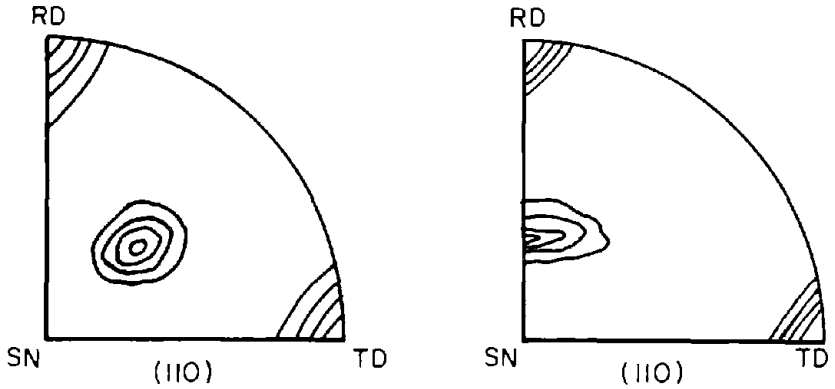

FIGURE 16. BETA-DEFORMATION TEXTURES FOR TITANIUM

TABLE 2. CHARACTERIZATION OF SHEET MATERIALS AND TEXTURES[61]

a. Commercially Pure Titanium

Unalloyed Titanium Grade	Heat	Thickness, in.	Condition[a]	Texture Type[b]
RC55	1	0.125	A.R.	α deformation
RC55	2	0.050	A.R.	Dual α deformation (ideal and TD Orientations)
RC55	3	0.130	A.R.	α deformation
RC55	4	0.140	ST 1400 F 1 hr	α deformation
RC55	4	0.140	ST 1700 F 1 hr	α deformation
Ti100A	1	0.065	A.R.	Dual α deformation
Ti100A	2	0.030	A.R.	α deformation
Ti75A	1	0.060	A.R.	α deformation
Ti75A	2	0.100	A.R.	Dual α deformation and transformed-β deformation

b. Ti-6Al-4V

Heat	Thickness, in.	Condition[a]	Texture Type[b]
1	0.060	A.R.	Dual (TD α deformation and Mg type)
2	0.130	A.R.	Transformed-β deformation
3	0.070	A.R.	Dual (TD α deformation and weak Mg type)
3	0.030	A.R.	Dual (strong TD α deformation)
3	0.060	STA – 1450 F 1/4 hr 1000 F 4 hr	α deformation (TD peak)
3	0.060	STA – 1650 F 1/4 hr 1000 F 4 hr	α deformation (TD peak)
3	0.060	STA – 1750 F 1/4 hr 1000 F 4 hr	Transformed-β deformation
4	0.040	A.R.	Random
5	0.040	A.R.	Dual (α deformation and TD poles)

c. Ti-4Al-3Mo-1V

Heat	Thickness, in.	Condition[a]	Texture Type[b]
1	0.060	STA – 1400 F 1/4 hr 1000 F 4 hr	Dual α deformation and Mg type
1	0.060	STA – 1500 F 1/4 hr 1000 F 4 hr	Dual α deformation and Mg type – slight peak
1	0.060	STA – 1600 F 1/4 hr 1000 F 4 hr	Complex α deformation and Mg type – stronger peak in RD
1	0.060	STA – 1700 F 1/4 hr	Transformed-β-deformation type
2	0.065	A.R.	Transformed-β-deformation type
3	0.060	A.R.	Very near ideal
4	0.020	A.R.	Alpha phase transformed β deformation – beta phase

Continued

TABLE 2. Continued

d. Ti-8Mn

Heat	Thickness, in.	Condition[a]	Texture Type[b]
1		A.R.	Near ideal
2	0.065	A.R.	α deformation – TD peak
3	0.030	A.R.	α deformation – very strong TD peak
4	0.120	A.R.	Dual (α deformation – strong TD peak + Mg peak)

e. Ti-4Al-4Mn

Heat	Thickness, in.	Condition[a]	Texture Type[b]
1	0.065	A.R.	α deformation – strong TD peak
2	0.055	A.R.	α deformation – strong TD peak
2	0.055	STA – 1300 F 3/4 hr 1000 F 8 hr	Dual (α deformation – TD peak + weak Mg peak)
2	0.055	STA – 1600 F 3/4 hr 1000 F 8 hr	Dual (α deformation – TD peak + weak Mg peak) slight RD peak
2	0.055	STA – 1700 F 3/4 hr	Beginning of β-deformation type

f. Ti-16V-2.5Al

Heat	Thickness, in.	Condition[a]	Texture Type[b]
1	0.030	STA – 1200 F 1/2 hr 975 F 4 hr	β deformation
1	0.030	STA – 1300 F 1/2 hr 975 F 4 hr	β deformation
1	0.030	STA – 1400 F 1/2 hr 975 F 4 hr	Complex
1	0.030	STA – 1450 F 1/2 hr 975 F 4 hr	Complex
1	0.030	A.R. + Aged 975 F 4 hr	β deformation
1	0.030	ST + WQ 1450 F 1/2 hr	Complex (coarse grain)
2	0.025	A.R.	β deformation
3	0.045	A.R.	β deformation
3	0.045	A.R. + 975 F 4 hr	Transformed-β deformation
4	0.025	A.R.	Transformed-β deformation
5	0.040	A.R.	β deformation
6	0.070	A.R.	Near transformed-β deformation
7	0.065	A.R.	Dual α deformation
8	0.130	A.R.	Dual α deformation

(a) A.R. – as received. ST – solution treated followed by air cooling. STA – solution treated, water quenched and aged.

(b) (0002) pole figure, except where noted.

Titanium-4Al-3Mo-1V

The alloy Ti-4Al-3Mo-1V showed several cases of transformed-beta-deformation textures (Heats 1, 2, and 4) in the heat-treated condition as illustrated in Table 2c. A dual-texture type similar to that found in Ti-6Al-4V was found in the case of Heat 1 and, with increasing temperature, it went to a beta-transformation-type texture. Heat 3 displayed a nearly ideal texture.

Titanium-8Al-1Mo-1V

The Ti-8Al-1Mo-1V alloy single sheet examined had a transformed-beta-deformation texture.

Titanium-6Al-6V-2Sn

The sheets of Ti-6Al-6V-2Sn examined also have textures which appear to be of the transformed-beta-deformation type.

Titanium-8Mn

The Ti-8Mn material examined, except for one sheet which was nearly random, had textures of the dual-alpha-deformation type with the TD pole being of high intensity. A single sheet examined had the ideal-type orientation, basal planes parallel to the sheet surface.

Titanium-4Al-4Mn

Two heats of the Ti-4Al-4Mn alloy showed a deformation-type texture with a single peak near or at the TD. Upon heating, Heat 2 developed a secondary peak near the SN; then, at 1700 F, a transformed-beta-deformation texture resulted. (Data are given in Table 2e.)

Titanium-16V-2.5Al

Ti-16V-2.5Al metastable beta alloy developed textures characteristic of the (100) [011] beta deformation in either the beta-structure component or in an alpha-transformation counterpart. (see Table 2f.)

Commercial Significance

It can be seen from the above review that a wide range of textures are formed in the titanium-alloy sheet produced commercially. This wide range of textures is of commercial significance from two major viewpoints. First, from the standpoint of anisotropy of properties, it appears that a beta-deformation or a transformed-beta-deformation texture will appear least anisotropic because it is orthotropic. Second, an alpha-deformation texture composed of basal poles in the transverse direction gives rise to highest degree of planar anisotropy. The technological barrier for the application of texture hardening or use of texture for dramatic improvements in many properties is not that the desired textures cannot be developed, but that mill techniques and procedures have not been determined and employed. It appears from textures found that virtually any described texture can be achieved.

EFFECT OF TEXTURE ON TITANIUM ELASTICITY

The increasing use of titanium and titanium alloys for critical structural applications has required that more precise information concerning elastic properties be made available. Unlike steel, titanium can exhibit considerable differences in Young's modulus and Poisson's ratio, depending upon alloying, heat treating, mill product shape, and processing history. The problem is further aggravated by the lack of basic information concerning the effects of preferred orientation upon the elastic properties. Probably the most complete study on this subject was reported by Roberts.[44]

Basically, there are two parts to the problem: (1) the anisotropy of the single-crystal properties and (2) the preferred orientation developed in the final polycrystalline mill product. Both of these factors are operative in a product that displays a high degree of anisotropy. It is apparent that if the single crystal is isotropic the final product will be isotropic, no matter what the preferred orientation. It is also true that if the product has a random texture the properties will be isotropic, no matter how anisotropic the single-crystal properties are. The authors of this report have studied the influence of preferred orientation on elastic properties and found wide variations, which indicates that these properties are very sensitive to texture.[66]

THEORETICAL BACKGROUND

The elastic constants, which can be correlated to other physical properties, have been determined for titanium single crystals, and the results of Flowers et al[67,68] are shown in Table 3. The C constants (stiffness) are usually used in ultrasonic work; the S constants (compliances) are used in strain-gage experiments and can be used to describe the variation in elastic properties of titanium.

Using the compliances in Table 3 and Hooke's Law[69,70], it can be shown that when stress is applied to a single crystal of titanium parallel to the basal plane, Young's modulus is:

$$E = 1/S_{11} = 14.5 \times 10^6 \text{ psi}, \qquad (1)$$

and when stress is applied perpendicular to the basal plane, Young's modulus is:

$$E = 1/S_{33} = 21.0 \times 10^6 \text{ psi}. \qquad (2)$$

TABLE 3. ELASTIC CONSTANTS OF HCP TITANIUM SINGLE CRYSTALS

Elastic Stiffness, 10^6 lb/sq in.		Elastic Compliances, 10^{-7} sq in./lb	
Constant	Value	Constant	Value
C_{11}	22.33	S_{11}	0.688
C_{12}	12.47	S_{12}	-0.325
C_{13}	9.74	S_{13}	-0.133
C_{33}	26.54	S_{33}	0.476
C_{44}	6.71	S_{44}	1.475

and when stress is applied perpendicular to the basal plane, Young's modulus is:

$$E = 1/S_{33} = 21.0 \times 10^6 \text{ psi.} \quad (2)$$

Furthermore, Young's modulus is symmetrical about the c axis, and its variation can be described by an equation which is a function of γ, the angle between the stress axis and the c axis. This equation is as follows[69]:

$$1/E = S_{11}(1-\cos^2\gamma)^2 + S_{33}\cos^4\gamma + (2S_{13} + S_{44})(\cos^2\gamma)(1-\cos^2\gamma). \quad (3)$$

A plot of the above equation for titanium, based on the constants determined by Flowers et al[66], is illustrated in Figure 17 which shows how Young's modulus for single crystals varies with testing orientation.

The next step is to translate these single-crystal properties to polycrystalline behavior. Alers and Liu[71] have examined the various methods and assumptions which are available to calculate Young's modulus for a polycrystalline sheet. Liu and Alers[72] have used these calculations to study the texture transition in Cu-Zn alloy sheet. These investigators concluded that, for the cubic case, one could not accurately calculate absolute values of Young's modulus; however, the variation of Young's modulus with testing direction could be determined.

Of the several models discussed, two are worth consideration[71,72]. One model assumes that all the grains within a polycrystalline aggregate are stressed uniformly; the other assumes that the strain is uniform. Neither case is completely valid, for there must be a discontinuity in stress and strain at or near the grain boundary of adjacent grains that have different orientations. However, the error from this source would probably decrease as an intense texture develops because of the smaller misorientation of adjacent grains. A very strong textured polycrystalline aggregate would probably behave much like a single crystal. The disagreement in the values calculated by the constant-stress or constant-strain model is reduced as the texture becomes more intense. As Liu and Alers[72] point out, the constant-stress model is more convenient to work with and in fact reduces to the equations commonly employed for single crystals.[69]

To employ Equation (3) it is necessary to express the orientation of the polycrystalline texture in terms of the specimen axis. This can be done by utilizing Matrices I and II where α is the angle between the rolling direction and the specimen axis and θ is the angle between the basal pole and the sheet normal.*

MATRIX I

	X	Y	Z
X′	$\cos\theta \sin\alpha$	$\cos\alpha$	$\sin\theta \sin\alpha$
Y′	$\cos\theta \cos\alpha$	$-\sin\alpha$	$\sin\theta \cos\alpha$
Z′	$-\sin\theta$	0	$\cos\theta$

and in contracted form:

MATRIX II

	X	Y	Z
X′	ℓ_1	m_1	n_1
Y′	ℓ_2	m_2	n_2
Z′	ℓ_3	m_3	n_3

where X′ is the tensile axis, Y′ is the transverse tensile direction, and Z′ is the sheet normal, and X, Y, and Z are coordinates of the texture where Z coincides with the maximum intensity of the basal poles or the C direction of a single crystal. Transforming Equation (3) by using the above contracted matrix, we find that:

$$1/E = S_{11}' = S_{33} + (1-n_1^2)(S_{11} - S_{33}) - n_1^2(1-n_1^2)(S_{11} + S_{33} - 2S_{13} - S_{44}). \quad (4)$$

Another elastic property that can be anisotropic is Poisson's ratio. The general definition of Poisson's ratio (μ) is the ratio of the contraction strain to the extension strain, at right angles and in the direction of the applied stress, respectively. The solution for the variation of extension strain as a function of orientation is given by Equation (4). To find Poisson's ratio, the variation of contraction strains with orientation is needed. Martin[73], using tensor analysis, has solved the general hexagonal case for sheet specimens cut at various angles from the rolling direction. His results are as follows:

$$\mu = -\frac{S_{12}'}{S_{11}'} \quad (5)$$

$$\mu = -\frac{S_{13} + n_3^2(S_{12} - S_{13}) + n_1^2 n_2^2 (S_{11} + S_{33} - 2S_{13} - S_{44})}{S_{33} + (1-n_1^2)(S_{11} - S_{33}) - n_1^2(1-n_1^2)(S_{11} + S_{33} - 2S_{13} - S_{44})}.$$

*For most titanium textures, the maximum intensity of the basal pole usually lies in the plane which contains sheet normal and transverse direction.

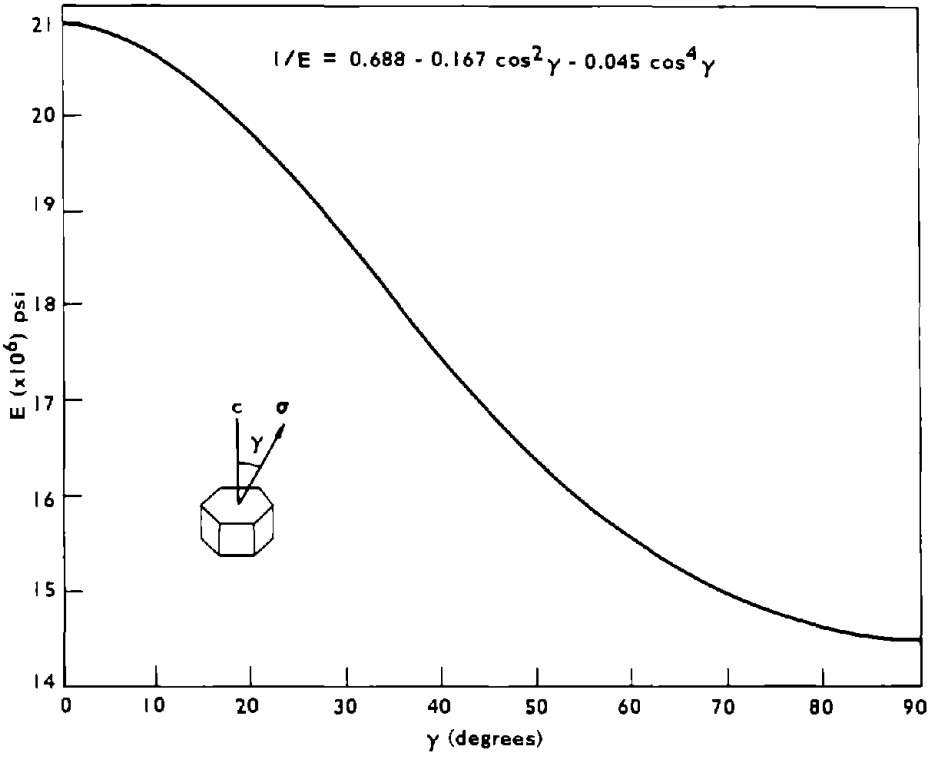

FIGURE 17. VARIATION OF YOUNG'S MODULUS (E) IN TITANIUM SINGLE CRYSTALS WITH THE DECLINATION ANGLE (γ)[66]

Equation (5) is illustrated in Figure 18 for various angles of α and θ employing the constants determined by Flowers, et al.[67] This equation also has the identical direction cosines as shown in Matrices I and II. It is interesting to study this figure for the boundary values. Examination of these curves reveals the large variation in Poisson's ratio in single crystals. When the stress axis is parallel to the basal plane, and the contraction strains are measured at right angles in the prism plane, Poisson's ratio will be approximately 0.20. On the other hand, if both strains are measured in the basal plane, Poisson's ratio will be about 0.47. Consequently, a variation in Poisson's ratio of more than two to one is possible.

In the case of certain highly alloyed compositions, titanium can exist in a body-centered cubic form. Under these conditions it becomes necessary to apply Hooke's law for the cubic crystal where only three compliances or three stiffness constants are employed. The variation of Young's modulus with crystal orientation can then be described by[69,70,74]

$$1/E = S_{11} - 2\,(S_{11} - S_{12} - 1/2S_{44})\,(\ell_1^2 m_1^2 + m_1^2 n_1^2 + \ell_1^2 n_1^2), \quad (6)$$

where ℓ_1, m_1, and n_1 are the direction cosines of the angles between the tensile axis and three edges of the unit cell as previously defined by Matrices I and II. Alternatively, ℓ_1, m_1, and n_1 would be the direction cosines of a polycrystalline material which has a strong simple texture and could be represented as a single crystal.

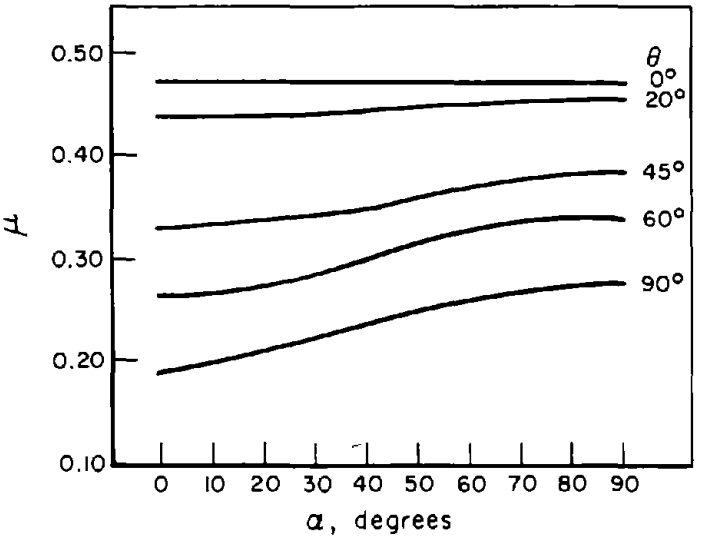

FIGURE 18. THEORETICAL POISSON'S RATIO (μ) AS A FUNCTION OF SPECIMEN ORIENTATION (α) WITH VARYING ANGLES OF (θ) IN TITANIUM[79]

Similarly, the equation for Poisson's ratio for the cubic crystal can be described as

$$\mu = -\frac{S_{12} + (S_{11} - S_{12} - 1/2S_{44})(\ell_1^2\ell_2^2 + m_1^2m_2^2 + n_1^2n_2^2)}{S_{11} - 2(S_{11} - S_{12} - 1/2S_{44})(\ell_1^2m_1^2 + m_1^2n_1^2 + \ell_1^2n_1^2)} \quad (7)$$

Unfortunately, the values of S_{11}, S_{12}, and S_{44} are not known for body-centered cubic titanium. However, it is demonstrated later how it is possible to use the foregoing to deduce the elastic constants from a strongly textured polycrystalline material with a known preferred orientation which can be represented as a single crystal.

Actual Titanium Elastic Anisotropy

Figure 19(a, b, and c) illustrates the (0002) pole figure for alpha-type and two extreme alpha-plus-beta-type textures. These textures are characteristic of the extreme of alpha-deformation textures which are commonly found in titanium sheet alloys.

Figure 19 illustrates the (2000) pole figure for the only body-centered cubic titanium alloy reported here. This is a {100}⟨110⟩ type of texture and is characteristic of body-centered cubic metals which have been subjected to heavy cold deformation. This type of texture is common in several beta-stabilized titanium alloys.

Typical sheet tension-strain-gage results for Young's modulus and Poisson's ratio are illustrated in Figures 20 and 21. The data are presented along with solid lines derived from the constant-stress model previously discussed. No calculated curve is drawn on the Ti-4Al-3Mo-1V alloy test results for it has been established that the alloying elements in this material significantly changed the elastic constants.[15] For the hexagonal phase materials, Figures 20 and 21 (a, b, and c), Young's modulus was calculated from Equation (4) and Poisson's ratio from Equation (5). In order to utilize Equations (4) and (5), a value for the angle θ must be established. This angle was determined by using a value of Young's

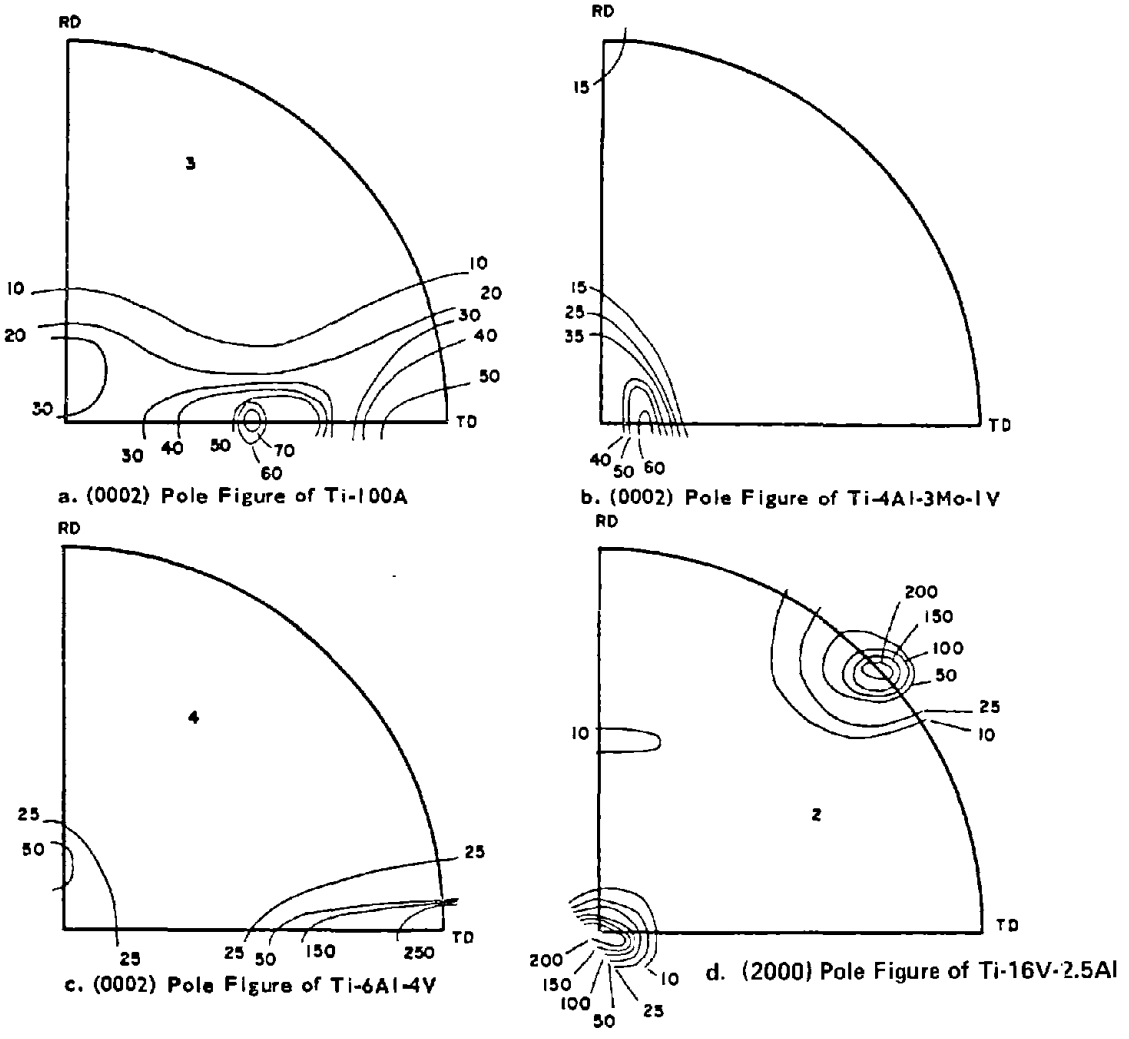

FIGURE 19. POLE FIGURES OF TITANIUM SHEET ALLOYS

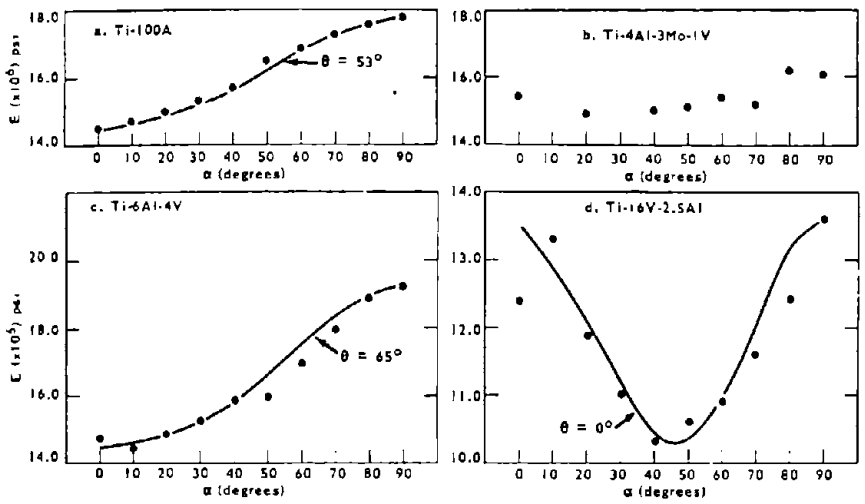

FIGURE 20. ACTUAL AND CALCULATED VARIATIONS OF YOUNG'S MODULUS E AS A FUNCTION OF SPECIMEN ORIENTATION α

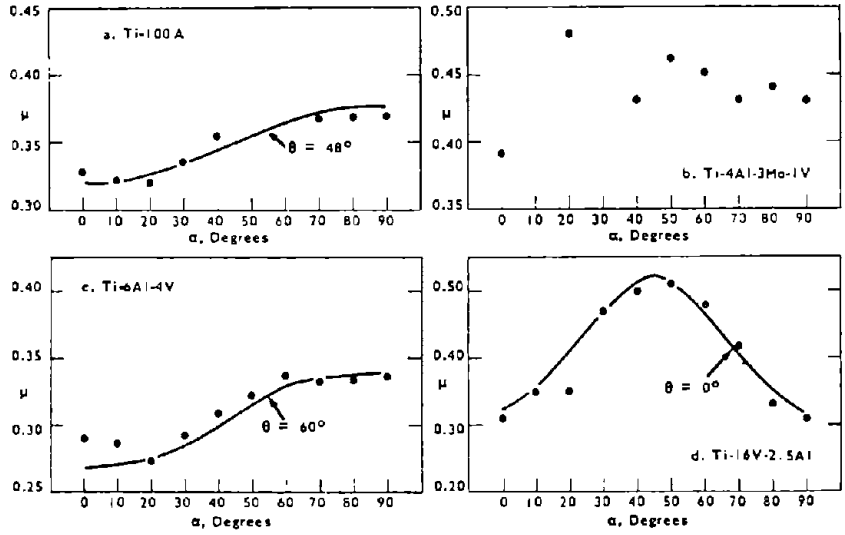

FIGURE 21. ACTUAL AND CALCULATED VARIATIONS OF POISSON'S RATIO (μ) AS A FUNCTION OF SPECIMEN ORIENTATION α

modulus measured from a transverse test. Figures 20 and 21 show that the test points compare favorably with the curves drawn from data calculated from the constant stress model.

Figures 20d and 21d illustrate the test results for the body-centered cubic metastable beta alloy. Since the compliances or stiffness constants for this body-centered cubic titanium alloy are unknown, it was necessary to deduce them. This was done by utilizing a knowledge of the texture. In this example, the Ti-16V-2.5Al sheet had a very intense {100}⟨110⟩ texture so the procedure was simplified. As a tension specimen cut at an angle of 45 degrees to the rolling direction would have its axis parallel to the [100] direction, by Hooke's law

$$1/E_{45} = S_{11}. \tag{8}$$

Furthermore, since S_{11} is defined as the extension strain parallel to the edge of a unit cell, a measurement of the lateral contraction strain would determine S_{12} because:

$$\mu_{45} = -S_{12}/S_{11}. \tag{9}$$

Finally, S_{44} can be determined by employing a longitudinal specimen since

$$G = 1/S_{44}, \quad (10)$$

where G = shear modulus calculated as follows:

$$G = E/2(1 + \mu). \quad (11)$$

Thus, from the above equations, it is possible to determine experimentally the elastic constants for this body-centered cubic titanium alloy. The resultant values are $S^P{}_{11}{}^* = 0.972$, $S^P{}_{12}{}^* = -0.40$, and $S^P{}_{44}{}^* = 1.8\ 10^{-7}$ sq in./lb. Employing these constants and Equation (6) for Young's modulus and Equation (7) for Poisson's ratio, it is possible to calculate the variation of these properties within the plane of the sheet. Figures 20 and 21 illustrate that calculated data compare favorably with the actual test data. Similar results could be obtained by considering the sheet orthotropic and applying the method described by Pursey and Cox.[74]

Several investigators[64,75,76] have attempted to characterize the texture through the measurement of elastic constants. Other investigators[77,78] have attempted to follow the procedure, outlined above, for calculating or estimating the elastic properties from the single-property data and the pole figure. Neither has met with great success, although the latter can give good results when the pole figure consists of only a simple single-point texture.

Summary

Moderately accurate predictions of elastic anisotropy can be made for polycrystalline aggregates with elementary textures. The constant-stress model is adequate for describing the behavior patterns found in titanium sheet material.

It appears that considerable improvements in values of Young's modulus or Poisson's ratio may be achieved through texture control. This could provide an improved material for critical applications.

EFFECT OF TEXTURE UPON UNIAXIAL MECHANICAL PROPERTIES

Yield Strength

Titanium and titanium alloys[79-81] exhibit anisotropy with regard to their plastic properties. The magnitude of plastic anisotropy in such polycrystalline hexagonal materials is much greater than that found in face-centered and body-centered cubic materials. This is probably due to the fact that the slip directions all lie in the basal plane. The fact that these slip directions are coplanar gives rise to a simplification when analyzing for strains to determine the plastic-flow anisotropy. Yielding has been shown to be governed by the critical resolved shear stress (CRSS) for the case of slip.[69] Thus, it is clear that the orientation is the controlling factor for the stresses that appear on various slip planes. The applied tensile stress for yielding would vary as the reciprocal of the Schmid factor (CRSS) which is the trigonometric resolution of the tensile stress upon the slip plane and in the slip direction. Since the hexagonal crystal major axis of symmetry is the c axis, the yield strength should be primarily sensitive to the angle gamma between the stress axis and the basal pole. Rotation of the crystal around the c axis has only a slight effect for various gamma angles. The yield-strength factors (K_p) for the $\{10\bar{1}0\}\langle 11\bar{2}0\rangle$ and $\{10\bar{1}1\}\langle 11\bar{2}0\rangle$ families are included in Figure 22 which shows the relationship between yield strength and orientation for these families. The yield-strength factors for basal slip are not included because it is not considered a major deformation mechanism, although it is observed in titanium.

The variation of yield strength as a function of orientation when twinning is involved is less clear; however, the observations of Reed-Hill[82] for zirconium probably would apply to titanium also because the c/a ratios are nearly the same. In the case of twinning, both the magnitude and the direction of the stress need be considered. For example both the $\{10\bar{1}2\}$ and $\{11\bar{2}1\}$ type twinning systems form when the tension axis is near the basal pole. On the other hand, the $\{11\bar{2}2\}$ type forms when the tension axis is parallel to the basal plane. Reed-Hill[82] has also shown how the Schmid factors vary for $\{10\bar{1}2\}$ $\{11\bar{2}1\}$ and the $\{11\bar{2}2\}$ twin types for zirconium. These would be nearly the same for titanium, and it is easy to construct the curves for yield-strength factors on the basis of his assumption.

From the foregoing discussion, and the work of Rogers[83], it is evident that the yield strength of a crystal is influenced by both the crystal orientation and the mode by which it deforms. Thus, a polycrystalline material with a very strong texture should also be strongly governed by the same factors.

The variation in the yield strength in strongly textured material is discussed below for several commercial sheets of various alloys. From the known textures of unalloyed titanium sheet, it is apparent that the stress axis for a longitudinal specimen will be 90 degrees from the basal pole. Hence, the critical resolved shear stress will be a maximum for the $\{10\bar{1}0\}\langle 11\bar{2}0\rangle$ family. Thus, K_p for the slip on $\{10\bar{1}0\}$ can be determined from this orientation. As the angle of the specimen is rotated toward the transverse

*S^P denotes that this constant was determined from polycrystalline material.

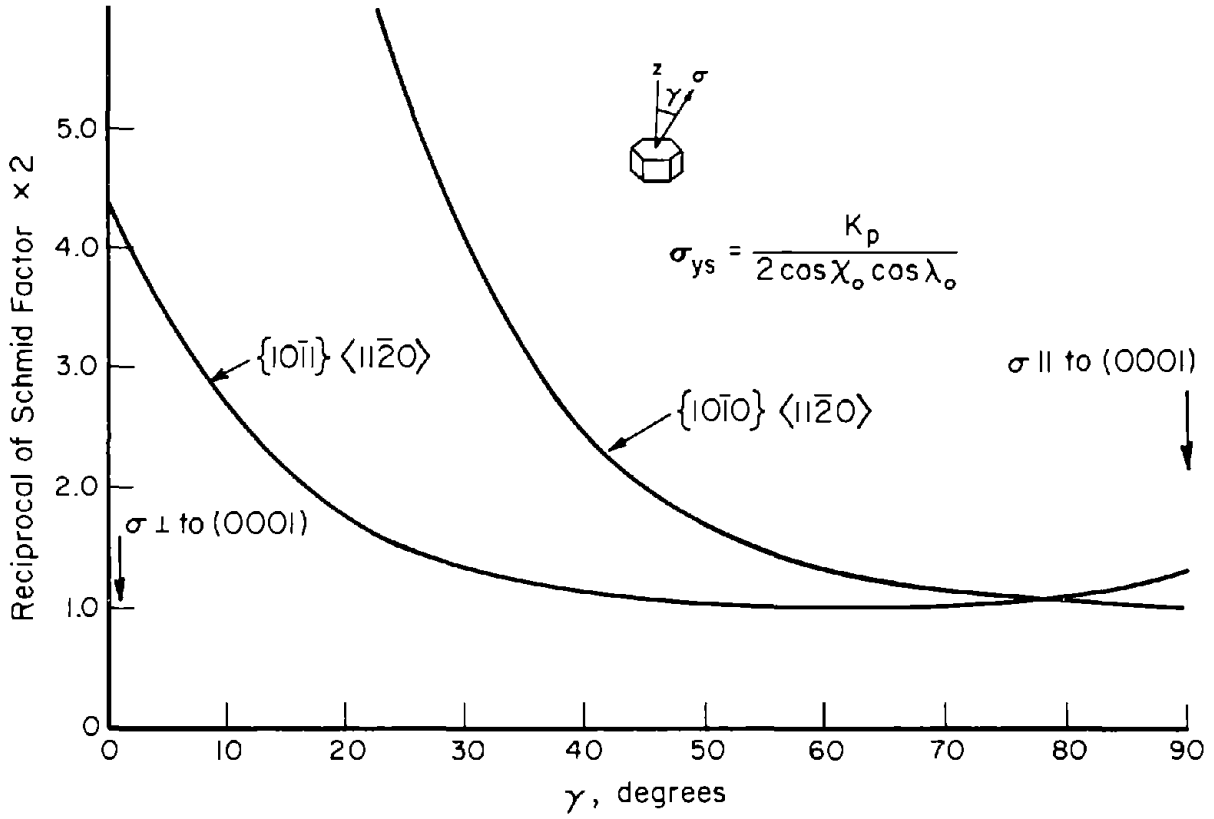

FIGURE 22. VARIATION OF YIELD STRENGTH WITH STRESS-AXIS DECLINATION ANGLE (γ) [79]

direction, gamma will decrease from 90 degrees to some intermediate value, depending upon the texture. As the declination angle, (γ), decreases, relative stresses on the various planes change, and the deformation modes are forced to change also.

As previously mentioned, for textures that have basal pole tilts toward the transverse direction, a longitudinal specimen will deform by slip on the $\{10\bar{1}0\}\langle 11\bar{2}0\rangle$ family. This is because gamma is near 90 degrees and the resolved stress is highest on this plane. With increasing angles of alpha (varying the specimen axis from the rolling direction toward the transverse direction), gamma decreases and the applied stress required to cause yielding by deformation on the $\{10\bar{1}0\}$ planes would increase. With this changing specimen orientation, maximum stress soon shifts from the $\{10\bar{1}0\}$ slip planes to the $\{11\bar{2}2\}$ twin planes and hence the mode of deformation changes. Similarly, the maximum stress shifts from the $\{11\bar{2}2\}$ twin planes to the $\{10\bar{1}1\}$ slip planes with increasing alpha and so on. Thus, it is clear that the measured yield strength of a strongly textured material should be dependent upon texture orientation and the relative yield strengths for various modes of deformation (see Figure 23). It is evident that when the texture is known, certain specific specimen orientations can be employed to determine the critical stresses for deformation by that mode. It has been known for a long time that the critical stresses for deformation by various modes are sensitive to factors such as grain size, alloying, temperature, strain rate, and many others.

Figure 24(a through m) shows typical textures and Figure 25(a through m) shows resulting yield-strength variation. For the alpha-deformation type, the variation will be small when the basal poles are near the sheet normal and large when they are near the transverse direction. An example of this large variation is shown in Figure 25(a and m).

For the other two texture types, the variation of yield strength with specimen orientation is small. In some cases, the value of yield strength is somewhat less in the region of specimen orientations around 45 degrees with high yield strength appearing in the rolling and transverse directions. Figures 25 i and l illustrates this.

Tensile Strength

The variation of tensile strength with specimen orientation is dependent upon two major factors. The first is the yield strength and the second is strain hardening. Strain hardening increases the range between the yield and tensile strengths. Materials at equivalent yield strengths

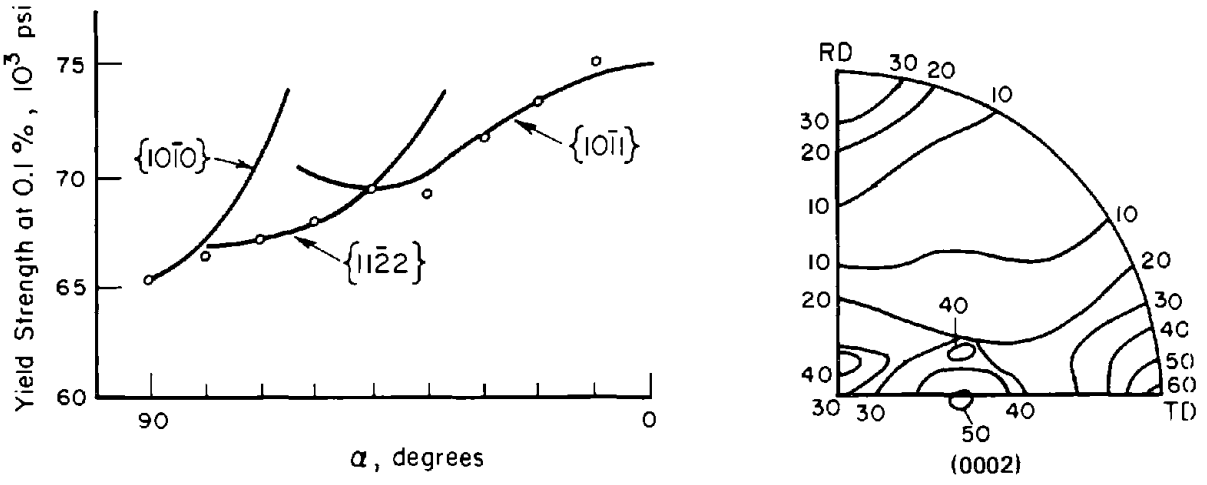

FIGURE 23. TEXTURE AND COMPARISON OF THEORETICAL CURVE AND ACTUAL TEST VARIATION OF YIELD STRENGTHS AS A FUNCTION OF SPECIMEN ORIENTATION (α) [79]

Note: α = angle between rolling direction and specimen axis

but different strain hardening will have various tensile strengths. It has been reported [69] that the twinning mode of deformation produces little or no strain hardening conversely to the slip mode. Thus, a specimen that deforms primarily by twinning will have a lower tensile-to-yield strength ratio than one that deforms by slip.

Figure 26 portrays typical data for a series of test specimens from sheet at various angles, alpha. For angles of alpha around 45 degrees, there is a minimum, and the tensile strength increases on either side of this. This behavior pattern is generally what would be expected since, from the yield-strength analysis, the {11$\bar{2}$2} twin mode would be operative at intermediate angles of alpha. As alpha increases or decreases, it can be seen that the {10$\bar{1}$0} or the {10$\bar{1}$1} slip mode would predominate. At large deformations in the loading region approaching the ultimate tensile strength, the deformation modes would probably be quite complex. Figure 27, which shows the tensile-yield strength ratio for this case, illustrates these points more clearly.

Since both yield strength and the rate of strain hardening can vary with specimen orientation, a complicated pattern can easily develop, as shown in Figure 28. An analysis of these curves reveals that except for the case where the basal poles are near the sheet normal [Figures 28(j and k)], which we cannot explain, the curves follow two types: an alpha type and a beta type. The alpha-phase type included both the alpha-deformation texture and the alpha-transformed-beta-deformation type. The primary feature of these curves is a low value of tensile strength at specimen orientation around 40 to 50 degrees, a high value in the rolling direction, and sometimes higher value in the transverse direction.

The beta-phase type [Figure 28(d and e)] shows a high at 40 to 50 degrees and a low in the rolling and transverse directions.

Plastic Strain Ratios

One of the important properties of anisotropic materials is the difference in plastic straining in different directions. These variations in plastic flow for different orientations quite frequently give rise to "ears" in deep-drawing operations. This plastic flow anisotropy may also reveal itself in many ways in other metal-forming operations. It has been shown that the deep drawability is quite sensitive to the normal anisotropy for sheet materials. [84,85] The normal anisotropy R is usually defined for sheet specimens as follows:

$$R = \frac{\epsilon_w}{\epsilon_t}, \qquad (12)$$

where ϵ_w is the width strain measured in a tension test and ϵ_t is the thickness strain.

Because the volume at constant stress does not change during plastic strains, various strain ratios can be used to define the plastic-flow anisotropy and they are interrelated. During the course of one investigation, it was found that greater precision could be obtained by using strain gages oriented at 90 degrees and bonded to the face of the specimens. Under these test conditions, the width and longitudinal strains are measured, and it is convenient to

Ti-6Al-4V

a. Heat M2803
0.033" thick

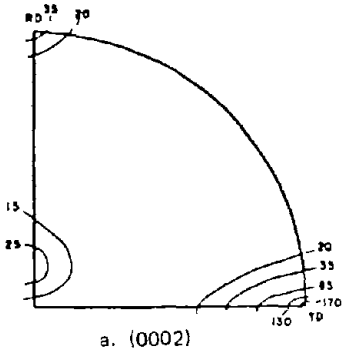

a. (0002)

b. Heat M7199

c. Heat B22075

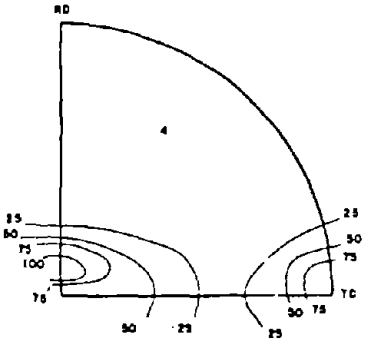

b. (0002)

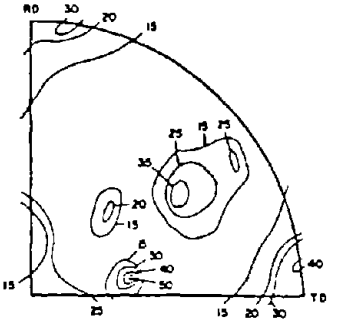

c. (0002)

Ti-16V-2.5Al

d. Heat B22117

e. Heat 24990

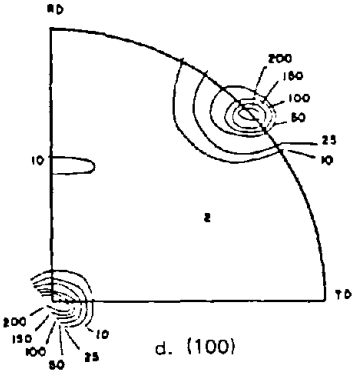

d. (100)

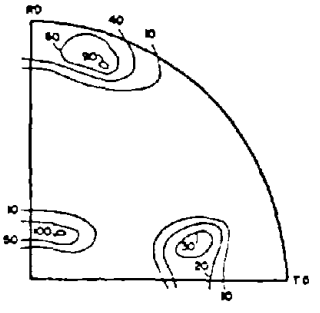

e. (110)

f. Heat M23346

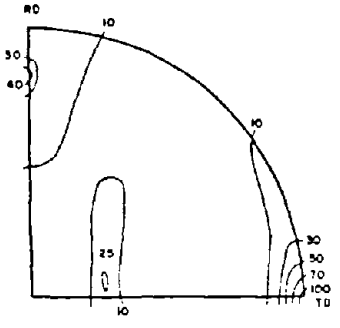

f. (0002)

FIGURE 24. POLE FIGURES OF VARIOUS TITANIUM ALLOYS[81]

RC130A

g. Heat 3442

j. Heat 5221-16

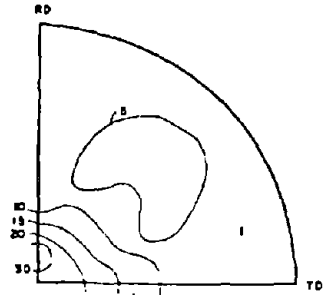

g. (0002)

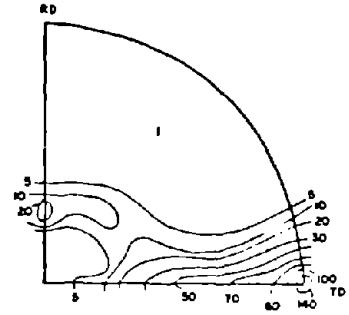

h. (0002)

Ti-6Al-6V-2Sn

i. Heat H

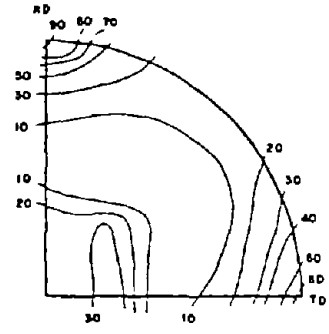

i. (0002)

Ti-4Al-3Mo-1V

j. Heat X70006

k. Heat M8173

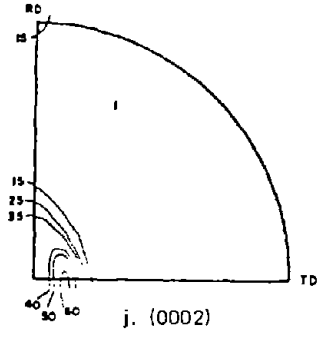

j. (0002)

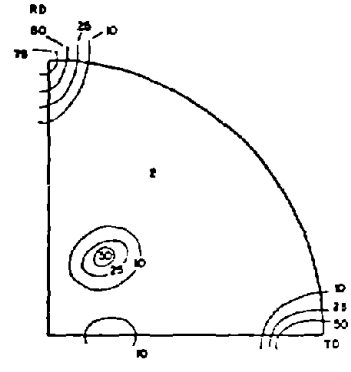

k. (0002)

l. Ti-8Al-1Mo-1V
Heat V1848

m. RC130B
Heat B3263-B1

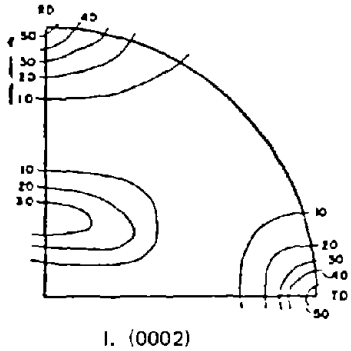

l. (0002)

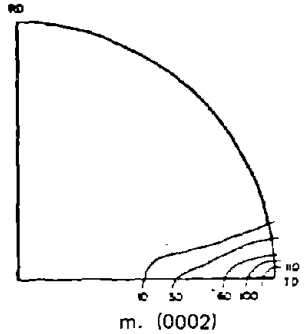

m. (0002)

FIGURE 24. Continued

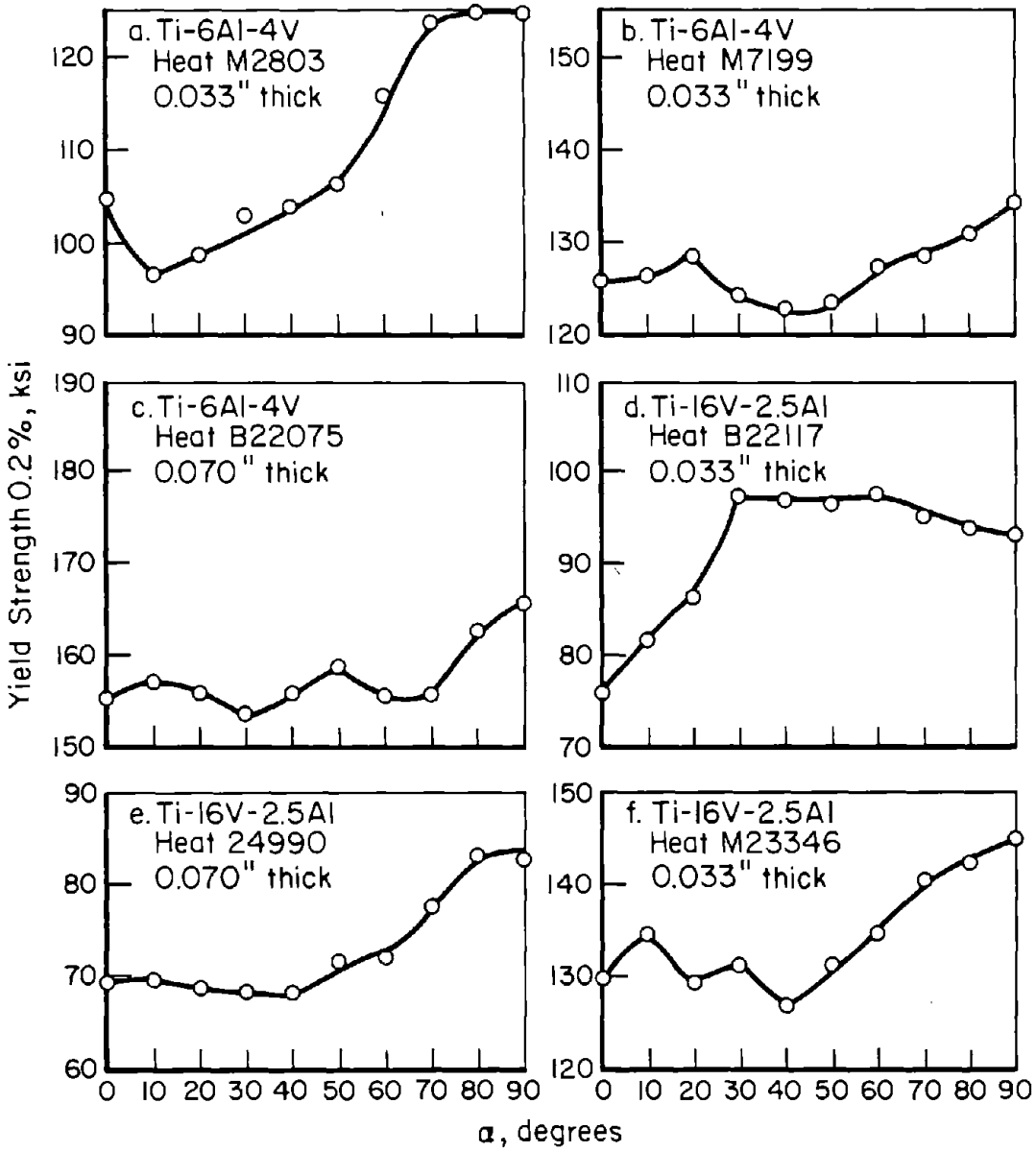

FIGURE 25. VARIATION OF YIELD STRENGTH WITH SPECIMEN ORIENTATION (α) [81]

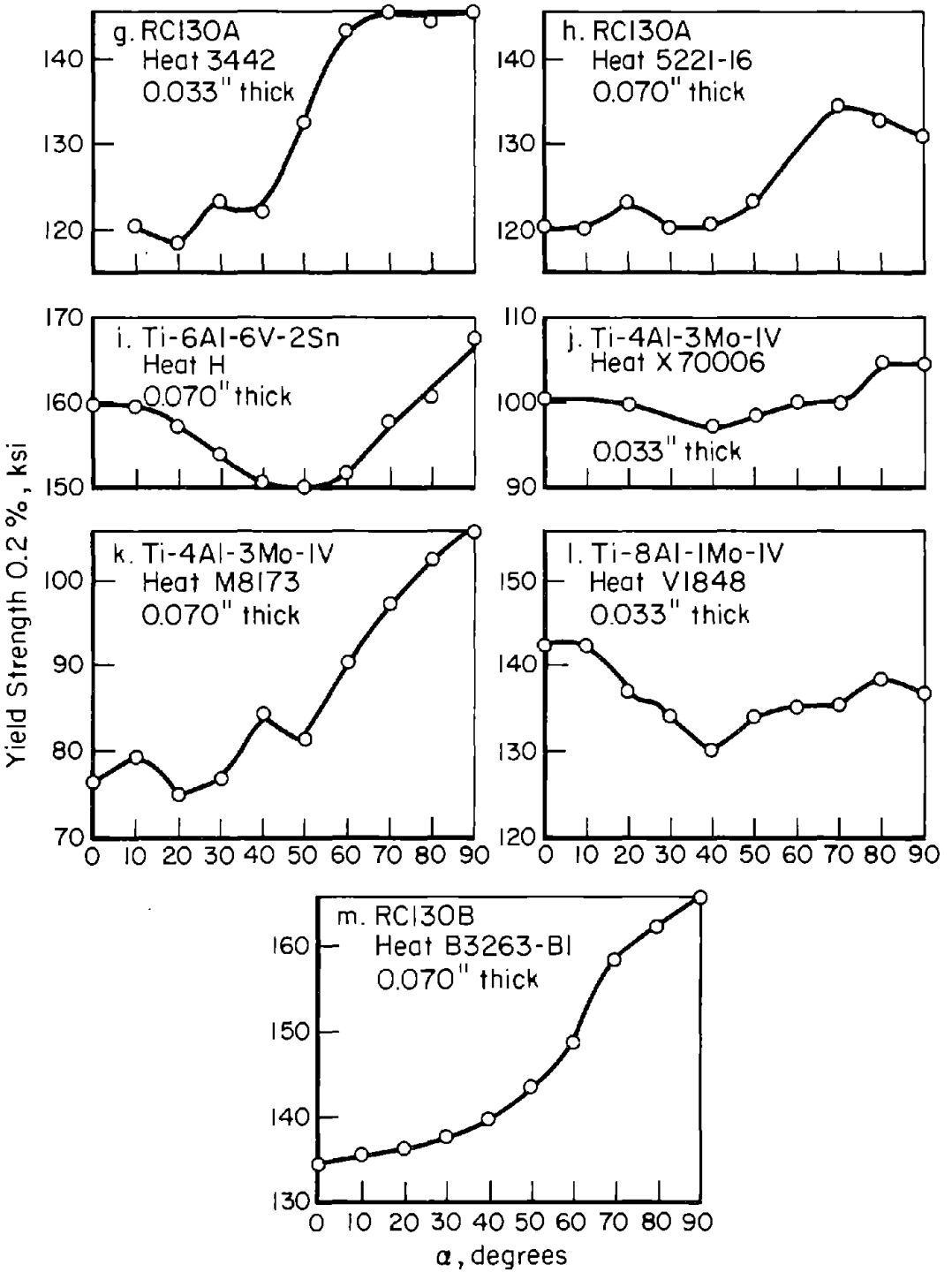

FIGURE 25. Continued

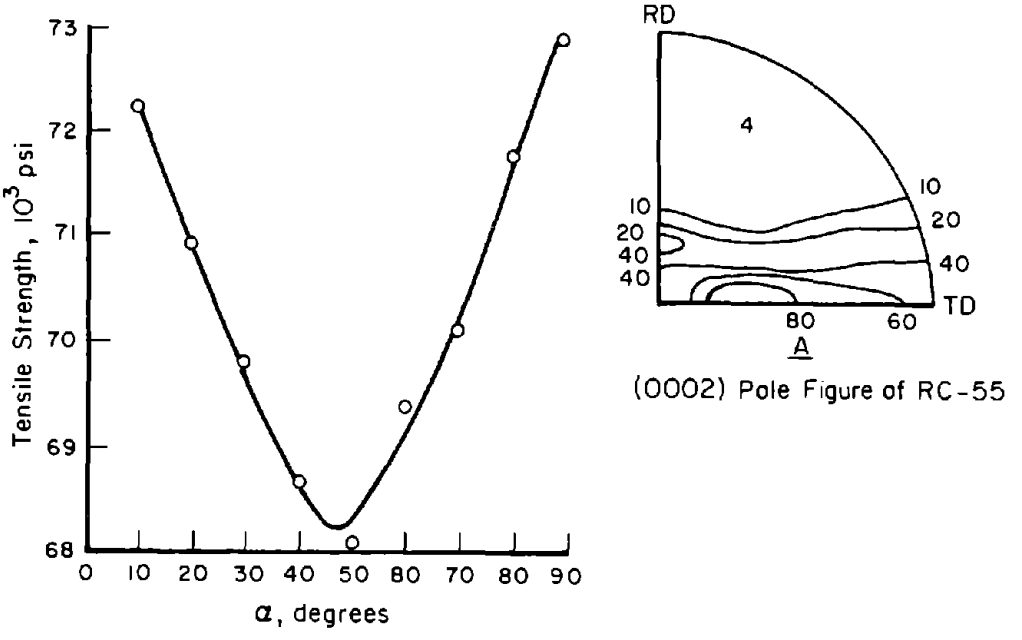

FIGURE 26. TEXTURE AND VARIATION OF TENSILE STRENGTH AS A FUNCTION OF SPECIMEN ORIENTATION (α) IN UNALLOYED TITANIUM[79]

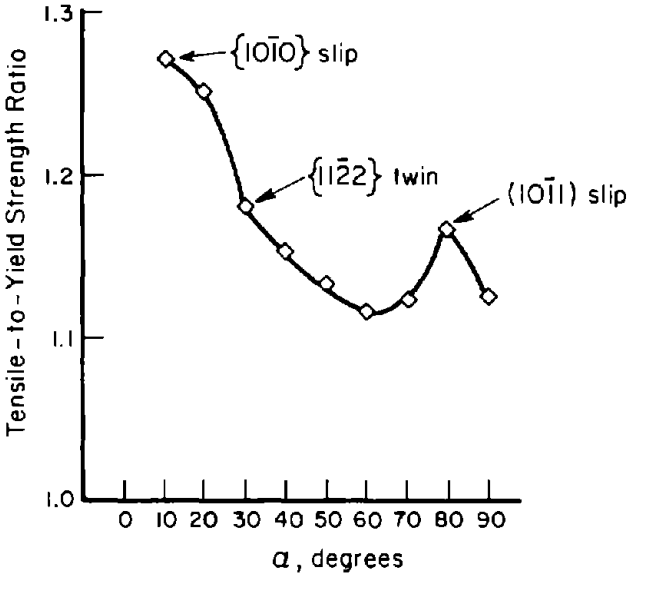

FIGURE 27. VARIATION OF TENSILE-TO-YIELD STRENGTH RATIO AS A FUNCTION OF SPECIMEN ORIENTATION (α) IN UNALLOYED TITANIUM[79]

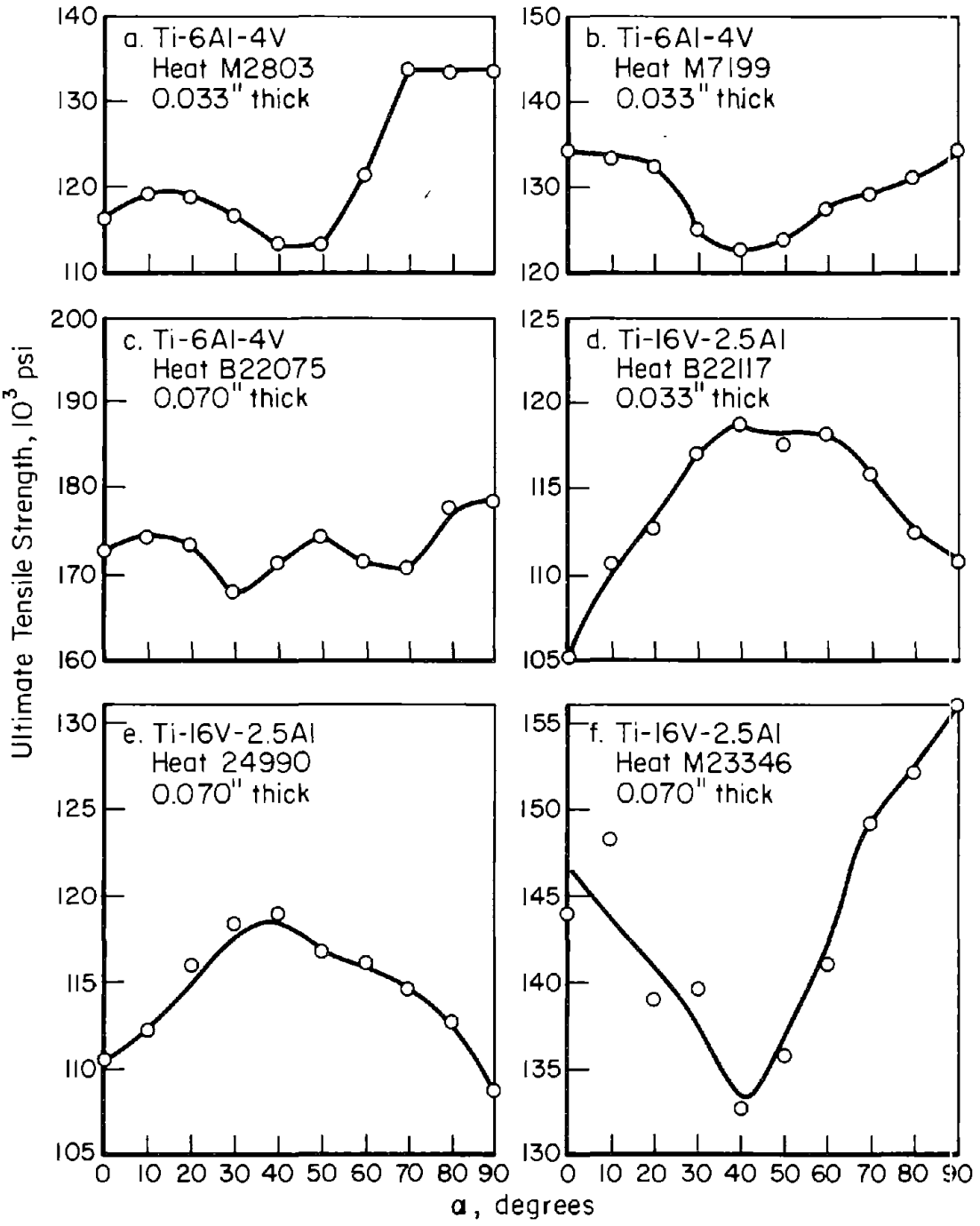

FIGURE 28. VARIATION OF TENSILE STRENGTH WITH SPECIMEN ORIENTATION (α)

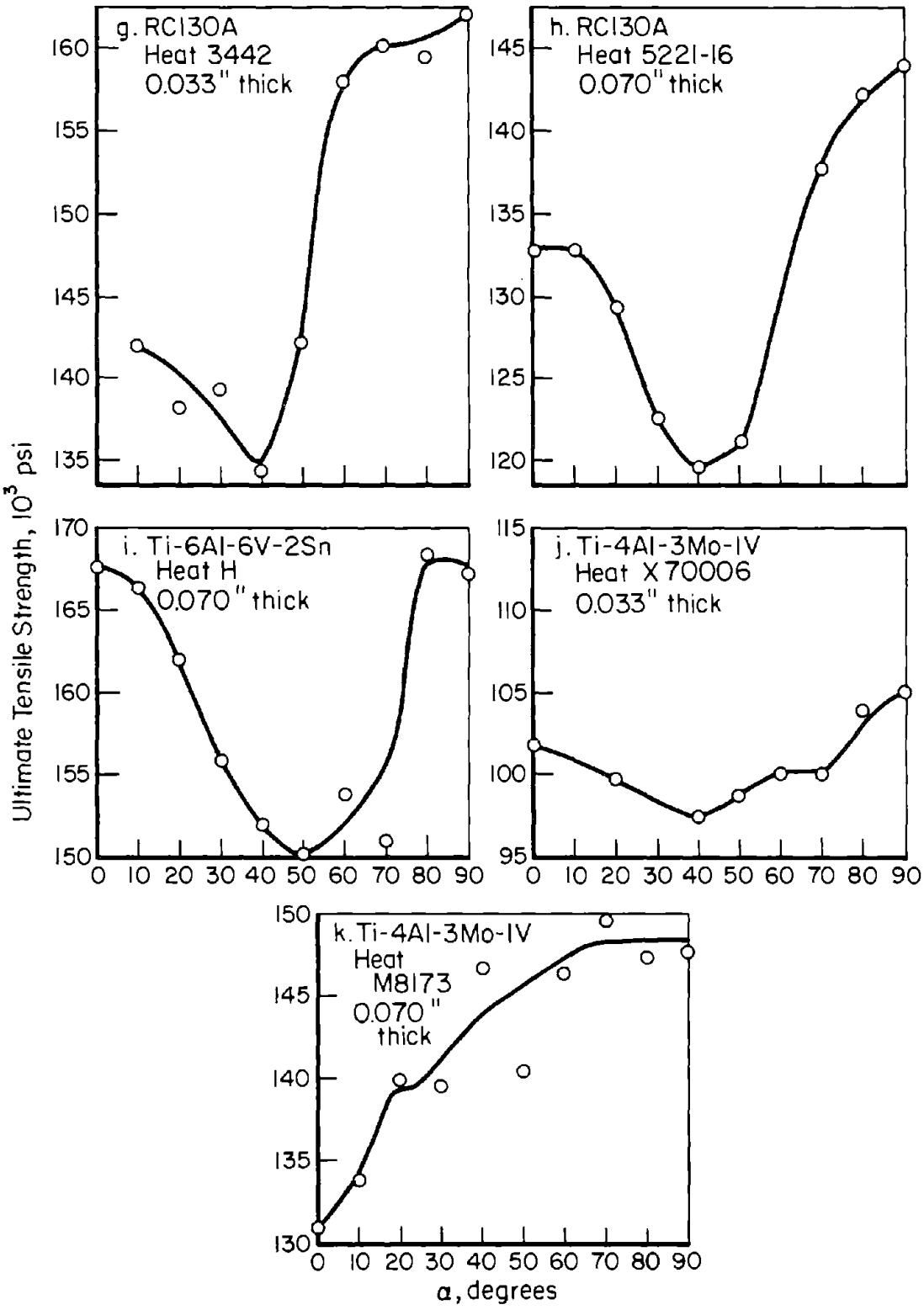

FIGURE 28. Continued

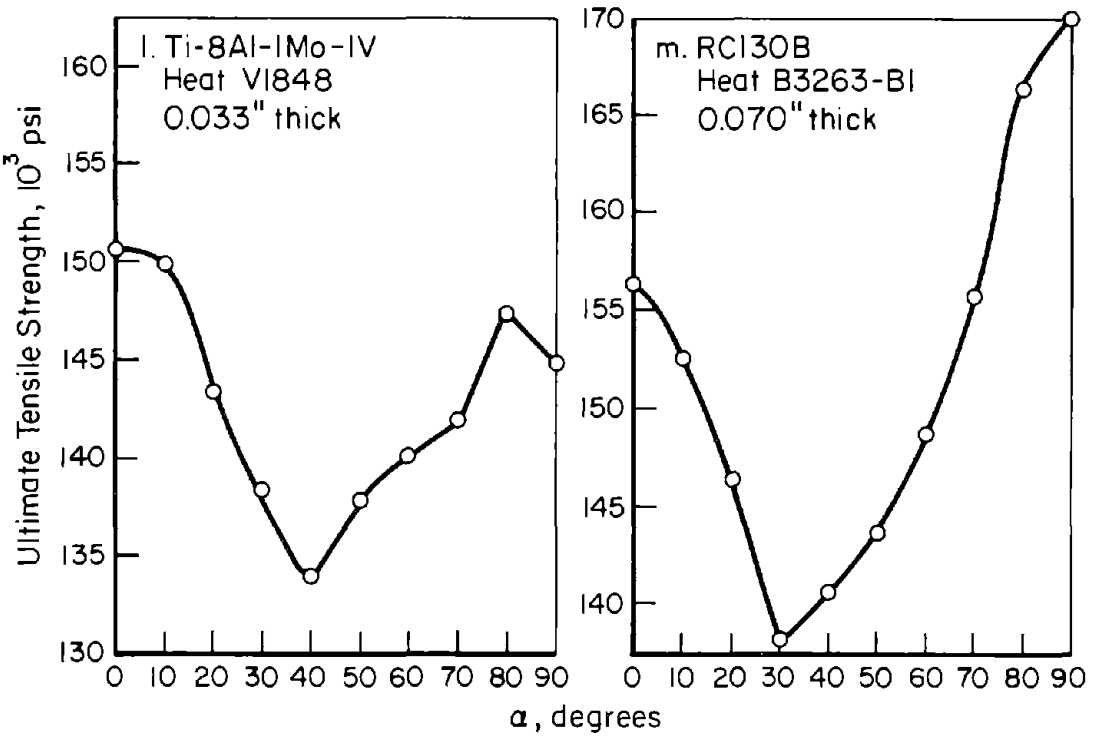

FIGURE 28. Continued

represent the anisotropy as a ratio of these strains as follows:

$$\mu_p = \frac{\epsilon_w}{\epsilon_t} \qquad (13)$$

and

$$R = \frac{\mu_p}{1-\mu_p} \quad .$$

Since the anisotropy is related to the deformation mechanisms and texture, it should be possible to predict the texture from the measure values of R or μ_p. Utilizing the direction cosines and assuming ϵ_z equals zero, it can be shown for a longitudinal test that

$$\mu_p = -\cos^2\theta \quad . \qquad (14a)$$

Thus, a test in the longitudinal direction in the normal titanium sheet texture should measure the average basal-pole tilt and should be quite sensitive, due to the range of values from zero to one. The strain ratios would also be dependent upon specimen orientation and for the case outlined above, that is, ϵ_z equal to zero, the variation of μ_p would depend upon alpha as follows:

$$\mu_p = \frac{\cos^2\theta \cos^2\alpha + \sin^2\alpha}{\cos^2\theta \sin^2\alpha + \sin^2\alpha} \quad . \qquad (14b)$$

Figure 29 illustrates this equation. It predicts that when a specimen is tested for alpha angle of 45 degrees, μ_p will be equal to one and independent of theta. This is because the resolution of the ratio of strains is independent of the orientation of this type of texture. As the stress axis moves away from lying in the basal plane toward the basal normal, the possibility of a deformation mode which will produce a strain component in the Z direction increases. It has previously been shown in the case of yield strengths that for only slight increases in alpha (20 degrees), the deformation mode changed from $\{10\bar{1}0\}\langle 11\bar{2}0\rangle$ slip to $\{11\bar{2}2\}$ twinning. This twinning mode has a ϵ_z strain component, and it is difficult to assess the amount. In order to develop a more complete picture, it is necessary to solve the general case.

Poisson's Ratio

Figure 30 portrays the variation in μ_p as a function of alpha. The experimental data are compared with the theory when a value of 45 degrees is chosen for theta. The experimental data fit the theoretical curve fairly well up to an angle of 30 degrees for alpha, and then diverge. The divergence is probably due to the increasing ϵ_z strain with increasing alpha. The probability of larger ϵ_z strain as the stress axis moves out of the basal plane toward the c axis or Z direction obviously increases. Thus, the strain-ratio behavior pattern is not expected.

Of all the mechanical properties, the ratio of plastic strains is probably more sensitive to texture than the others studied. This is clearly evident from the large variations shown in Figure 31. As pointed out

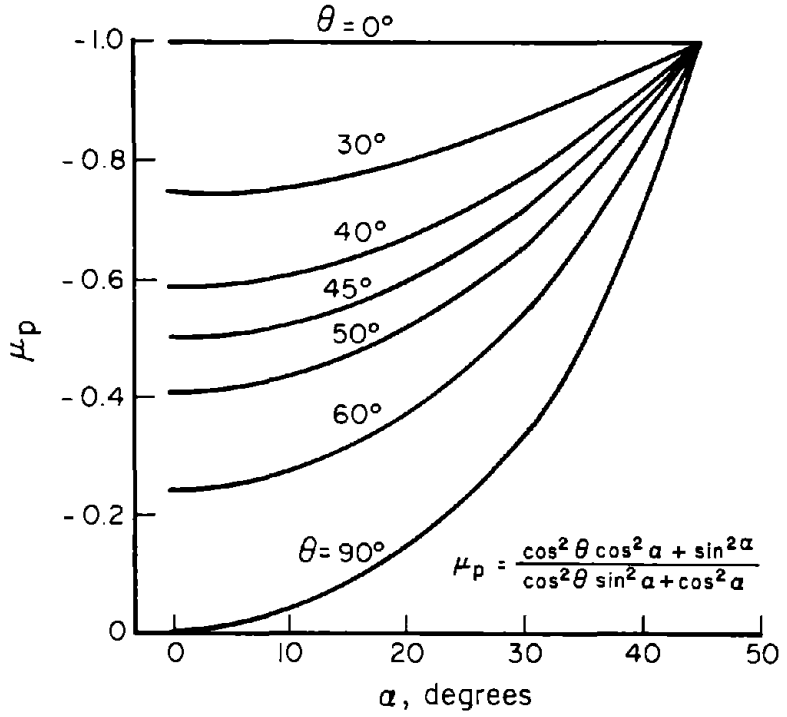

FIGURE 29. VARIATION OF PLASTIC STRAIN RATIO (μ_p) AS A FUNCTION OF SPECIMEN ORIENTATION (α) FOR VARIOUS CONSTANT BASAL PLANE TILTS (θ DEGREES)[79]

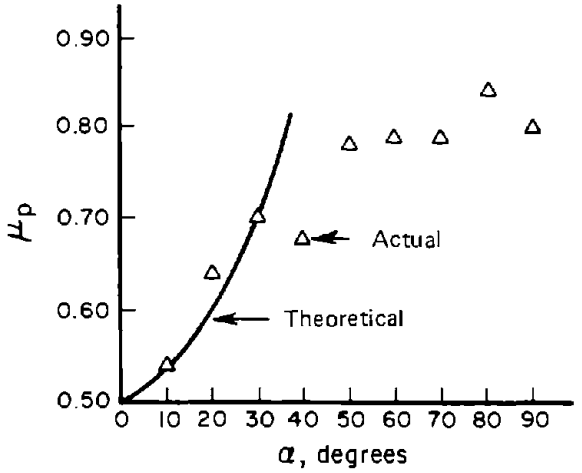

FIGURE 30. COMPARISON OF THEORETICAL AND ACTUAL PLASTIC STRAIN RATIOS (μ_p) AS A FUNCTION OF SPECIMEN ORIENTATION (α)[79]

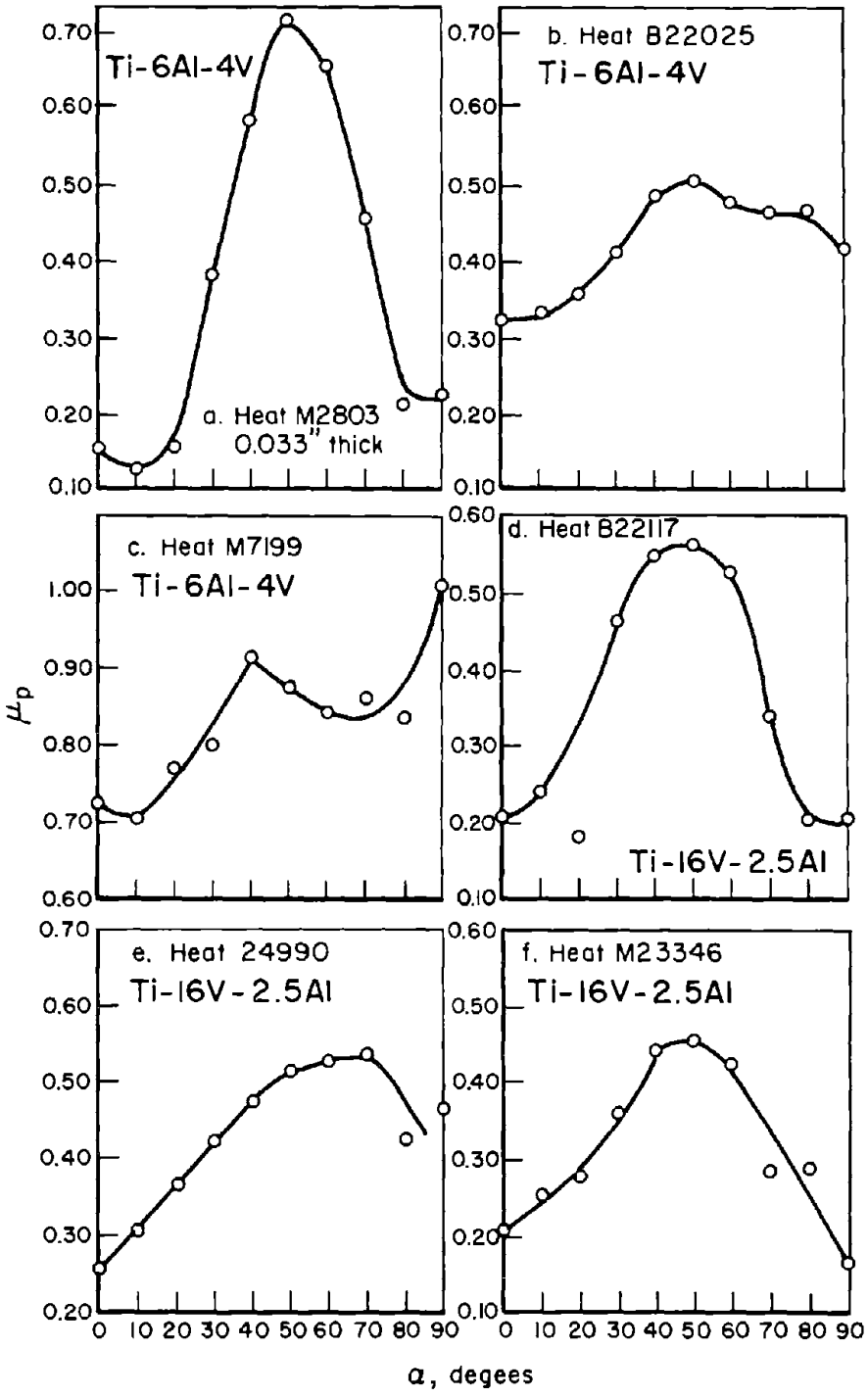

FIGURE 31. VARIATION OF POISSON'S RATIO IN THE PLASTIC ZONE (μ_p) WITH SPECIMEN ORIENTATION (α)

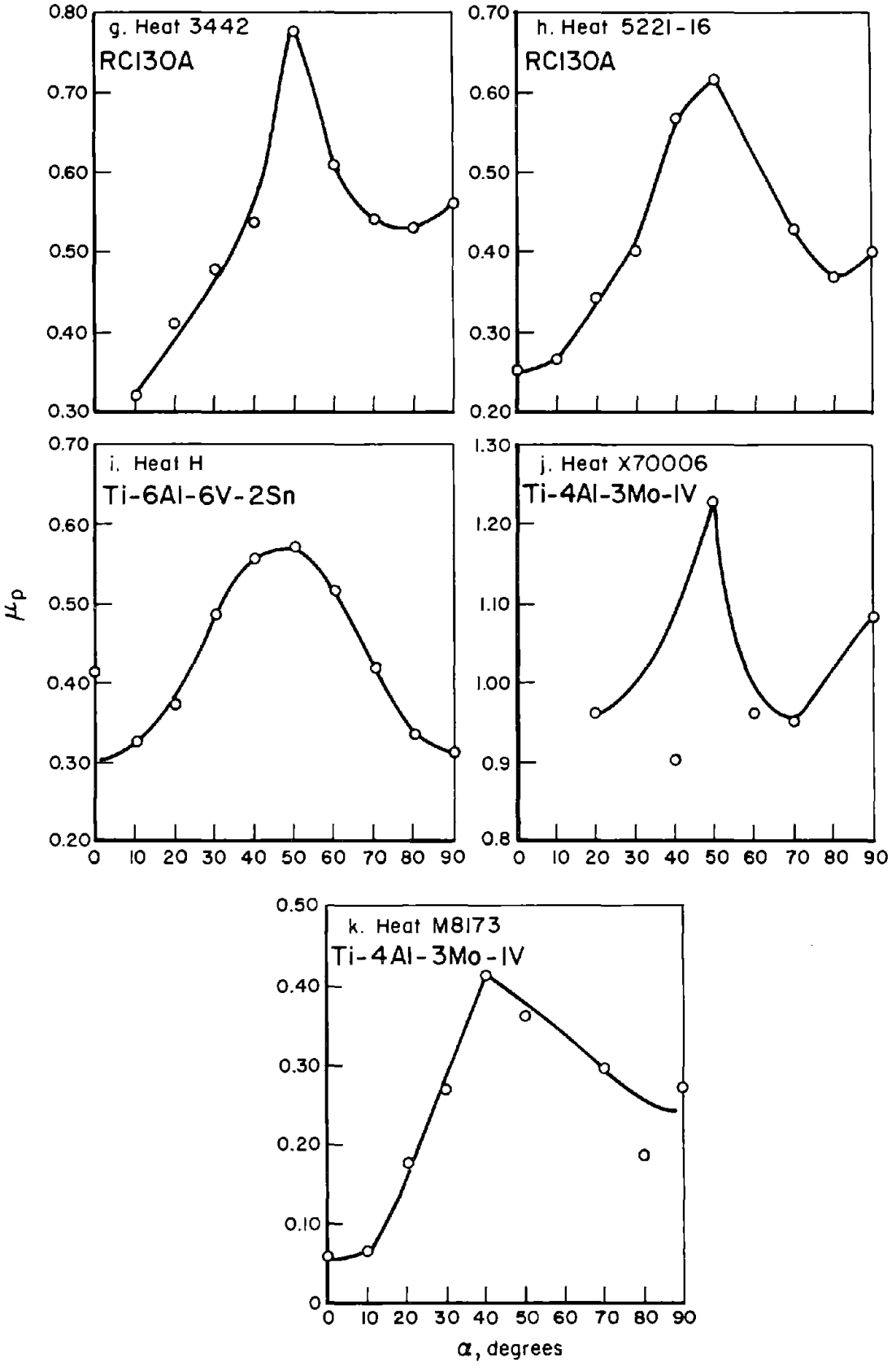

FIGURE 31. Continued

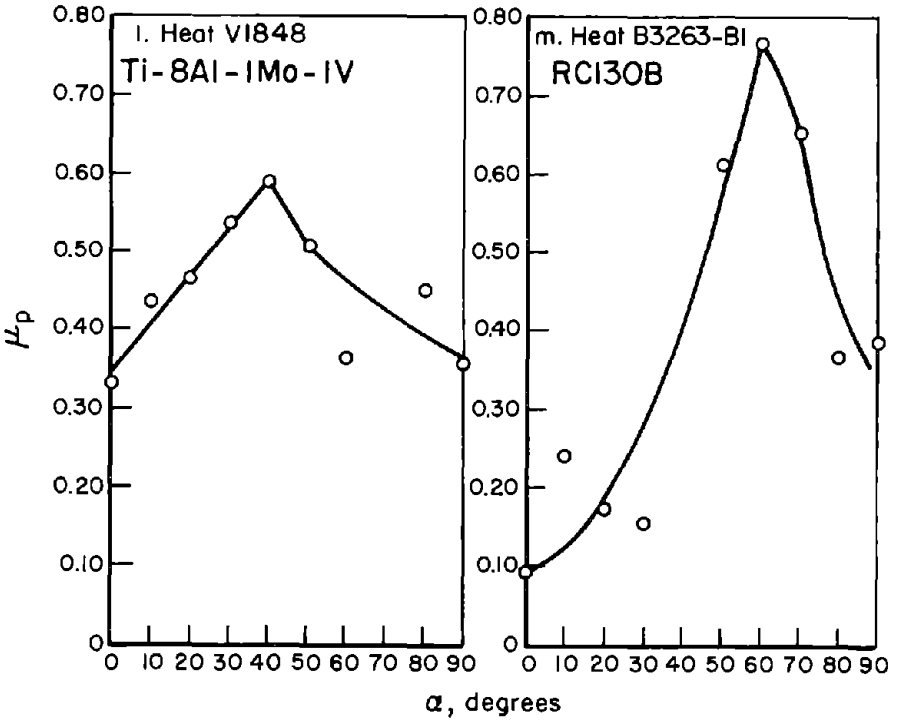

FIGURE 31. Continued

previously [15], the values of Poisson's plastic strain ratios are related through constancy of volume to the more commonly used value, the strain ratio R. R is very important because it defines the biaxial yield locus as is discussed in the next section. It is difficult to describe the pattern displayed by this data. It appears, however, that the lowest value of R or μ_p is in the rolling direction and, as the specimen orientation moves to the transverse direction, the value increases to a maximum at 40 to 50 degrees and then decreases. The value for the transverse test, in general, is somewhat higher than that for the rolling direction. It seems the alpha-deformation-type texture produces the largest spread in values when the basal poles are tilted farthest toward the transverse direction.

Compression Yield Strength

It has been shown that tensile properties are anisotropic in nature, and the compression properties can also be anisotropic. Compressive elastic properties, Young's modulus, and Poisson's ratio are equivalent to the tension values because the sign of the stress does not matter. Nor does the sign of the stress matter in the case of plastic flow by slip. However, when twinning is involved, the twin mode is dependent upon the direction of the stress. Thus, for certain types of textures, the tension and compression yield strengths are not equivalent. A striking example of this, (Table 4) is seen if an intense TD texture is tested for yield strength in tension and compression. [2]

Compression yield strength is useful as an indicator of the balanced biaxial plane stress strength of pressure vessels. This is because the balanced biaxial yield and compression yield are equivalent since hydrostatic tension does not effect yield behavior. In this case, we are interested in c direction compression and ideal textures produce the highest values.

Summary

We have shown that titanium and titanium alloys can be anisotropic with respect to their uniaxial tensile properties. The most sensitive measure of this anisotropy appears to be the strain, although the other mechanical properties such as yield strength and tensile strength are also influenced. We have shown the general behavior patterns observed in commercially obtainable textures of several types. The patterns of behavior observed can be described in a qualitative way and further work is needed to more fully develop a quantitative understanding of the interrelationships between texture and mechanical properties of titanium sheet materials.

TABLE 4. TENSION AND COMPRESSION PROPERTIES OF HIGHLY TEXTURED, CONTINUOUSLY ROLLED, Ti-6Al-4V SHEET[2]

Thickness, inch	Grain Direction	TUS, ksi	TYS, ksi	Elongation in 2 Inches, percent	E_T, 10^6 psi	CYS, ksi	E_C, 10^6 psi
	L	144.2	125.5	10.0	14.8	126.4	15.6
0.050	T	158.5	155.2	10.0	19.4	196.5	19.7
	45°	133.5	130.6	10.8	15.9	143.3	16.4
	L	152.0	134.5	8.2	14.8	134.7	15.7
0.060	T	163.5	162.0	9.3	18.8	192.5	19.9
	45°	137.3	135.8	11.7	16.0	145.2	17.4
	L	146.3	129.4	8.8	—	133.6	—
0.080	T	153.3	147.5	8.5	—	172.3	—
	45°	136.1	129.8	10.5	—	143.3	—
	L	143.7	129.0	10.8	14.7	134.1	15.3
0.125	T	150.9	142.5	10.0	17.7	165.1	17.1
	45°	139.5	131.9	12.8	16.2	143.1	16.6
	L	136.9	124.6	12.7	14.8	130.0	15.9
0.150	T	148.8	147.3	11.3	18.9	177.4	19.4
	45°	133.3	130.9	14.7	15.3	149.8	18.0

BIAXIAL ANISOTROPIC YIELDING BEHAVIOR

In the past, mechanical anisotropy was regarded as undesirable, and every effort was made to eliminate it. Recently there has been a shift in viewpoint, for attempts are being made to employ plane-stress anisotropic yielding theory for achieving an engineering advantage in hydraulic tubing and pressure vessels. Of special interest have been applications involving thin-wall pressure vessels such as those used in missiles.

To perceive the potential benefits which would arise from designing with anisotropic materials, first consider a polycrystalline aggregate which is random and will likely be isotropic. Then the isotropic criterion for yielding proposed by von Mises[86] would be:

$$(\sigma_x-\sigma_y)^2 + (\sigma_y-\sigma_z)^2 + (\sigma_z-\sigma_x)^2 + 6\,(\tau_{yz}^2+\tau_{zx}^2+\tau_{xy}^2) = 2Y^2, \quad (15)$$

where Y is the yield stress in tension, σ is normal stress, and τ is shear stress. When σ_x, σ_y, and σ_z are the principal stresses, then

$$(\sigma_x-\sigma_y)^2 + (\sigma_y-\sigma_z)^2 + (\sigma_z-\sigma_x)^2 = 2Y^2. \quad (16)$$

For plotting simplicity and to represent the plane-stress state ($\sigma_z = 0$) for the above-mentioned thin-wall pressure vessels, the equation reduces to:

$$\sigma_x^2 + \sigma_y^2 - \sigma_x\sigma_y = Y^2. \quad (17)$$

Equation (17) is plotted in Figure 32 along with the Tresca criteria[87], illustrating the variation of biaxial yield strength. The maximum yield strength occurs in the 2-to-1 field, either tension-tension or compression-compression, and a value of 1.15 times the yield in uniaxial tension is predicted.

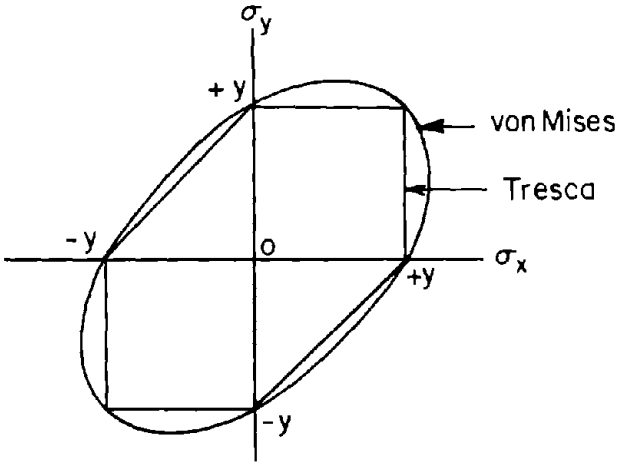

FIGURE 32. von MISES AND TRESCA YIELD CRITERIA ($\sigma_z = 0$)[86,87]

To consider yielding of anisotropic materials, it is necessary to generalize the yield equations. Hill's formulation seems the most applicable.[88] Backofen[71,89] recognized the importance of this theory and carried much investigation in this area. He assumed orthogonal symmetry and chose the principal axis as the Cartesian axis of reference. Then if the yield criterion is assumed to be a quadratic in stress components, it must be of the form

$$F(\sigma_y-\sigma_z)^2 + G(\sigma_z-\sigma_x)^2 + H(\sigma_x-\sigma_y)^2 + 2L\,\tau^2_{yz} + 2M\,\tau^2_{zx} + 2N\,\tau^2_{xy} = 1, \quad (18)$$

where F, G, H, L, M, and N are parameters defining the current state of anisotropy.

For principal stresses

$$F(\sigma_y-\sigma_z)^2 + G(\sigma_z-\sigma_x)^2 + H(\sigma_x-\sigma_y)^2 = 1. \quad (19)$$

The anisotropic parameters F, G, and H can be evaluated by performing two tension tests. If we are considering sheet or plate material, then the rolling, transverse, and thickness directions are usually designated as x, y, and z, respectively. The x direction uniaxial tension yield strength is X, y direction is Y, and the z direction is Z.

It is easy to show that

$$\frac{1}{X^2} = G+H \quad (20)$$

$$\frac{1}{Y^2} = H+F \quad (20a)$$

$$\frac{1}{Z^2} = F+G\,. \quad (20b)$$

From an x-direction tension test, one can measure X and a value of incremental strain ratio which is a measure of the current state of anisotropy. This strain ratio, designated R, is defined as

$$R = \frac{\delta\epsilon_y}{\delta\epsilon_z}\,. \quad (21)$$

From the strain-increment relations it can be shown that

$$R = \frac{H}{G}\,. \quad (22)$$

Similarly, for a y-direction test it can be shown that P, which is defined as

$$P = \frac{\delta\epsilon_x}{\delta\epsilon_y}\,, \quad (23)$$

is also

$$P = \frac{H}{F}\,. \quad (24)$$

Substitution of R and P for G, H, and F into Equation (19) yields

$$R(\sigma_y-\sigma_z)^2 + P(\sigma_z-\sigma_x)^2 + RP(\sigma_x-\sigma_y)^2 = P(1+R)X^2 = R(1+P)Y^2. \quad (25)$$

and for plane-stress ($\sigma_z = 0$) then

$$P(R+1)\sigma_x^2 - 2RP\,\sigma_x\sigma_y + R(P+1)\sigma_y^2 = P(R+1)X^2 = R(P+1)Y^2. \quad (26)$$

If the properties show rotational symmetry about the z axis, planar isotropy, then X = Y and R = P so that

Equation (26) simplifies to

$$\sigma_x^2 - \left[2R\Big/(R+1)\right]\sigma_x\sigma_y + \sigma_y^2 = X^2 \quad (27)$$

Equation (27) is plotted in Figure 33. Under the restrictions specified, it can be seen that the yield ellipses specified by Equation (27) predict large increases in strength for both biaxial tension and biaxial compression.

The effect of anisotropy (R and P) can be shown for yielding in various stress fields which are of engineering importance. If we define the plane-stress state ($\sigma_z = 0$) as

$$\frac{\sigma_y}{\sigma_x} = \omega\,, \quad (28)$$

Equation (26) becomes

$$\sigma_x^2\left[\frac{P(1+R)}{R(1+P)} + \omega^2 - \omega\,\frac{2P}{1+P}\right] = Y^2\,, \quad (29)$$

and with rotational symmetry about z (P = R and X = Y), then

$$\sigma_x^2\left[1 + \omega^2 - \omega\,\frac{2R}{R+1}\right] = X^2\,. \quad (30)$$

For a cylindrical thin-wall pressure vessel, $\omega = 1/2$, yielding in the side wall is governed by

$$\frac{\sigma_x}{x} = 2\sqrt{\frac{R+1}{R+5}}\,. \quad (31)$$

For a spherical thin-wall pressure vessel, yielding is predicted by

$$\frac{\sigma_x}{x} = \sqrt{\frac{1+R}{2}}\,. \quad (32)$$

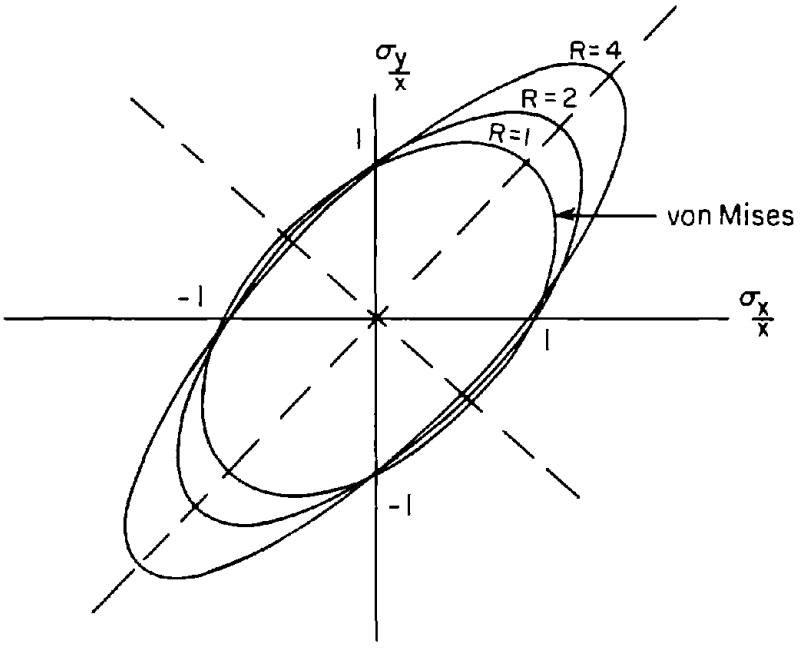

FIGURE 33. HILL'S YIELD CRITERIA FOR PLANE-STRESS ($\sigma_z = 0$) AND WITH ROTATIONAL SYMMETRY AROUND Z[89]

Equations (31) and (32) are plotted in Figure 34.

The foregoing analysis is based upon continuum plasticity and does not consider the crystallographic nature of the deformation process. In order to consider the crystallographic aspects of plastic yielding, it is necessary to select a crystal structure. Probably the most interesting are those metals which are hexagonal close packed (hcp) since they usually exhibit the largest degree of anisotropy. This is because the number of deformation mechanisms available is limited. All of the slip directions, $\langle 11\bar{2}0\rangle$, which are the close packed directions, are coplanar and make an angle of 90 degrees to the c axis. In hcp metals, twinning plays an important role in plastic deformation but, unlike slip, twinning is sensitive to the direction of the applied stress. By assuming an ideal orientation of a (0001) $[10\bar{1}0]$ texture, and that the critical stresses for prism slip, $\{11\bar{2}2\}$ twinning are in the ratio of 1:1.5:2, it is possible to construct a yield locus considering the crystallographic nature of plastic yielding. This is shown in Figure 35 along with the Hill locus of R = P = 5. It can be readily seen that the continuum-plasticity and crystal-plasticity results are in disagreement. The main difference is in the compression-compression quadrant where the directionability of the twinning deformation takes effect.[90]

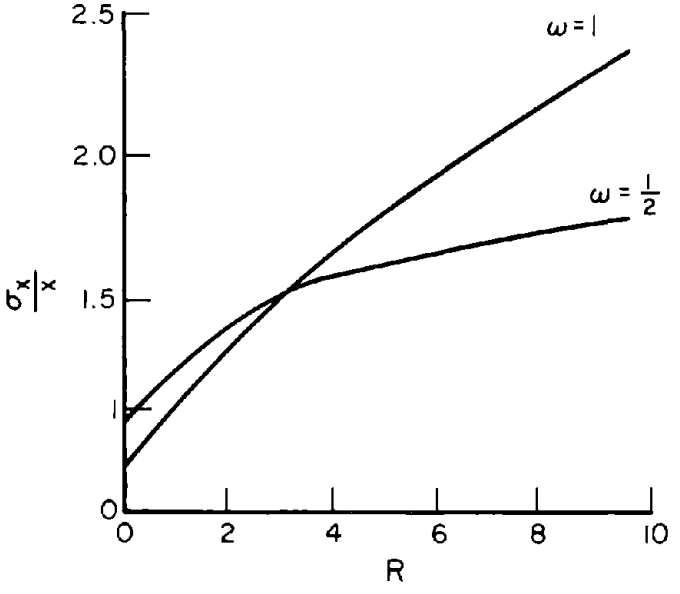

FIGURE 34. STRENGTHENING RATIO $\frac{\sigma_x}{x}$ VERSUS R FOR ($\sigma_z = 0$) AND (R = P X = Y) NORMAL ISOTROPY

Symbols defined in text

Many experiments have been conducted to compare the continuum plasticity and crystallographic plasticity

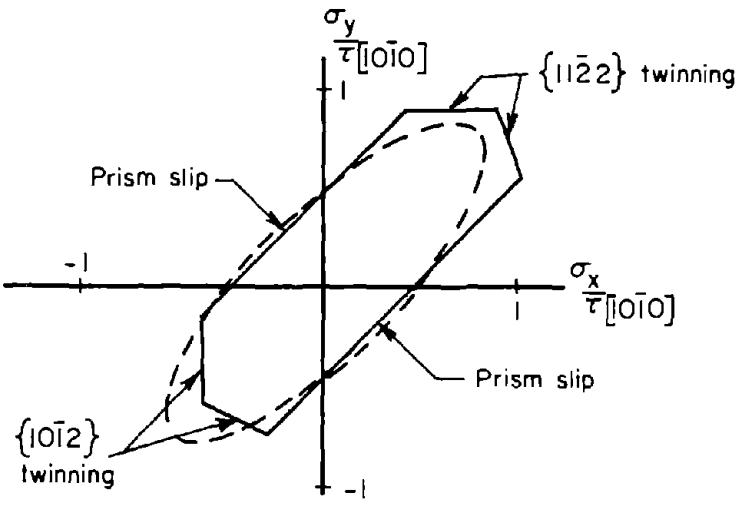

FIGURE 35. YIELD LOCUS CONSIDERING CRYSTALLOGRAPHY ($\sigma_z = 0$), $[10\bar{1}0]\langle 11\bar{2}0\rangle$ SLIP, $\{10\bar{1}2\}$ AND $\{11\bar{2}2\}$ TWINNING WITH CRITICAL STRESS RATIO OF 1:1.5:2[90]

Hill locus for R = P = 5 is indicated by dotted line

with the experimental yield loci, but few results are available on strongly anisotropic material. Probably the most complete, recent yield-locus determination for an hcp metal (Ti-4Al-0.250$_2$) was carried out by Lee and Backofen[91], who used a series of uniaxial, plane-stress tension and compression tests. In addition to determining the stresses, they also measured the slope of the locus by considering that the strain vector is normal to the locus and computing the tangent to the locus.

$$\tan \delta = \frac{d\epsilon_x}{d\epsilon_y} \quad , \tag{33}$$

where δ is the angle from the x axis to the tangent of the yield locus.

For an x-direction uniaxial tension test,

$$\tan \delta = \frac{(1+R)}{R} \quad ; \tag{34}$$

and for y-direction test

$$\tan \delta = \frac{(1+P)}{P} \quad . \tag{35}$$

The results of these experiments are shown in Figure 36. It can readily be seen that isotropic theory is poor because it fails to predict the potential strengthening that is possible in the tension-tension quadrant. Hill's anisotropic theory also is deficient because it fails to predict the weakening that occurs in the compression-compression quadrant. Obviously, a more generalized theory that considers the directionality of the twinning deformation is needed.

Results of Experiments With Textured Titanium Pressure Vessels

Although the indications of texture strengthening are clear, the practical applications have been slow to develop. This has been because of two problems. The first is associated with the difficulty in obtaining highly anisotropic sheet or plate with the high R values in high-strength titanium alloys such as Ti-6Al-4V; second, there have been practical problems such as welding connected with the fabrication of end items stems from these materials.

There have been many investigations into the yield and burst behavior of pressure vessels fabricated from titanium sheet metal. One was carried out by Sliney.[92,93] His work was limited to two sheets of Ti-5Al-2.5Sn, which were made into pressure vessels by roll and weld techniques. One of the sheets had a low R and not the correct anisotropy. However, the other sheet showed much improved properties as shown by the data of Table 5.

An important observation made by Sliney which has also been observed by other researchers is the high ratios of burst to ultimate strength for pressure vessels as tabulated at the bottom of page 43.

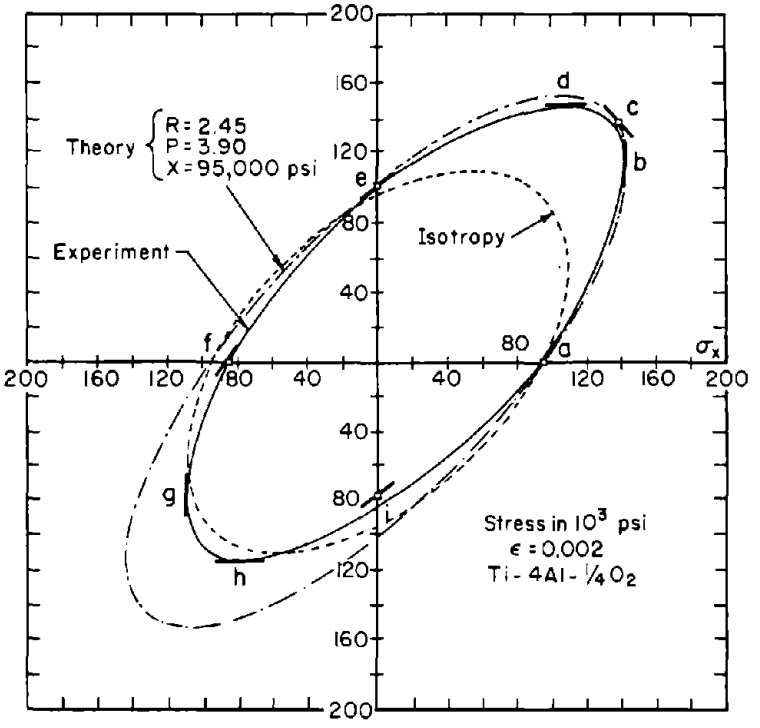

FIGURE 36. PLANE-STRESS ($\sigma_z = 0$) YIELD LOCUS FOR A TITANIUM ALLOY SHEET[91]

Points and slopes were determined as follows: a and f, x-direction tension and compression; e and i, y-direction tension and compression; c, z-direction compression; b, d, g, and h, plane-strain compression. The loci predicted by the von Mises and Hill criteria are shown for comparison.

TABLE 5. MEASURED AND PREDICTED UNIAXIAL-BIAXIAL YIELD STRENGTH RATIO

	Vessel			
	1A	2A	1B[a]	2B[a]
Measured Hoop Yield to Uniaxial Yield Ratio, $\frac{\sigma_h}{X_o}$	1.25	1.25	1.00	1.10
Calculated[b] $\frac{\sigma_h}{X_o}$	1.35	1.39	1.37	1.36

(a) Sheet B had poor anisotropy.

(b) $$\frac{\sigma_h}{X_o} = \frac{(1+R_T)\,R_L\,K^2}{(1+R_T)\,R_L K^2 + (R_L+1)\,R_T - 2\,R_L R_T K}$$.

Tabulation:

	Vessel			
	1A	2A	1B	2B
$\frac{\sigma_B}{UTS}$	1.81	1.70	1.36	1.36

These high ratios of burst to ultimate strength may be due to the fact that R may change with the strain and stress system, and the yield- or flow-strength locus is a function of the current strain ratio or incremental strain ratio, and not the initial strain ratio.

Sullivan[94,95] also ran pressure tests on anisotropic-titanium-alloy pressure vessels to demonstrate texture strengthening. This program was carried out over a range of temperatures above and below room temperature. The results are shown in Figure 37. Notch-toughness and uniaxial tensile tests were conducted for both smooth and flawed vessels. The alloys he employed were Ti-5Al-2.5Sn and Ti-4Al-0.$2O_2$. Both alloys develop the "ideal" or desired texture during processing.

Workers at Douglas[96-98] have also pursued the texture strengthening of titanium-alloy pressure vessels. Their work on Ti-5Al-2.5Sn alloy vessels has also shown large increases in both biaxial yield strength and biaxial burst strength. One of their programs[94] resulted in the curves shown in Figures 38 and 39. These curves clearly demonstrate the vastly improved biaxial properties achievable through texture strengthening.

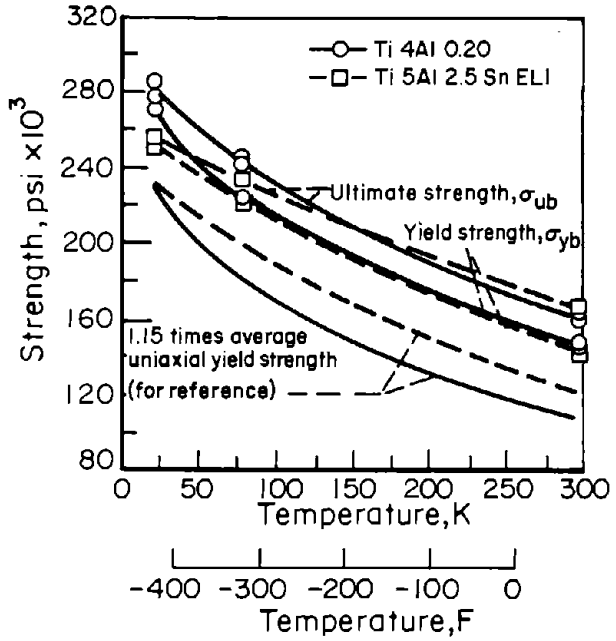

FIGURE 37. BIAXIAL YIELD AND ULTIMATE STRENGTH OF Ti-4Al-0.20 AND Ti-5Al-2.5Sn ELI SHEET IN A 1 TO 2 STRESS FIELD AS FUNCTION OF TEST TEMPERATURE[94]

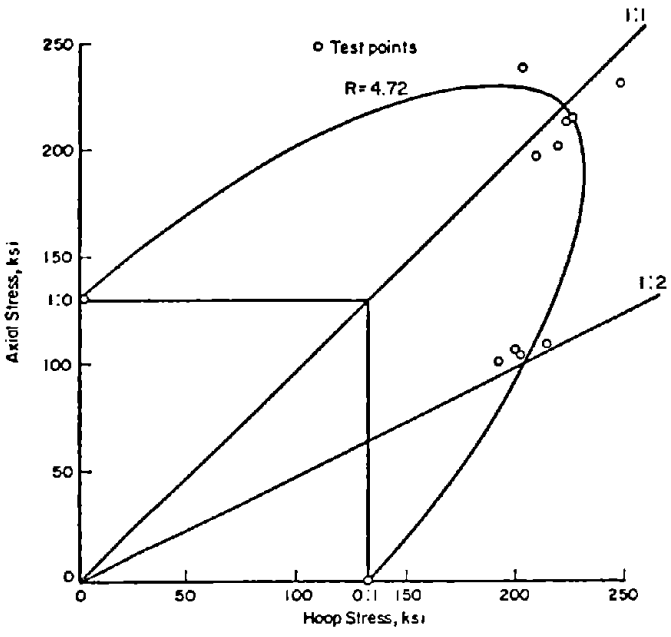

FIGURE 38. BIAXIAL BURST STRENGTHS OF Ti-5Al-2.5Sn ALLOY PRESSURE VESSELS[96]

Note: R calculated from uniaxial strength and hoop strength for approximate 1:2 stress state. Predicted strength for a 1:1 stress state was 221 ksi. Average experimental hoop stress obtained was 224 ksi.[96]

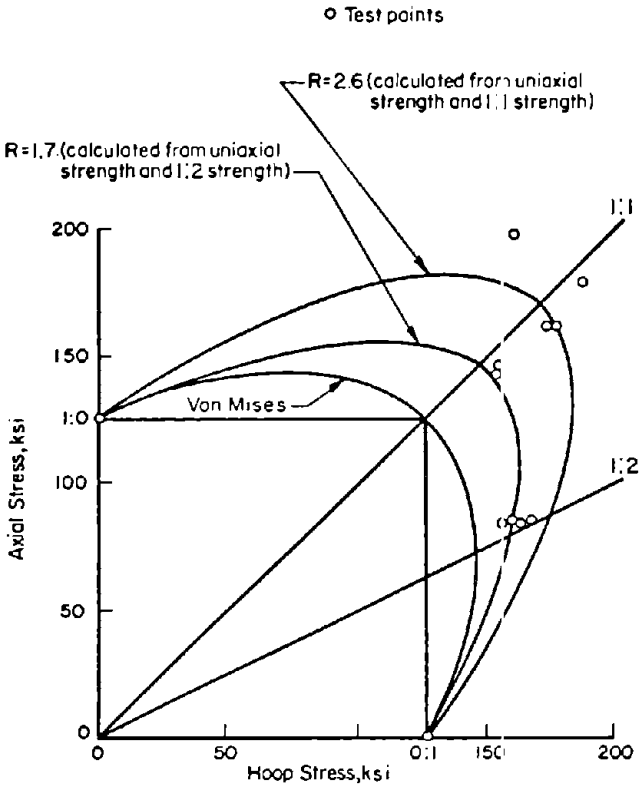

FIGURE 39. BIAXIAL YIELD STRENGTH CF Ti-5Al-2.5Sn ALLOY PRESSURE VESSELS[96]

The Douglas investigators[97] have also worked on Ti-6Al-4V, a higher strength alloy, which unfortunately does not develop the ideal texture so easily. The results of this work clearly illustrate that Ti-6Al-4V with a lower R can have a higher burst strength (see Figure 40). Another important point brought out by these invest gators was the variation of R with plastic strain and stress state.

A program carried out at Lockheed[99,100] has also demonstrated the value of texture strengthening. This program was designed to come to grips with the multifaceted features in the manufacture of highly textured-strengthened pressure vessels. Phase I centered on sheet rolling and heat treatment to determine suitable processes by which texture-strengthened sheet could be produced, a difficult task at this stage of development. Phase II was an investigation of a shear-forming process for producing Ti-6Al-4V cylinders. Phase III was a study to determine the effect of different welding procedures on texture. Phase IV was a demonstration of a spherical-tank fabrication and hydroburst test using texture-strengthened Ti-6Al-4V. The program was a very successful one in that it demonstrated that texture strengthening can be achieved in real pressure vessels. The results of the program are shown in Figure 41. Here actual biaxial strengths are given along with predicted biaxial strengths from the known uniaxial yield strength and R values. Other investigations[101,102] have also demonstrated the value of texture strengthening.

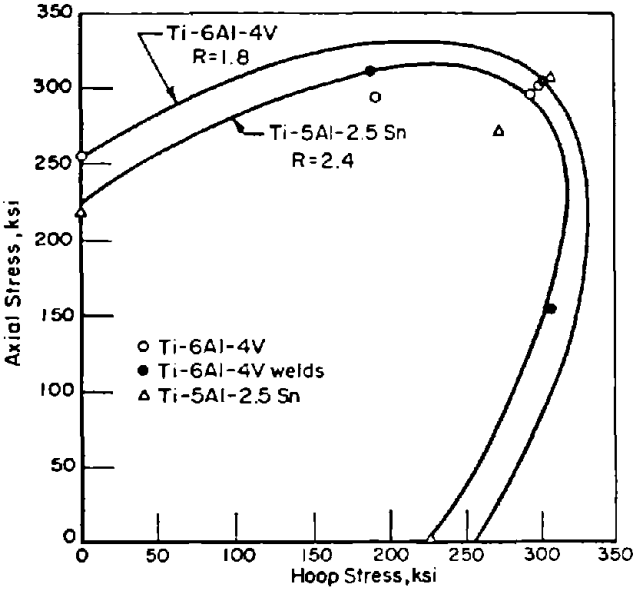

FIGURE 40. BURST LOCI [97] AT -423 F FOR PRESSURE VESSELS OF TWO TITANIUM ALLOYS[97]

The increased strength of these spherical pressure vessels (average yield strength of 221,700 psi and burst strength of a range of 254,000 to 263,000 psi) clearly demonstrates the value of texture control. Here again, this program pointed up the difficulty of obtaining high-R materials, and more work needs to be carried out in this area. area.

The research on anisotropic yielding can be also applied to hydraulic tubing. Considerable work has been carried out on zirconium for this type of application probably because this is a principal application of zirconium. Only limited work with titanium has been accomplished viz., that on the development and control of crystallographic texture in Ti-3Al-2.5V alloy [103] tubing. Spurr and Quist[104] have related the effects of crystallographic texture on the mechanical and fracture properties of the same alloy.

Summary

The utilization of texture as a method for improved performance in engineering applications is more highly developed in the case of plane-stress or biaxial-stress applications than in other fields. It, however, appears that considerable work is necessary in both the mill and the secondary-fabrication sides of the problem. The most important barrier yet to be overcome is the commercial

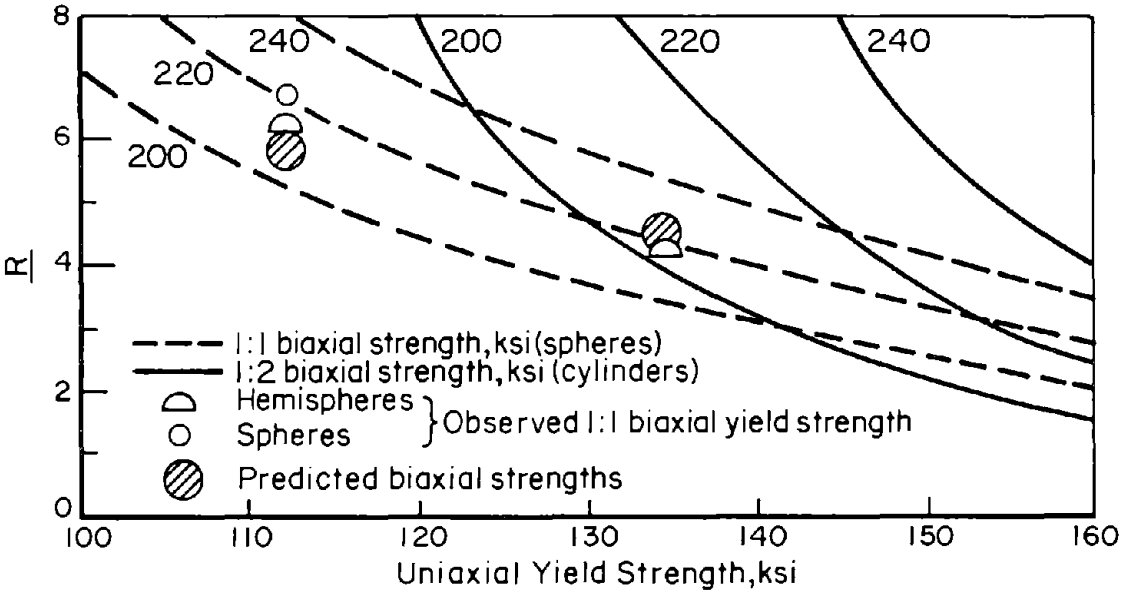

FIGURE 41. OBSERVED BIAXIAL YIELD STRENGTHS OF Ti-6Al-4V SPHERICAL PRESSURE VESSELS AND PREDICTIONS FROM HILL'S THEORY [99]

production of the "ideal" texture in which high R's can be guaranteed or specified. Such processing procedures are currently being worked on [64] and undoubtedly the answers will be forthcoming. It is apparent that large improvements in biaxially stressed pressure vessels can be achieved through texture control. These large gains will not be easy to come by, yet they are possible if the resources are devoted to this area.

EFFECT OF TEXTURE ON KNOOP HARDNESS

Hardness varies with crystallographic and indenter orientation in hexagonal-close-packed single crystals. [105-107] For titanium it has been established that on the basal plane, no variation of hardness exists with varying indenter orientation. On the prismatic planes, however, minimum hardness values will be found when the long axis of the Knoop indenter is parallel to the c axis, and maximum hardness values will be obtained when the long axis of the indenter is perpendicular to the c axis. Results clearly illustrate that hardness variations found in the titanium hcp single crystal are evident in the polycrystalline unalloyed titanium material. Definite indications of a preferred texture giving rise to hardness anisotropy are evident. [108]

The Knoop indenter may be used advantageously to detect hardness anisotropy because of its unidirectional design, which accentuates the directionality of the material, and the fact that the long dimension of the indentation is not affected by elastic recovery. In a study by Zarkades [108], readings were taken at 10-degree intervals. For measurements made on the longitudinal and rolling planes, this interval was the angle between the long axis of the indenter and the rolling direction and was designated as alpha (α). On the transverse planes, however, α was the angle between the long axis of the indenter and the transverse direction. Reported Knoop hardness numbers (Khn) were an average of a minimum of two readings at each orientation and were calculated from the formula,

$$I = \frac{L}{A_p} = \frac{L}{\ell^2 C_p} \quad ,$$

where

I = Knoop hardness number
L = load in kilograms
A_p = unrecovered projected area of indentation, mm^2
ℓ = measure length of long diagonal, mm
C_p = constant relating ℓ to the projected area (for the Knoop indenters, it is equal to 7.028×10^{-2} kg/mm^2).

The hardness data obtained on commercially pure titanium sheet were averaged and plotted as shown in Figure 42. It is evident that the hardness variation existing within a plane of polycrystalline hcp material is similar to the variation found in the titanium hcp single crystal (see Figure 42a.) As would be expected, a similar variation of hardness was found on the transverse plane, as shown in Figure 42b. The surface or rolling plane was also examined and, in this instance, results plotted in Figure 42c are the average of four indentations at each orientation. Less regularity in change of hardness with indenter orientation was observed.

The X-ray pole figure for this material, Figure 42d, shows some degree of preferred orientation of the aggregate with the maximum intensity at a tilt of the (0002) planes of approximately 22 degrees toward the transverse direction. Knowing that no hardness variation is found in the basal plane of single-crystal titanium, one could expect to find no variation of hardness when the basal plane lies in the plane or surface of the polycrystalline sheet material. This type of texture is considered ideal. As the texture under study is not ideal, results shown in Figure 42c reflect the basal tilt causing the variation of hardness data within the rolling plane. Comparison of average values in Figure 42 clearly illustrates the variation of hardness that can be found between planes of a textured material. It is observed that little difference exists between the longitudinal and transverse planes, while a large variation is found between rolling and cross-section planes.

Since primary concern was with hardness variations of textured materials and not of a single crystal as such, tests were conducted to ensure that results obtained were indeed measurements of a preferred-orientation polycrystalline aggregate. The ASTM grain size number for the commercially pure material was 8. Photomicrographs of the specimens showed hardness indentations covering a various number of grains (typically nine), depending on the material and the orientation of the indenter.

The directionality of hardness has been utilized to develop the plane-stress yield locus of sheet material and indicate a measure of material anisotropic resistance to plastic deformation. [109-112] Knoop-hardness readings are taken on surfaces normal to the three principal directions with the Knoop-indenter orientations, as shown in Figure 43. The proposed methods for the construction of the yield locus from hardness values of Wheeler and Ireland [109] and Wonsiewicz and Wilkening [111] define the stress for the X and Y directions as:

$$\sigma_x = \frac{Khn}{(1 - \alpha + \alpha^2)^{1/2}}$$

$$\sigma_y = \frac{\alpha Khn}{(1 - \alpha + \alpha^2)^{1/2}} \quad ;$$

however, Wheeler and Ireland propose α to be 3/5, 5/3, -2/3, 2/5, 5/2, and -3/2 for indentations positions

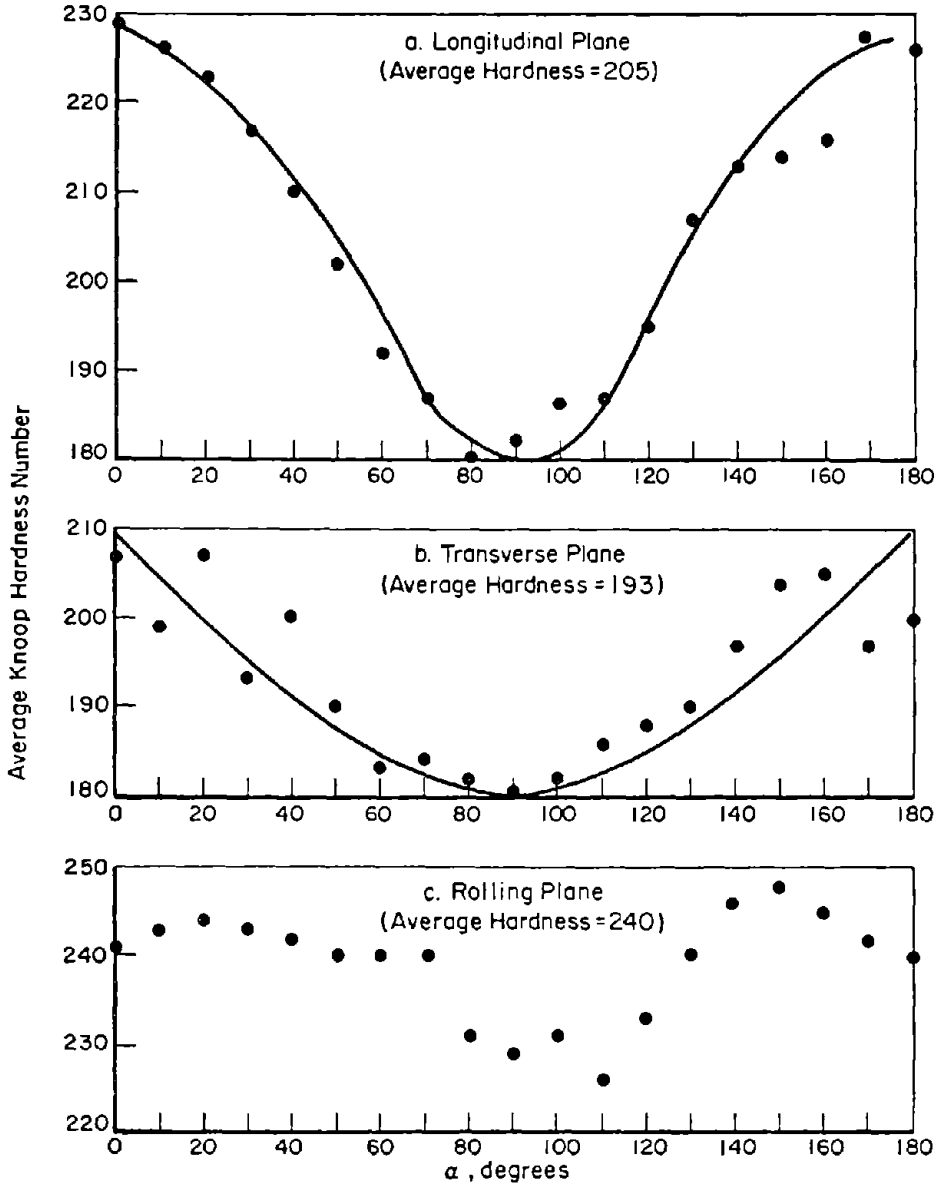

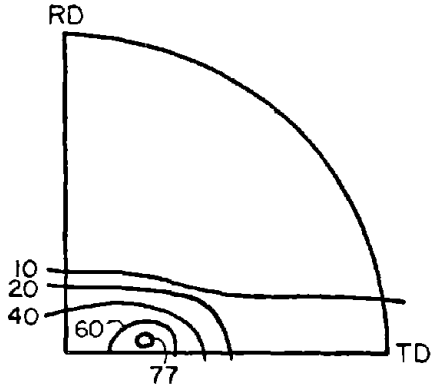

d. Pole Figure (0002)

FIGURE 42. KNOOP HARDNESS VARIATION AS A FUNCTION OF INDENTER ORIENTATION FOR UNALLOYED TITANIUM SHEET[108]

a through f, and Wonsiewicz and Wilkening propose α to be

$$\alpha = \frac{A\,(R+1) + R}{AR + R + 1} \quad ,$$

having A equal to $d\epsilon_y/d\epsilon_x$, so that α is 1/7, 7, -7/8, -1/8, -8, and -8/7.

Yield loci are illustrated in Figure 44 and the approach was successful for titanium with anisotropy ratios R up to 6.[113] As seen in Figure 44a, the agreement of hardness data with proposed theories and tensile results is excellent but may be fortuitous. For material with high through-the-thickness plastic-flow anisotropy, the data for the c and f impressions (Figure 41) fall outside the Hill ellipse, as shown in Figure 44b.

Summary

Hardness anisotropy similar to that for hexagonal-close-packed (hcp) structured material does occur in body-centered cubic (bcc) and face-centered cubic (fcc) metals.[114,115] With cubic material (bcc) and (fcc), it is a function of indenter orientations, with the plane of indentation having a minor effect.

Although microhardness testing is primarily a laboratory testing method, it is being utilized more and more for quality control. When specifications are requested with certain Knoop-hardness-number limitations, the initiator of such specifications should be cognizant of the anisotropic characteristics of the crystals and the texture of the aggregate for the polycrystalline material.

Complete mathematical analyses and exhaustive studies are needed to fully explain the phenomenon and to define the modes and processes of plastic deformation taking place during a hardness test. Once this is accomplished satisfactorily, hardness measurements may be used to determine the degree of anisotropy of polycrystalline metals.

EFFECT OF TEXTURE ON TOUGHNESS AND STRESS CORROSION CRACKING

Charpy Impact and Transition Temperature

Most of the work conducted concerning titanium texturing has centered around the increases in strength that can be expected in biaxial loading. This work on preferred orientation has dealt mainly with yield and flow, with very little attention being directed toward fracture or toughness. The basic problem of predicting the effects of texture upon the toughness is extremely difficult and complicated because it includes yield and flow effects. For the sake of simplicity, toughness can be viewed as the integral of the area under the stress-strain curve. From this it can be seen that the total work on toughness is a function of both the strength levels and the fracture ductility. The problem is a complicated one, as the strength level and the fracture ductility are related. The effects of texture on yielding and flow are fairly well understood from the work of Hill[88] and Backofen et al[21], yet the quantitative definition of the effects of texture on fracture is illusive and ill defined. Recent work has revealed that significant toughness variations can be found in titanium plate as a function of specimen and notch orientation.[116] This impact-energy anisotropy was found to be related to texturing.

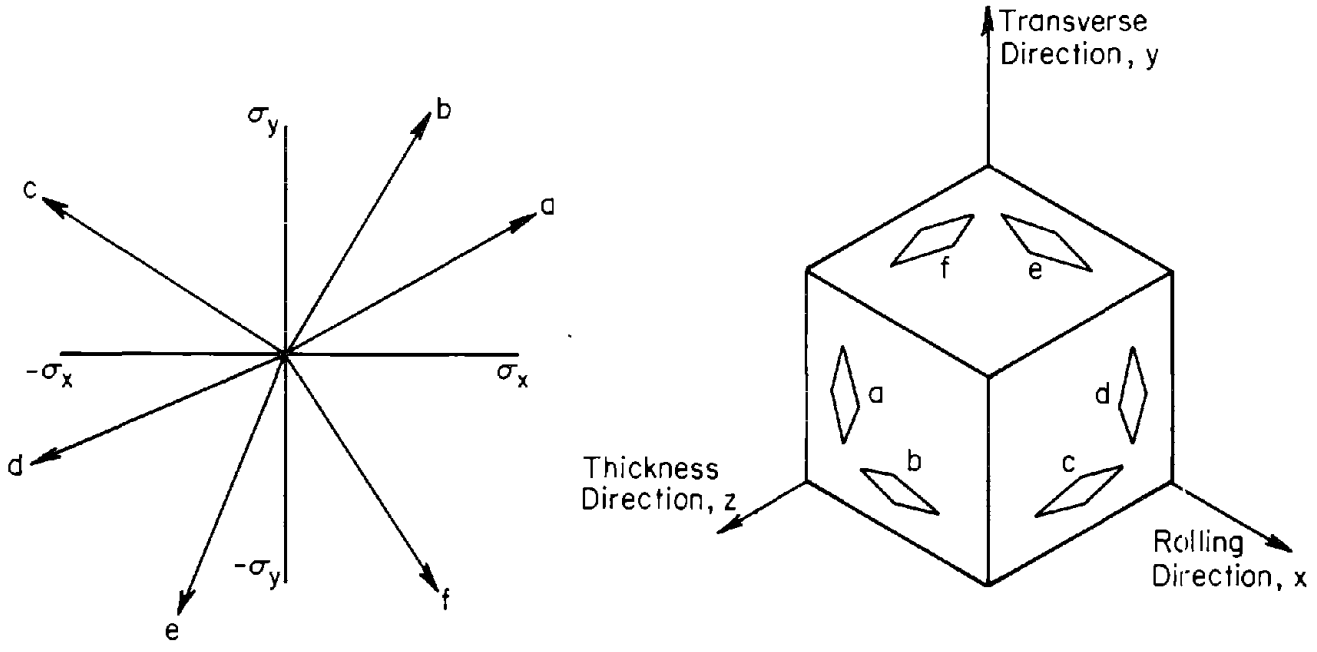

FIGURE 43. CORRESPONDENCE BETWEEN ORIENTATION OF THE KNOOP HARDNESS IMPRESSION AND THE BIAXIAL STRESS RATIOS[113]

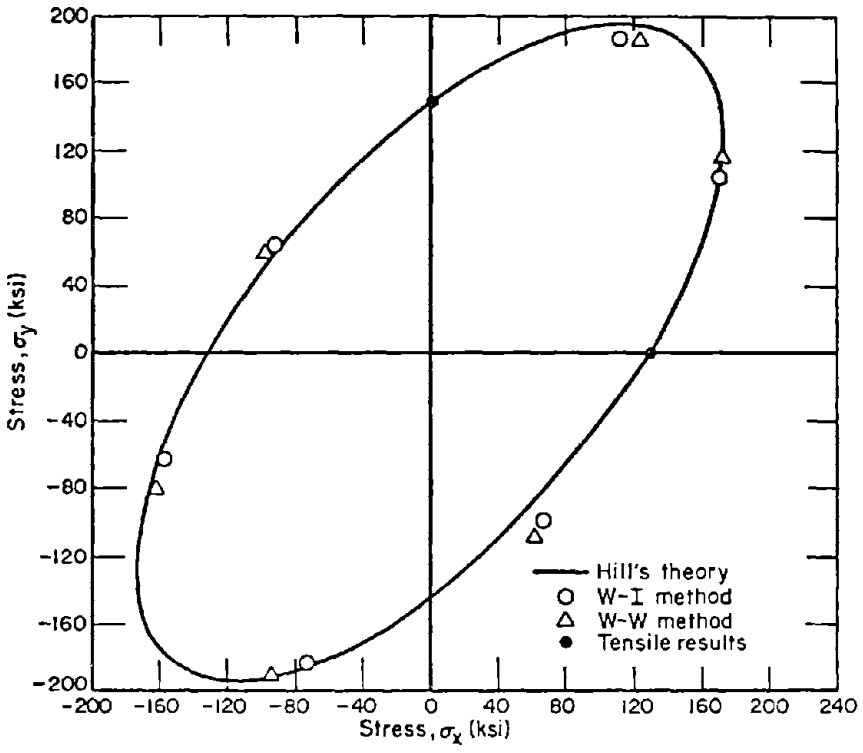

a. Rolled at 1400 F (R = 1.6, P = 2.9)

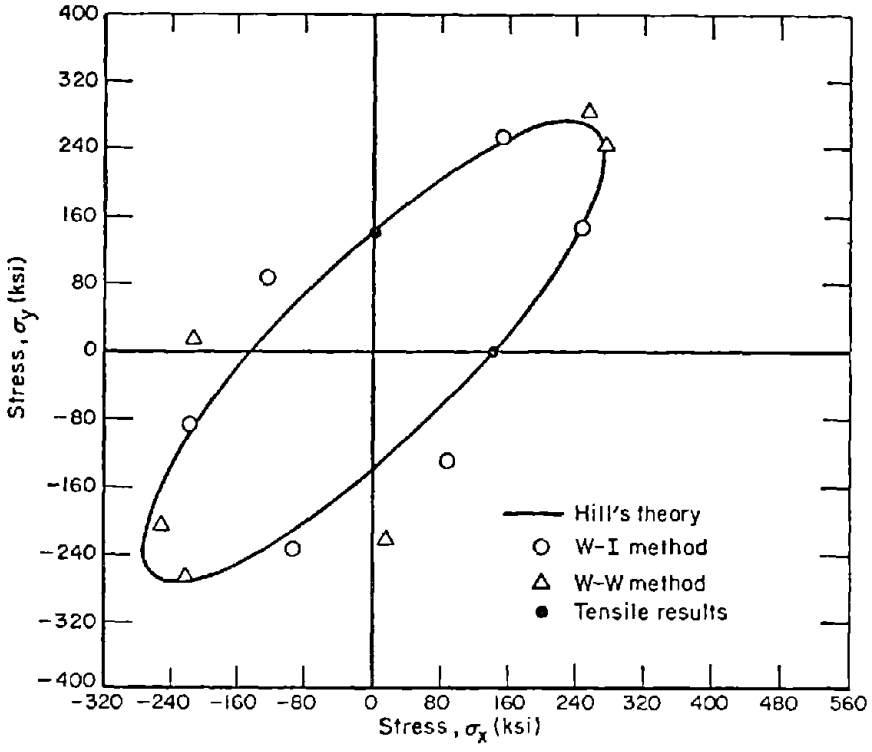

b. Unidirectional Rolled (R = 4.9, P = 6.1)[113]

FIGURE 44. YIELD LOCUS OF Ti-6Al-4V[113]

R and P are strain ratios, defined in text. W-I and W-W refer to References [109] and [111], respectively.

In the study mentioned[116] standard 0.394-inch-square Charpy V-notch specimens were machined at 10-degree increments from the rolling direction to the transverse direction. Two notch orientations were examined. One orientation has the specimens notched parallel to the plate surface, and the second orientation has the notch normal to the plate surface or in a through-thickness direction. With ASTM designations for longitudinal and transverse directions, specimens with notches as indicated would be RT, WT, and RW, WR. In this form, the first letter indicates the direction the notch is normal to, and the second letter the direction of crack propagation (see Figure 45).

To help define the specimen orientation and crack propagation in relation to the texture, a system is shown in Figure 46 where the strong texture is considered as a single crystal, and only the principal specimen and hexagonal unit cell directions need to be considered. For the first letter, the specimen axis is referred to the pole of the plane which lies parallel to it, and the second letter specifies the direction of crack propagation. P and B stand for prism and basal poles. Furthermore, a and c are conventional hexagonal directions; thus, for a titanium texture which had a strong concentration of basal poles in the transverse direction, the $(10\bar{1}0)$ poles usually are strongly concentrated in the rolling direction so that a

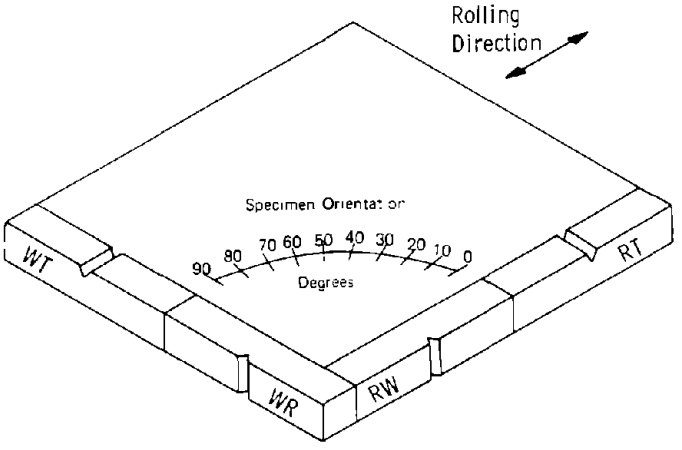

FIGURE 45. SCHEMATIC OF CHARPY SPECIMEN AND NOTCH ORIENTATION[116]

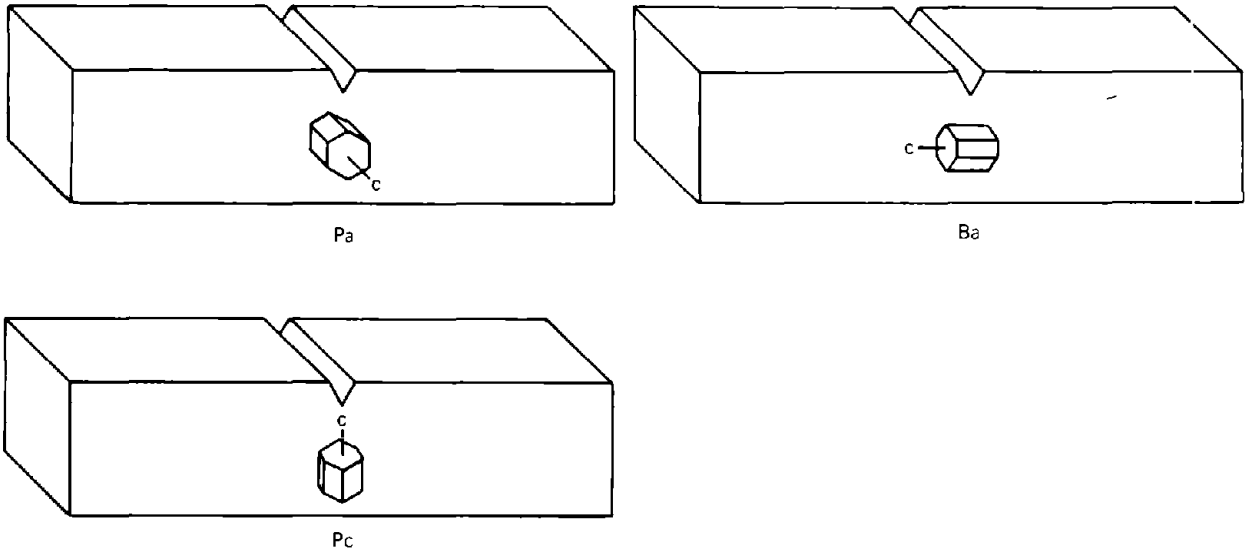

FIGURE 46. SCHEMATIC OF TEXTURE VERSUS NOTCH AND SPECIMEN ORIENTATION[116]

transverse-face-notched (WT) specimen would have a crystallographic or texture designation of Ba.

Since the primary concern was about the effects of texture, it was necessary to rule out the effect of fibering. Mechanical fibering is noncrystallographic in nature and brings about anisotropy through existing elongated grain structure, inclusions, porosity, and segregation. Although not completely conclusive, the variation of toughness caused by fibering can be detected by the metallographic observations of delaminations associated with the fracture surfaces.[117] The effect of an elongated second phase can also be evaluated in this manner to a lesser degree. A large number of fracture samples were studied, and delaminations of the type associated with mechanical fibering were not found in the magnitude as described by English.[117] Nor did there seem to be a pronounced preferential fracture path associated with the elongated alpha-beta duplex structures found in some of the alloys. Also, the Charpy energies did not show the anisotropy difference for the WT and WR orientation normally attributed to mechanical fibering or elongated grain structure.

The results of the study by Zarkades and Larson are shown in Figures 47 to 50. To orient the reader, complete pole figures, tensile and microstructural properties are included. Analysis of the data indicate that Charpy-impact fractures can be categorized into two general types, brittle and ductile. In the case of brittle fracture (less than 10 ft-lb) very little anisotropy of toughness was found (see Figure 48).

It appears from preliminary observation that the anisotropy of Charpy-impact properties is related to plastic-flow anisotropy. One of the most dramatic cases found was for the Ti-4Al-4V alloy, as shown in Figure 49. Charpy specimens for that case were taken from the top and bottom of a 1.0-inch plate, and average impact values are plotted. Another case showing significant anisotropy was the Ti-6Al-4V alloy, as shown in Figure 50. For the Ti-4Al-4V alloy, the RW and WR specimen orientations gave about 25 ft-lb. The WT orientation was also low at about 35 ft-lb. However, the RT results were three times as high, or about 75 ft-lb. These results can be explained if we examine the texture orientation and the alloy's ability to plastically deform. From a texture standpoint, the highest energy-absorbing orientations are those with a Pa designation. Considering the fact that slip occurs in the $[11\bar{2}0]$ direction, it can be seen that the Pa orientation would be the "softest" and hence the greatest plastic deformation would be allowed; for the other orientation, either $(11\bar{2}2)$ or $(10\bar{1}2)$ twinning would be required for deformation. Subsequent to the twinning, the lattice reorientations would not be favorable for slip.

The high toughness of the Pa orientations unfortunately was not demonstrated for "ideal" textures in this program, for they were generally brittle. However, they were clearly shown in the work of Hatch,[118] (see Table 6). For ideal textures, the tough orientation (Pa) would occur for all edge-notched specimens (RW and WR). Backofen[119] studied impact energy transition for a duplex texture in Ti-5Al-2.5Sn and showed the effect of specimen orientation. These results are illustrated in Figure 51.

TABLE 6. CHARPY IMPACT AND R VALUES FOR Ti-4Al[(a)], 0.5-INCH PLATE ROLLED AT 1700 F [118]

Test Direction	Charpy V-Notch Impact Energy, (ft-lb)		R[(b)]
	Edge Notch	Face Notch	
L	RW 63.5	RT 17.5	5.1
T	WR 67.0	WT 17.3	9.5

(a) Oxygen content = 0.21 percent
(b) R = strain ratio, $\epsilon w/\epsilon t$.

In order to verify the effect of texture on the transition temperature, several specimens were cut from unalloyed grade Ti-75A. This plate had a texture with a basal pole intensity near the plate normal with little transverse spread. The tough Pa specimen orientation would correspond to the through-thickness notch orientation. From examination of data at several test temperatures, it can be seen that the transition temperature is lower and the toughness is higher for the Pa specimen orientation (see Figure 52).[116] These results are in agreement with the results for Zircaloy 2 which has deformation modes similar to those of titanium.[120,121]

The RW or WR orientation specimen for material with a near ideal texture would have a texture orientation of Pa and the RT and WT would have a Pc orientation. The argument is that for the soft Pa orientation, plastic flow occurs and high energy is absorbed. For the Pc orientation, higher levels of strength are required to induce flow, and then fracture occurs at lower strains, resulting in a less tough condition. As the temperature is raised, the Pc orientation becomes tougher due to a relaxation of the higher stresses by the introduction of c + a slip or slip with a non-basal vector.

A better understanding of the relationship between plastic deformation and fracture can be had from studying Figure 53 and References [122] and [123]. At high temperatures, the critical resolved stress for $(10\bar{1}0)$ $[11\bar{2}0]$ slip is low, and the specimen in a Pa orientation (Figure 53a) is favorable for this type of deformation. As the temperature is lowered, the critical resolved stress for $(10\bar{1}0)$ $[11\bar{2}0]$ slip rises until $(11\bar{2}2)$ twinning begins; microcracks are then formed at the twin-matrix interface and brittle fracture ensues. For the Pc specimen orientation (Figure 53b) a similar behavior is apparent; however,

Orientation	Thick (in.)	Yield Strength (psi) 0.1%	Yield Strength (psi) 0.2%	Tensile Strength (psi)	Elon. %	E x 10^6 (psi)	μ_E	μ_P
L	0.443	59,600	60,900	79,500	35.5	15.0	0.400	0.681
T	0.443	66,200	68,000	77,500	31.5	16.7	0.393	0.857

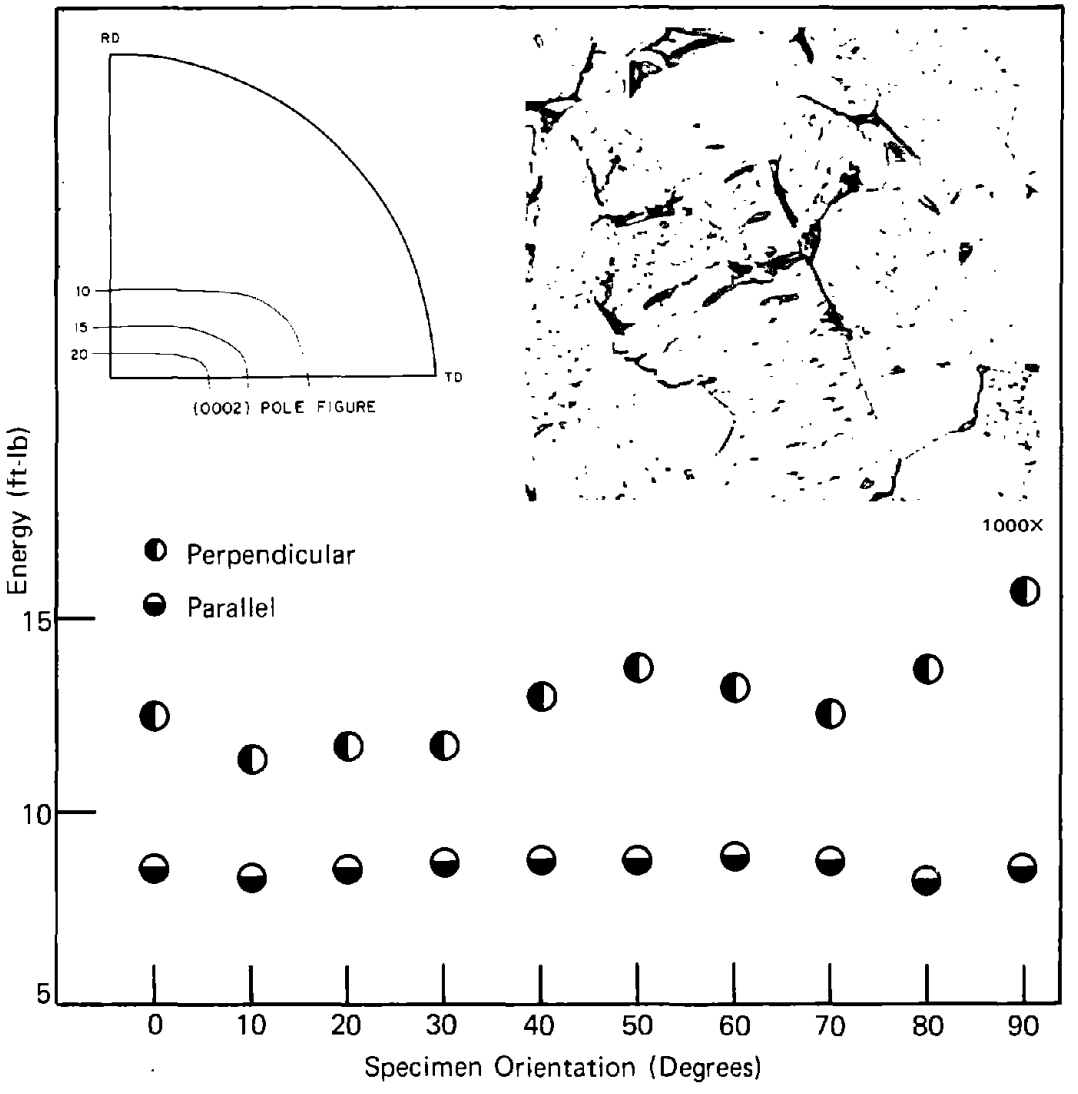

FIGURE 47. TYPICAL CHARPY IMPACT TEST DATA FOR UNALLOYED TITANIUM[116]

Orien-tation	Thick (in.)	Yield Strength (psi) 0.1%	0.2%	Tensile Strength (psi)	Elon. %	E x 10^6 (psi)	μ_E	μ_P
L	0.502	130,800	132,400	141,600	10.5	16.9	0.322	0.433
T	0.502	*	*	*	*	*	*	*

*Specimen broke in pinhole.

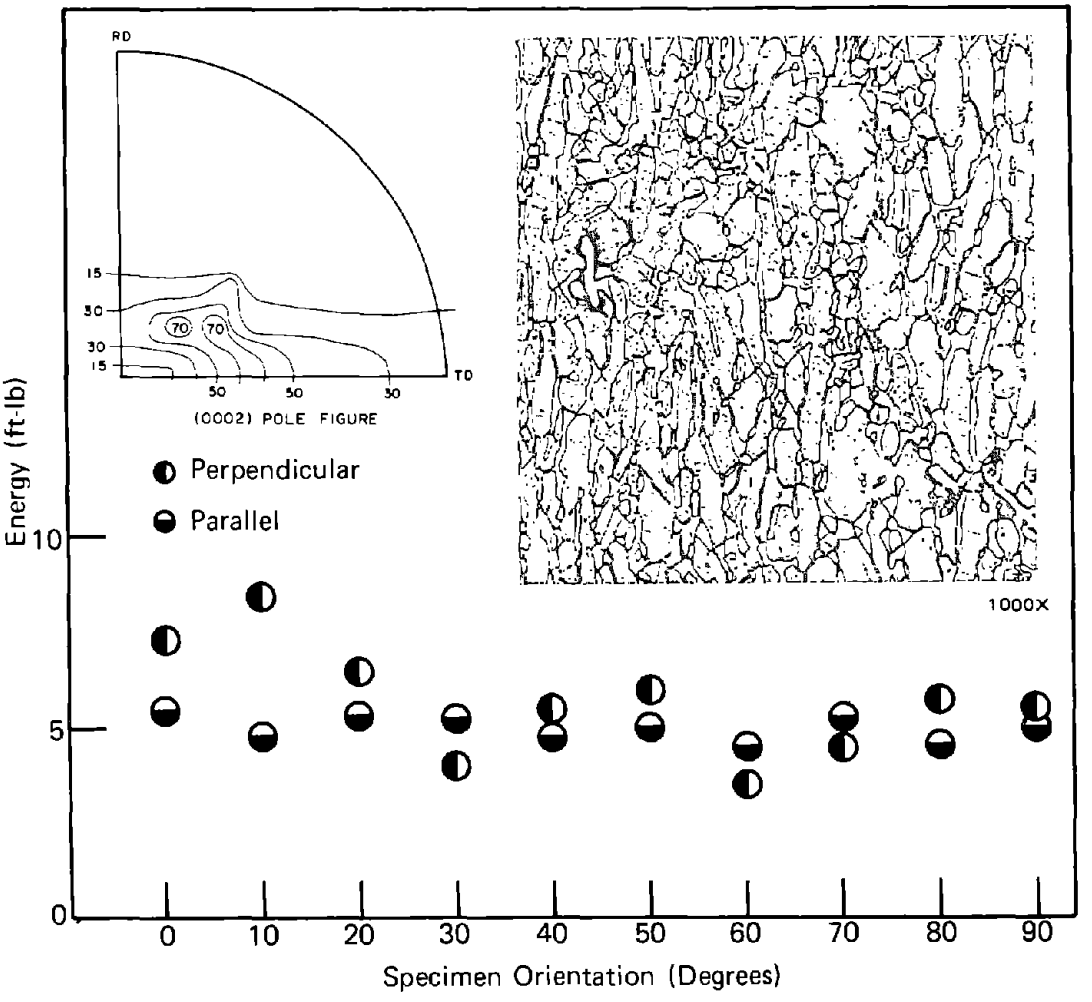

FIGURE 48. TYPICAL CHARPY IMPACT TEST DATA FOR Ti-8Mn ALLOY[116]

Orientation	Thick (in.)	Yield Strength (psi) 0.1%	Yield Strength (psi) 0.2%	Tensile Strength (psi)	Elon. %	E x 10^6 (psi)	μ_E	μ_P
L	0.460	93,500	97,400	110,700	19.0	16.5	0.242	0.188
T	0.475	99,600	102,500	115,600	21.5	16.2	0.246	0.226
L	0.472	112,300	114,800	119,100	17.0	17.7	0.250	0.369
T	0.507	118,300	120,700	127,400	20.5	19.7	0.300	0.321

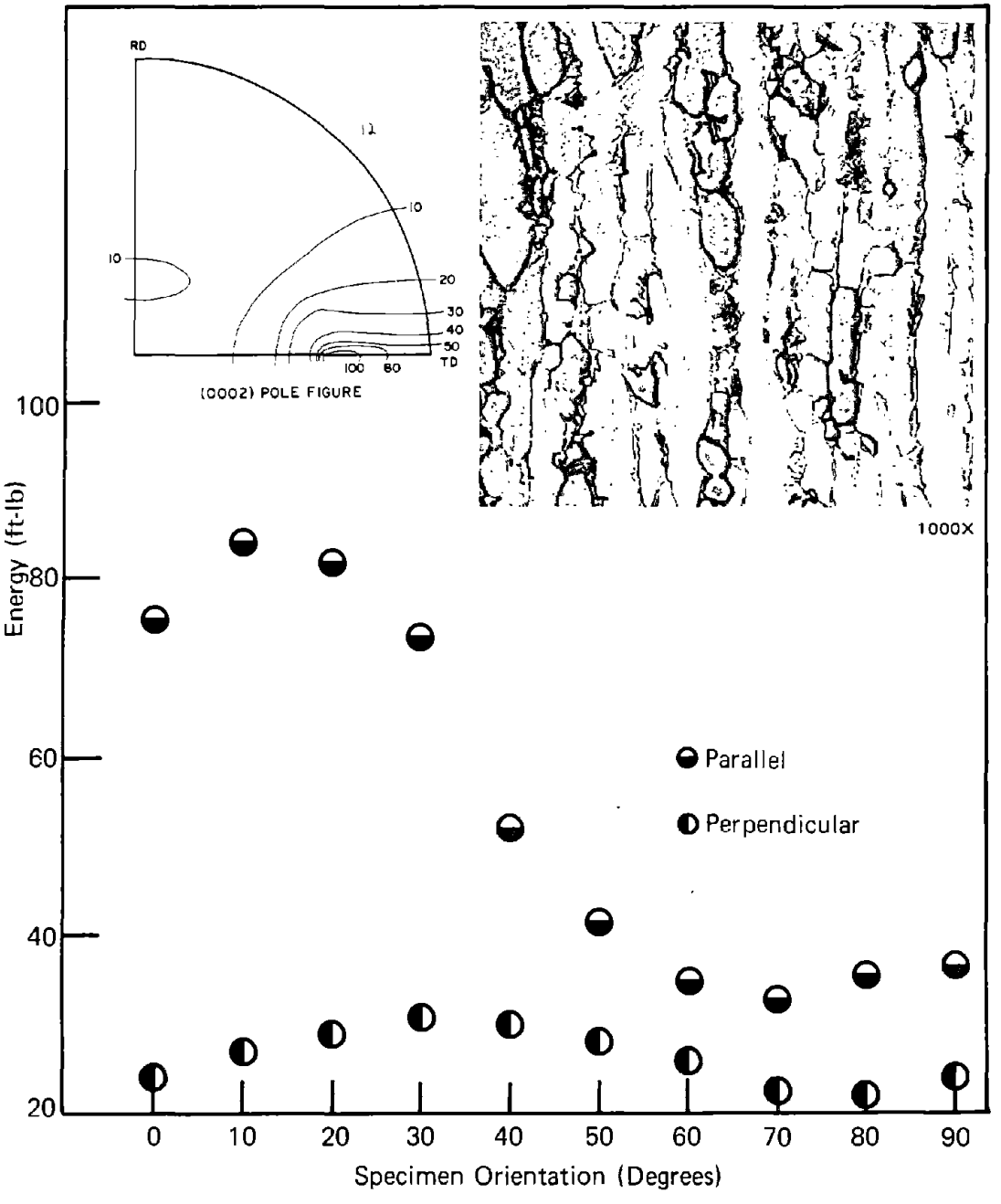

FIGURE 49. TYPICAL CHARPY IMPACT TEST DATA FOR Ti-4Al-4V ALLOY[116]

Orien-tation	Thick (in.)	Yield Strength (psi) 0.1%	0.2%	Tensile Strength (psi)	Elon. %	E x 10^6 (psi)	μ_E	μ_P
L	0.525	120,000	122,200	130,200	14.0	16.3	0.257	0.250
T	0.527	132,100	134,700	140,800	10.0	19.7	0.300	0.444

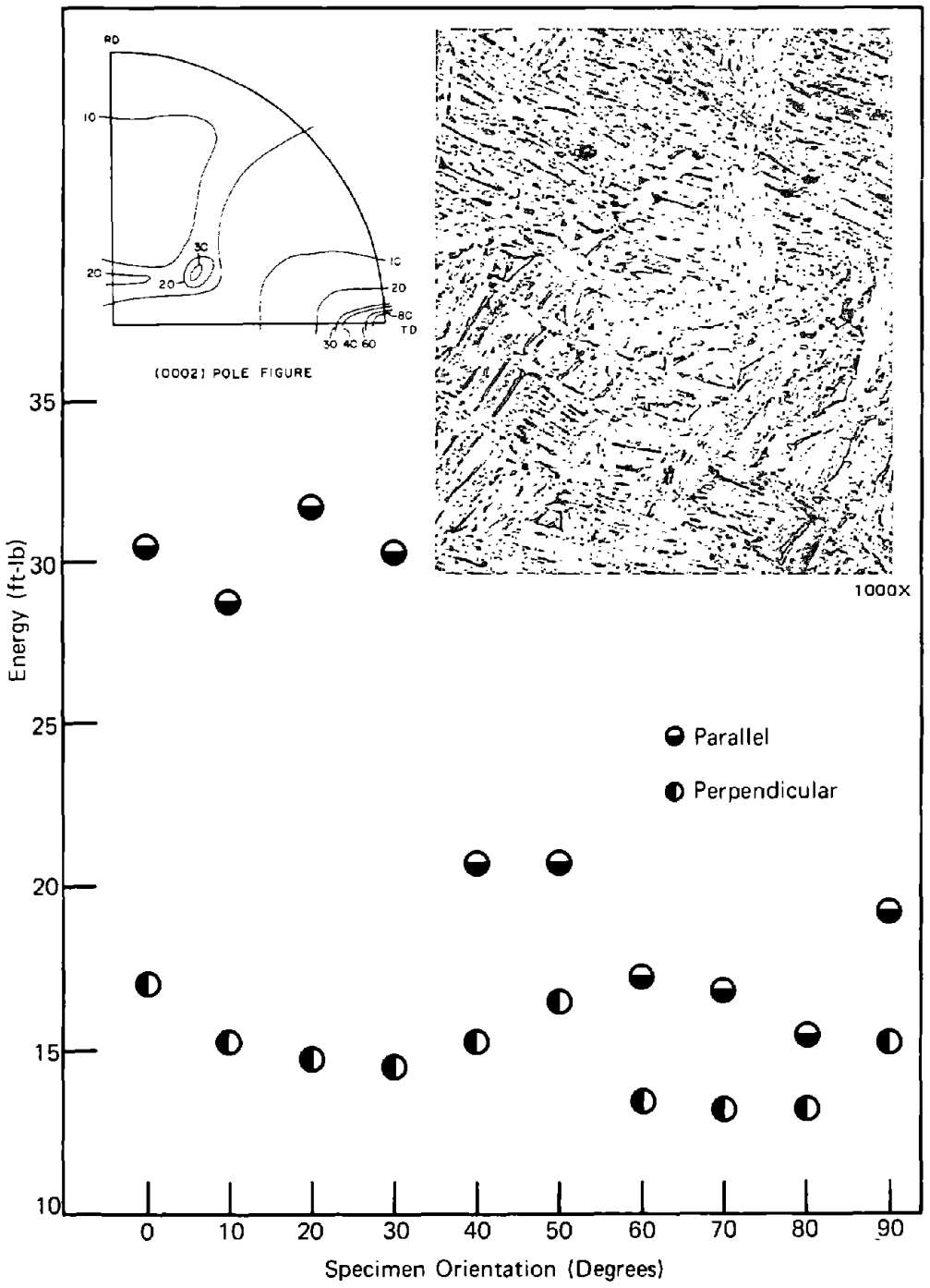

FIGURE 50. TYPICAL CHARPY IMPACT TEST DATA FOR Ti-6Al-4V ALLOY [116]

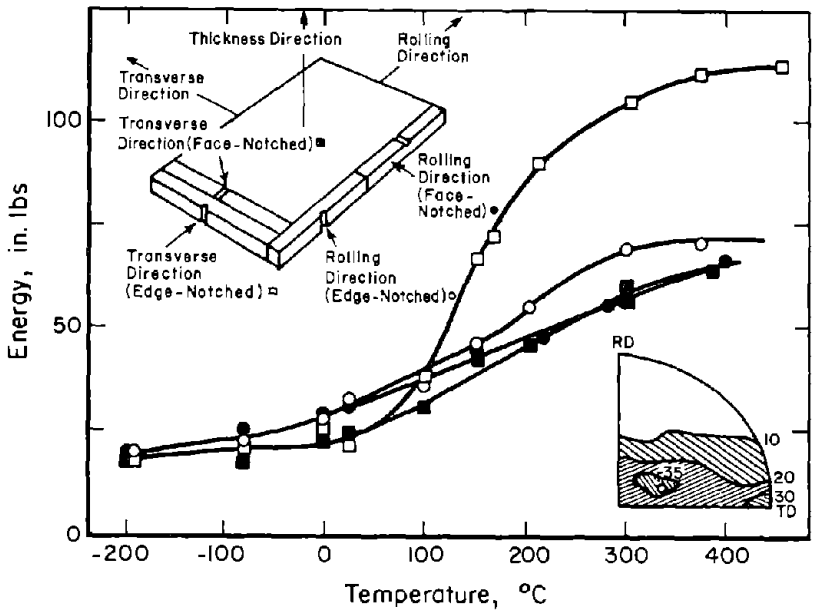

FIGURE 51. IMPACT STRENGTH OF Ti-5Al-2.5Sn[117]

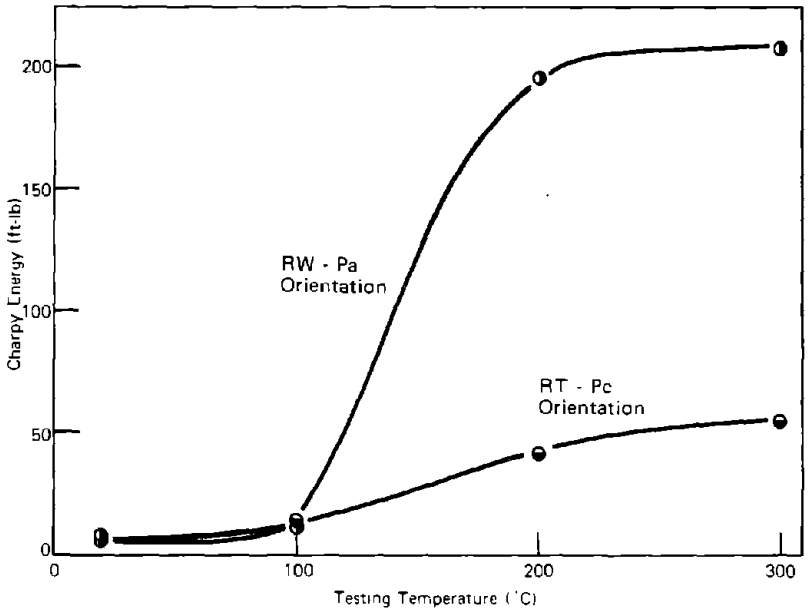

FIGURE 52. EFFECT OF TEXTURE ON THE TRANSITION TEMPERATURE OF UNALLOYED TITANIUM[116]

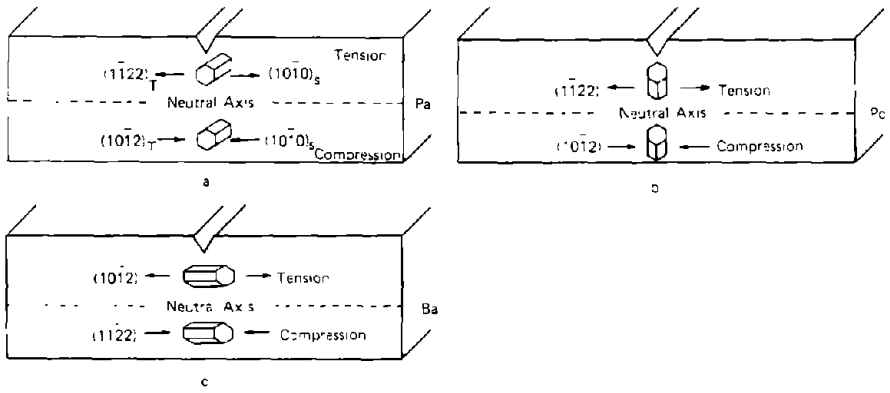

FIGURE 53. SPECIMEN DEFORMATION MODES AND TEXTURE ORIENTATION[116]

owing to the plane-strain constraints at the base of the notch, a higher temperature is needed for plastic flow and high toughness. Predictions are for large compressive deformations at the back side of the specimen. Finally, the Ba-orientation specimen is not favorably oriented for slip or any of the known slip systems since the stress is perpendicular to the $[11\bar{2}2]$ direction. In this case $(10\bar{1}2)$ twinning probably occurs, and the reoriented matrix would now be favorably oriented for $(11\bar{2}2)$ twinning and susceptible to fracture (Figure 53c).

While the mechanisms proposed above are somewhat speculative, and further research is required, they do provide a simple model for the description of texture and its influence on toughness, and this beginning of understanding should allow us to utilize textures to produce high-toughness materials.

Fracture Toughness, K_{Ic} and K_c

Very little information has been published on the influence of texture upon fracture toughness, K_{Ic} or K_c. Although there has been some discussion[95,124,125], most of the reports have not had pole figures and fracture-toughness values for the same material. Probably the most complete investigation was carried out on the SST program at the Boeing Co.[1-8] This program has shown that a large anisotropic variation in fracture toughness is present in Ti-6Al-4V extrusions, plate and sheet. Unfortunately, no clear simple description of the nature of the directional fracture-toughness properties is available at this time. However, textures can affect fracture toughness parameters K_{Ic} and K_c through a complicated influence upon strength and ductility. Plane-stress (K_c) toughness values are influenced in a different way than are plane-strain (K_{Ic}) values. The influence of preferred orientation upon toughness is very specific with each texture-specimen orientation relationship.

The plane-stress (K_c) values are usually lower in the longitudinal direction, as illustrated in Table 7. This appears to reflect the higher strength in the transverse direction when the texture consists mainly of basal poles parallel to the transverse direction. An "ideal" texture of course would have similar longitudinal and transverse properties. As the constraint of the notch increases or as plane-strain conditions are approached, there is a shift to higher longitudinal values (see Table 8). It is possible to also have higher K_c values in the longitudinal direction of a product that has strong transverse basal poles. This usually occurs in a thicker product as seen in Table 9. The variation of fracture toughness with texture and specimen orientation is a complex matter, and it really depends upon whether ductility or strength dominates in contributing to the energy consumed during fracture. In the case in Table 9 ductility dominates.

TABLE 7. FRACTURE TOUGHNESS (K_c) OF CONTINUOUSLY ROLLED Ti-6Al-4V SHEET[2]

Heat	Thickness, inch	K_c, ksi $\sqrt{in.}$ Grain Direction L	T
A	0.050	135.3	165.2
		134.8	167.2
B	0.060	149.5	178.7
C	0.016	134.9	140.0
D	0.035	131.0	161.9
E	0.058	158.4	203.9
		160.1	196.4
F	0.050	141.4	187.9
G	0.031	136.4	184.6
		136.0	188.6

TABLE 8. FRACTURE TOUGHNESS OF THICK CONTINUOUSLY ROLLED Ti-6Al-4V SHEET[2]

Specimen	Thickness, inch	Grain Direction	K_c, ksi $\sqrt{in.}$
1	0.125	T	109.5
2	0.110	L	148.5
3	0.110	L	154.1
4	0.110	L	154.3
1	0.150	T	157.0
2	0.150	L	163.0
3	0.150	L	165.1
4	0.150	L	160.5

TABLE 9. FRACTURE-TOUGHNESS DATA FOR 20-ft-long HAND-MILL Ti-6Al-4V SHEET[2]

Specimen	Thickness, inch	Grain Direction	K_c, ksi $\sqrt{in.}$
1	0.158	T	87.5
2	0.158	T	82.8
3	0.158	T	99.5
4	0.158	L	190.8
5	0.158	L	193.9

Frederick[125] reported the fracture toughness of 0.080-inch sheet of A-70 commercially pure titanium tested at -423 F. The results of these tests are shown in Figure 54. The basal pole figure is also included, which

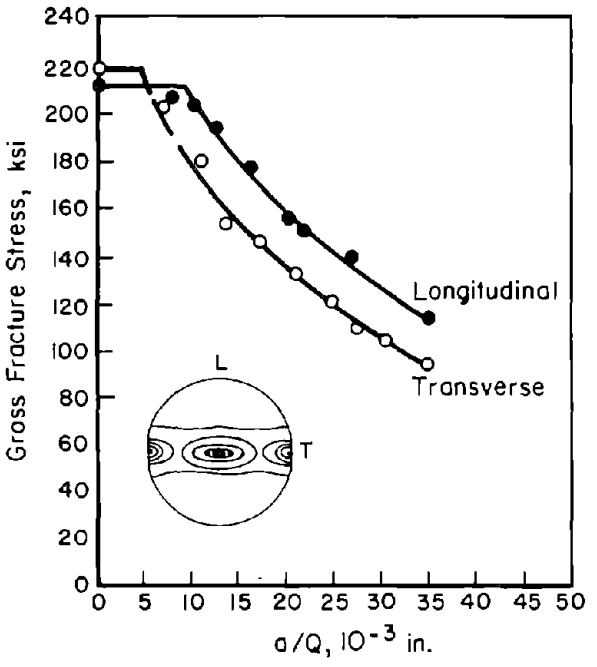

FIGURE 54. THE INFLUENCE OF ORIENTATION ON THE FRACTURE TOUGHNESS OF UNALLOYED TITANIUM SHEET TESTED AT -423 F[125]

Note: a = depth of crack
Q = shape factor after ASTM STP 381, p 249

reveals a duplex type of texture with both ideal and TD peaks. It is evident from this figure that the fracture toughness is somewhat higher in the longitudinal direction than in the transverse direction. This anisotropy in fracture toughness was attributed to the differences in ease of slip, the longitudinal specimens being favorably oriented for $(10\bar{1}0)\langle 11\bar{2}0\rangle$ slip.

The main bulk of the fracture-toughness data that are available come from the SST[1-8] program. Because of the interactions between chemistry, microstructure, and texture and their effect upon strength and ductility, the results are complicated. However, it can be shown that in many cases where there is a large component of basal poles in the TD, the K_c values are high in the transverse direction, as shown in Table 10. These results, which are for a mildly textured hand-mill sheet (see Figure 55 for texture), show that high K_c values are obtained in a direction perpendicular to the basal plane where the strength is highest. A more severely textured continuously rolled sheet (see Figure 55, Sheet B) was tested and the results also show a similar result as shown in Table 11.

Data on the effect of texture upon K_{Ic} values are much more limited and difficult to assess; however, it appears that the transverse values are high for conventional notch orientation, that is, through the plate. There are indications from other fracture tests that notches parallel to the plate surface can have very high toughness (see impact data in Figures 49 and 50). The main problem in understanding the influence of texture upon fracture toughness is the complicated three-dimensional interactions between specimen and notch orientation with the various types of textures. Probably the best way to elaborate upon the above discussion is to use illustrations from some of the limited data reported.

TABLE 10. AVERAGE FRACTURE TOUGHNESS OF Ti-6Al-4V SHEET

Gage	Direction	K_c
	Mill Annealed	
0.060	L	157.3
0.060	T	200.8
	Duplex Annealed	
0.075	L	170.2
	T	182.0
0.105	L	163.7
	T	172.8
0.100	L	148.2
	T	172.6

TABLE 11. FRACTURE TOUGHNESS AND STRESS-CORROSION RESISTANCE OF SUPER ELI CONTINUOUSLY ROLLED Ti-6Al-4V SHEET[8]

Specimen	Grain Direction	K_c, (ksi $\sqrt{in.}$)	Sustained K Level in 3.5% NaCl, (ksi $\sqrt{in.}$)
ST-310-3	Longitudinal	177.0	
ST-310-4	Longitudinal		No failure at 159 Failure at 177 (50 sec)
ST-310-1	Transverse	199.4	
ST-310-2	Transverse		No failure at 180, 200, 219 Failure at 239 (40 sec)

Harrigan[76] reported K_{Ic} fracture toughness values for textured Ti-6Al-2Sn-4Zr-6Mo for three specimen orientations along with the basal pole figure and tensile properties. These results are shown in Table 12 and Figure 56. The basal pole figure shows essentially a duplex texture with a heavy concentration of poles in the TD. The anisotropy of fracture toughness and tensile properties is

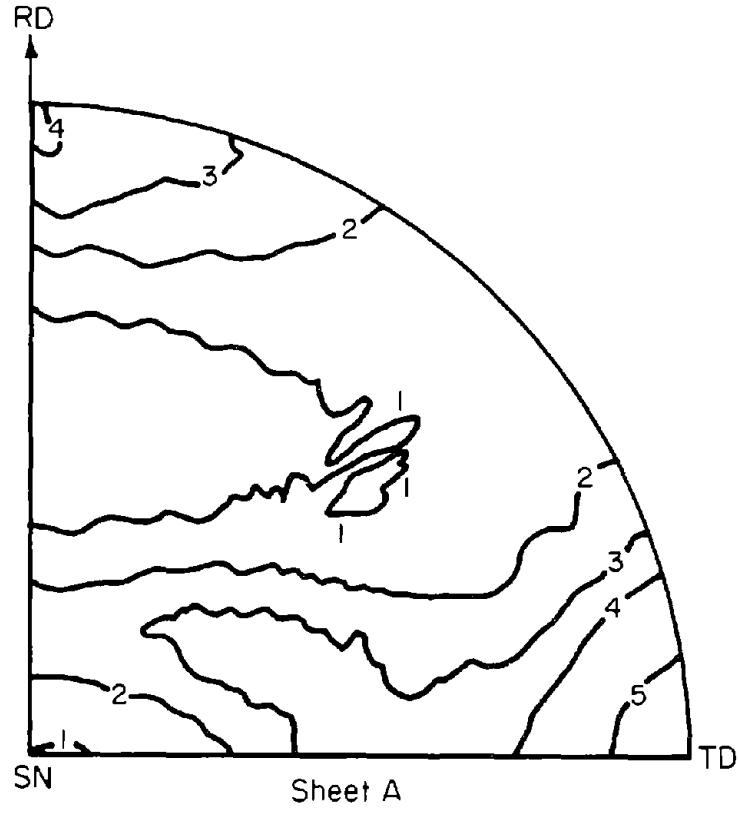

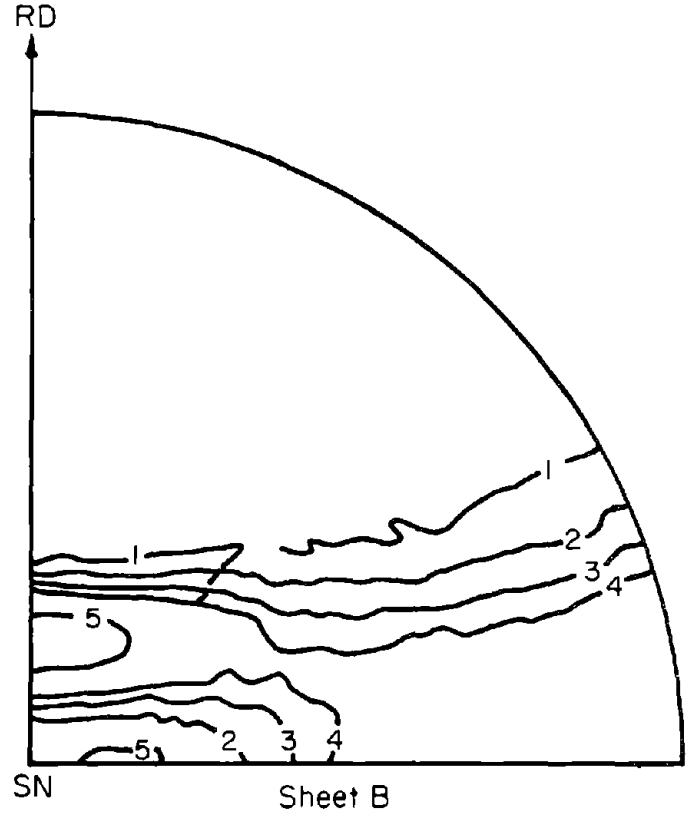

FIGURE 55. BASAL-PLANE POLE FIGURE FOR Ti-6Al-4V CONTINUOUSLY ROLLED SUPER ELI SHEET[8]

TABLE 12. SUMMARY OF MECHANICAL PROPERTIES FOR TEXTURED Ti-6Al-2Sn-4Zr-6Mo[76]

Orientation	F_{TU}, ksi	F_{TY}, ksi	Elong., %	R.A., %	K_{Ic}, ksi $\sqrt{in.}$
L or RW	148.7	138.2	11.5	18.0	67.8
T or WR	196.9	173.8	11.3	13.5	83.0
ST or TW	136.1	134.3	6.5	26.0	44.5

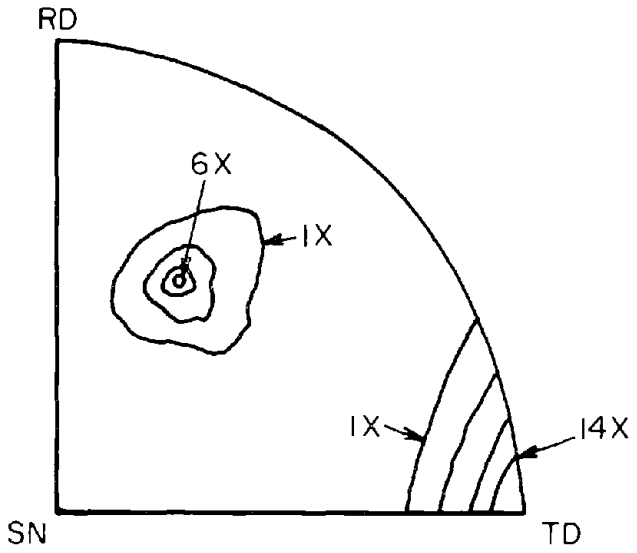

FIGURE 56. (0002) POLE FIGURE OF Ti-6Al-2Sn-4Zr-6Mo[76]

quite large. This investigation shows that the highest strength, modulus, and K_{Ic} are obtained in the transverse direction. Harrigan explains the higher transverse K_{Ic} as a modulus effect.

Backofen[21], using Hill's[88] mathematical theory of anisotropic yielding has shown that the effect of a notch in a textured product is dependent upon the specimen orientation and notch location. As an example, it was shown that an edge notch should be less embrittling, the higher the value of R. However, a face notch should become more embrittling. No actual values of K_{Ic} are available, although Hatch[113] does report some impact energy data which seem to support this.

Some results of the K_{Ic} testing showed only minor differences between WR and RW orientation in a plate with a heavy concentration of basal poles in the TD direction. These results are shown in Table 13. The higher K_{Ic} perpendicular to the highest concentration of basal poles, however, is still evident. The textures of the plates described in Table 13 are illustrated in Figure 57.

TABLE 13. FRACTURE TOUGHNESS OF ALPHA-PLUS-BETA-WORKED MILL ANNEALED Ti-6Al-4V PLATE[8]

Sheet	Specimen	Grain Direction	K_Q[(a)], ksi $\sqrt{in.}$
A	1	WR	54.4
	2	RW	68.5
B	5	WR	43.4, retest 48.5[(b)]
	6	RW	32.4, retest 52.5[(b)]

(a) K_Q values are provisional values for K_{Ic}.

(b) Not valid due to low deviation on load-deflection curve.

Stress-Corrosion Cracking

An excellent review of the status of stress-corrosion cracking of titanium has recently been published.[126] It has been shown that many material factors influence stress-corrosion cracking, among which are chemistry, microstructure, and texture. The sensitivity of stress-corrosion cracking to texture arises from the fact that the nature of stress-corrosion cracking is in part crystallographic. Several investigations have shown that stress-corrosion cracking occurs upon a plane about $(10\bar{1}7)$ near the basal orientation[127,128] (see Figure 58). This can lead to the development of large differences in the stress-corrosion cracking of various textured products.

One of the most outstanding examples where large effects can be demonstrated are in products that have highly textured basal poles which lie in the transverse direction.[129] Thus, through-notched samples cut longitudinally would not stress the basal plane, and transverse specimens would have the maximum stress on the basal planes.

Dramatic visual evidence of texture effects in stress-corrosion cracking in methanol-0.4 HCl can be obtained by observing the crack morphologies. This is illustrated in Figure 59. The crack path is very sensitive to the anisotropic nature of the cracking plane, and unusual crack-branching tendencies are observed. The influence of texture for crystallographic stress-corrosion cracking is manifested upon the threshold K_{Iscc} values. When the texture is such that the specimen does not stress the basal plane, then K_{Ic} is roughly equal to K_{Iscc}, or it can be said that the sample is not very susceptible to stress corrosion. On the other hand, when the texture is such that the maximum stress is applied to the basal plane, then the K_{Iscc} values will be very low. In these tests, longitudinal K_{Iscc} was 63 ksi $\sqrt{in.}$ and transverse K_{Iscc} was 28 ksi $\sqrt{in.}$, over a two-to-one difference.

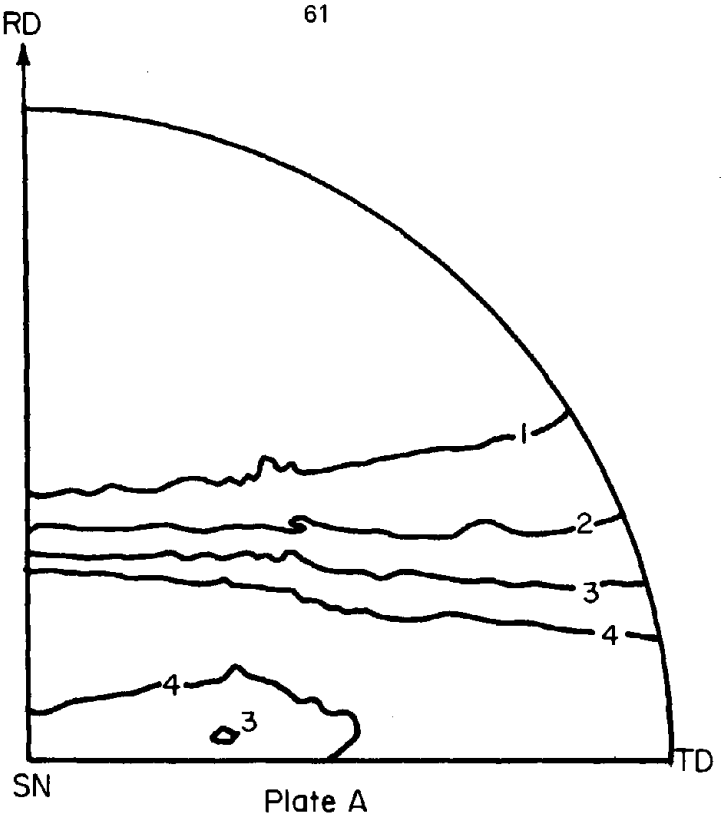

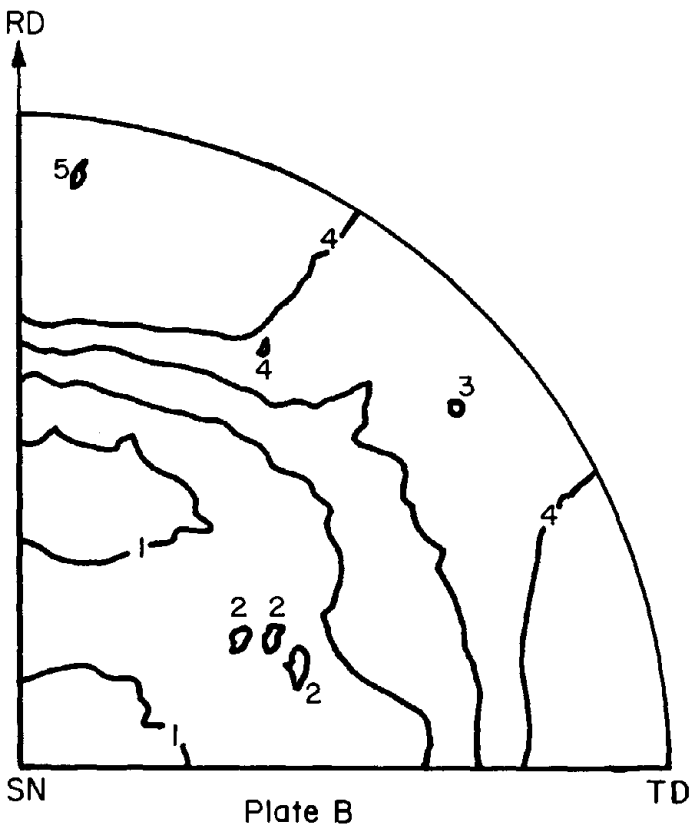

FIGURE 57. BASAL PLANE POLE FIGURE FOR ALPHA-PLUS-BETA-WORKED Ti-6Al-4V PLATE[8]

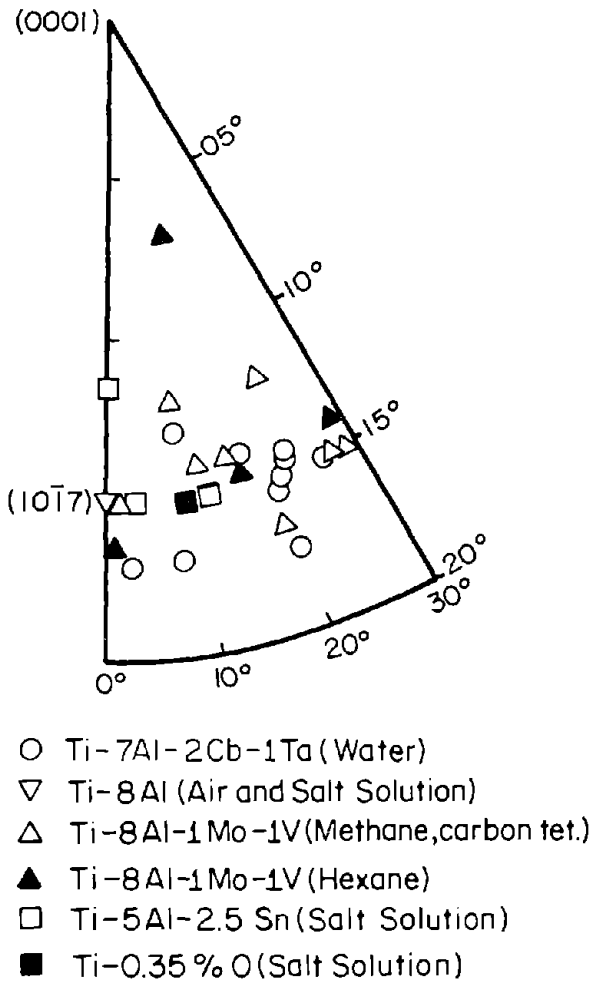

FIGURE 58. CENTRAL PORTION OF THE POLAR STEREOGRAPHIC PROJECTION OF A UNIT TRIANGLE OF THE HCP STRUCTURE SHOWING ORIENTATIONS OF CLEAVAGE PLANES IN TITANIUM ALLOYS TESTED UNDER CONDITIONS OF STRESS CORROSION [127]

The left side is the $\langle 11\bar{2}0 \rangle$ zone; the right side is the $\langle 10\bar{1}0 \rangle$ zone.

Differences in salt-water K_{Iscc} for longitudinal and transverse tests are further illustrated by data from the SST program[1] shown in Table 14. In almost every case the transverse tests were lower, which is indicative of textures which had high or moderate tendencies to develop TD peaks.

An excellent example of the directional characteristics of K_{Iscc} is shown in the work of Fager.[130] The results of his investigation clearly demonstrate the three-dimensional characteristics of stress-corrosion cracking and the influence of preferred orientation. These are shown in Figure 60. The crack morphology attributed to anisotropic crack propagation was also observed and is illustrated in Figure 61.

TABLE 14. LONGITUDINAL (RW) AND TRANSVERSE (WR) K_{Iscc} OF AS-RECEIVED Ti-6Al-4V PLATE[1]

Heat	K_{Iscc}, ksi $\sqrt{in.}$	
	Transverse	Longitudinal
A	36	55
B	36	–
C	36	53
D	36	55
E	44	–
F	35	65
E	36	36
G	45	–
H	36	–
I	36	36
J	36	–
K	37	–
L	36	–
M	36	55
L	53	–
M	22	53
N	35	–
O	35	46
P	35	–
Q	45	55

The crystallographic nature of stress-corrosion cracking suggests that texture could be employed as a means of alleviating stress-corrosion cracking. An "ideal" texture might be applied to resist stress-corrosion cracking. Collectively, the limited data available indicate the influence of texture upon stress-corrosion cracking, but also that much additional research work is needed to clearly define the interactions between cracking media, chemistry, microstructure, and texture.

EFFECT OF TEXTURE UPON FATIGUE

Of the various mechanical properties of metals that might be improved, fatigue is the most interesting and challenging. There has been an impressive amount of work on the fatigue properties of metals, yet, in spite of this, very little study has been made of fatigue anisotropy as related to texture. Chandrathil[131] studied fatigue of textured face-centered cubic sheet and concluded that it required work. He suggested that: "In the case of hcp metals the anisotropy of fatigue behavior might be expected to be particularly great when strong preferred orientations exist due to the limited number of slip systems".

Although considerable fatigue properties have been generated for titanium and its alloys, very little effort has been directed toward defining the effects of texture. The

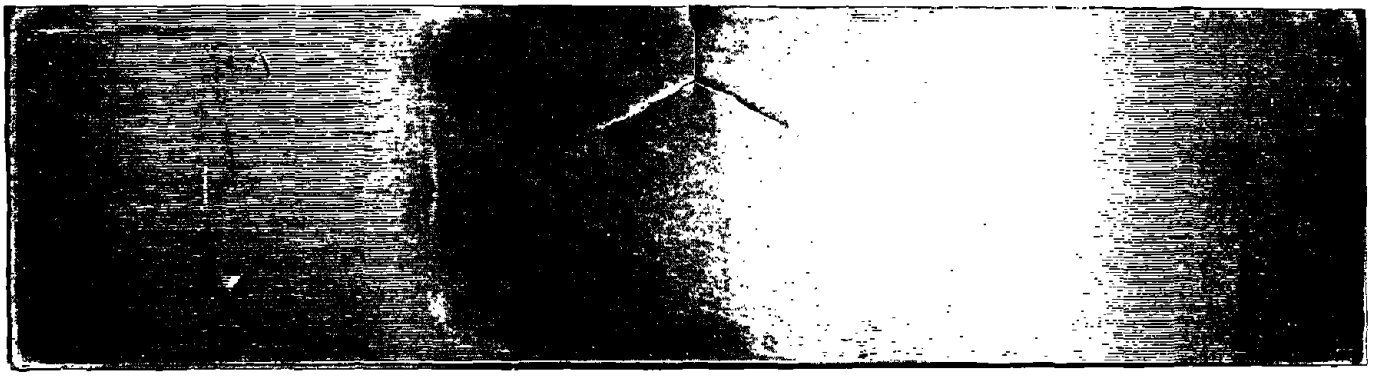

a. Longitudinal orientation, K_I = 63 ksi $\sqrt{in.}$

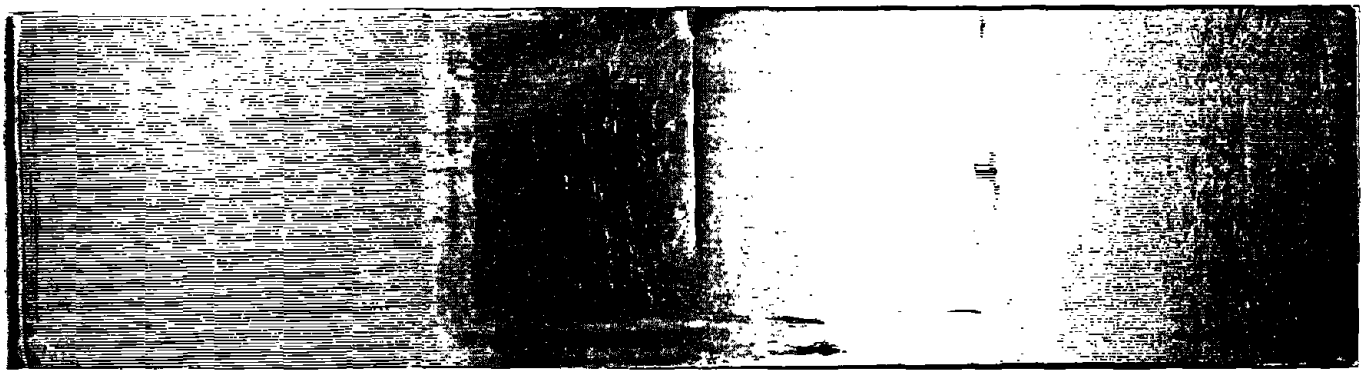

b. Transverse orientation, K_I = 28 ksi $\sqrt{in.}$

FIGURE 59. SCC MORPHOLOGY OF Ti-4Al-4V IN METHANOL-0.4 HCl

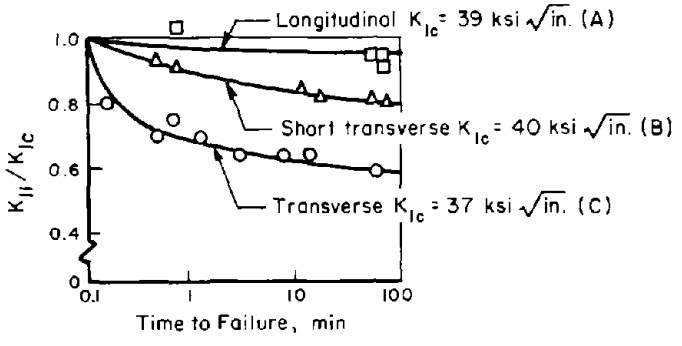

a. Stress-Corrosion Susceptibility as a Function of Specimen Orientation in Ti-8Al-1Mo-1V 0.5-in. Annealed Plate (Three-Point-Loaded Notched Bend Specimens)

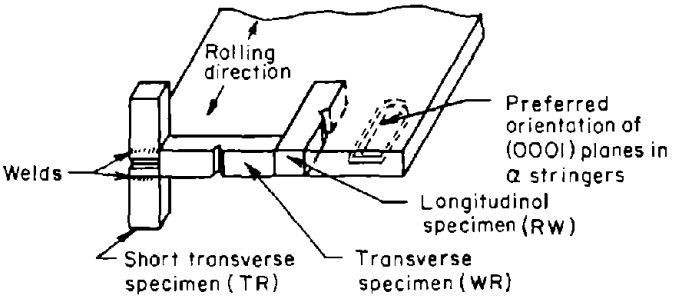

b. Orientation of Specimens in Ti-8Al-1Mo-1V 0.5-in. Plate

FIGURE 60. THE EFFECT ON STRESS CORROSION SUSCEPTIBILITY OF ORIENTATION OF Ti-8Al-1Mo-1V PLATE SPECIMENS[126]

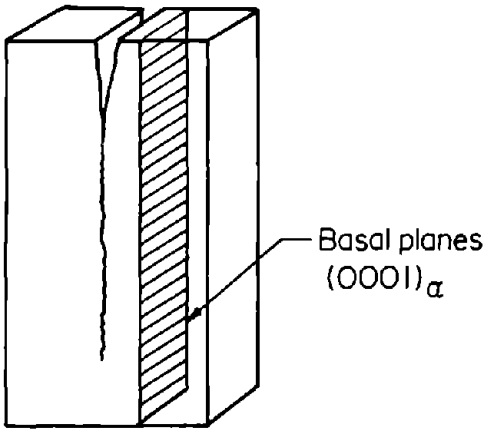

a. (0001) Planes Parallel to General Cracking Plane

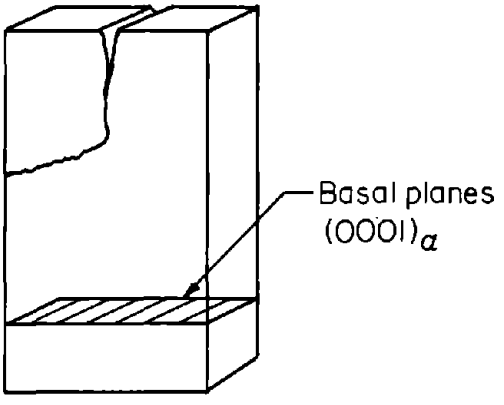

b. (0001) Planes Normal to General Cracking Plane

FIGURE 61. PROPOSED MECHANISMS FOR INFLUENCE OF TEXTURE ON CRACK PROPAGATION IN DCB SPECIMENS OF α OR $\alpha+\beta$ ALLOYS[126]

importance of texture can be demonstrated as an influence upon crack nucleation rather than on crack propagation. However, texture can be shown to also affect propagation through an influence upon slow-frequency propagation via a stress-corrosion-aided crack growth. One of the most disturbing aspects concerning the generation of smooth-bar fatigue data has been the scatter in the test data, and it is believed that texture plays a dominant role in influencing this scatter. Large variations have been found in both the endurance limit and the high-stress finite region.

The variation in fatigue properties as influenced by texture is also manifested in notched fatigue-crack-initiation results. Unfortunately, for both smooth and notch results, very little definitive results relative to the influence of texture are available. The limited results that have been obtained, however, are based upon fundamental reasoning and have been quite spectacular.

One of the most dramatic discoveries from recent texture research is related to a large improvement in fatigue properties. This finding could have widespread use in practical applications. Heretofore, there have been isolated cases of reported good fatigue properties in titanium, yet this has not been understood.[132] It is now believed that it is related to texture, as described in the following paragraphs.

Partridge[133] and others[134-136] have shown that the formation of deformation twins in hexagonal-close-packed metals like titanium can be very damaging to mechanical properties. In some cases, twin-matrix interactions have resulted in fracture nucleation sites, and the easy cyclic motion of a twin-matrix boundary can result in early crack initiation. Slip-band extrusions have also been noted as a mode of crack nucleation in fatigue-crack initiation.[137,138] Additional research has shown that slip-band extrusions and twin-matrix cracking are competing mechanisms.[139,140] It is possible to suppress twin formation and favor slip in single crystals by proper orientation. Likewise, it may be possible to suppress twin formation in highly textured polycrystalline material by similar considerations of orientation. Through consideration of texture-twin-orientation relationships, it should be possible to bring about a vast improvement in fatigue properties.

To test this hypothesis, two sets of smooth-bar fatigue samples from a highly textured Ti-4Al-4V[141] alpha-beta titanium alloy plate (see Figure 49 for static properties) were tested.

The first set was with the c axis of the texture parallel to the loading axis. This orientation is such that the principal mode of deformation is twinning. The second set was oriented in the a direction; slip is the principal mode of deformation. These specimens were tested in tension-tension (R = 0.1) and the results are shown in Figure 62.

As can be seen from Figure 62, there is a vast difference in the high-stress finite life region as was predicted. The c orientation (which forms twins) has a very short finite life. The a (slip orientation) samples have more than two log cycles superiority in this region and a remarkably long duration. Actually, one sample of the a orientation ran over 1.5×10^6 cycles at 90 percent of the yield strength.

Another important feature of these tests is the high ratio of 0.73 of the endurance limit to tensile strength for both orientations. This ratio has been widely variable in titanium, running from 0.25 to 0.80.[132] This large spread has been confusing and of concern to the designers. In retrospect, it now appears that since ease of cross slip is thought to be related to the endurance limit, the relationship between specimen orientation and texture can be controlled to suppress cross slip, thus favoring a high ratio of endurance limit to ultimate tensile strength.

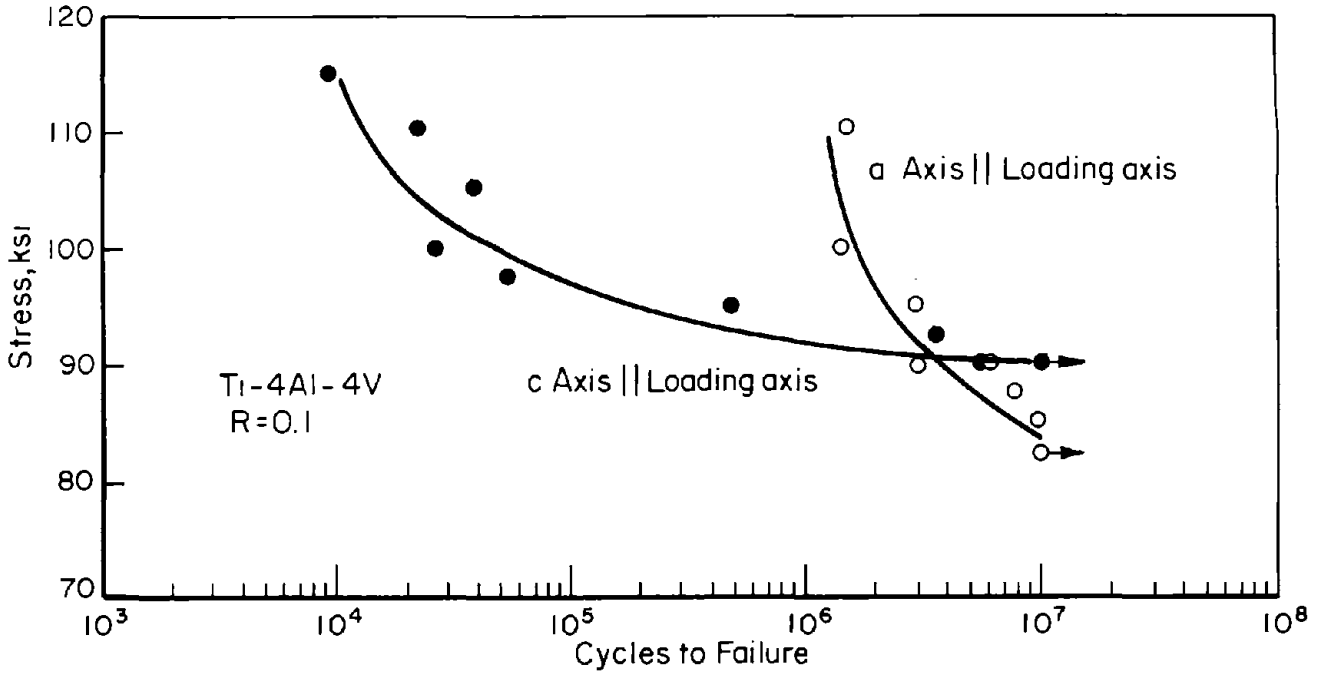

FIGURE 62. EFFECT OF SPECIMEN ORIENTATION ON FATIGUE LIFE

The high endurance limit could also be related to the perfect nature of the texture and lack of the stress concentrations that might be expected between adjacent anisotropic hexagonal grains. Just imagine the incompatibility of two adjacent hexagonal grains which are 90-degrees apart in orientation.

Since these improved fatigue properties appear to be related to crack nucleation rather than propagation, a difference in crack origin should be apparent. Scanning-electron-microscope studies clearly revealed this. Figure 63 illustrates the important crack-nucleation differences. For the good – fatigue, slip, orientation – examination of the test sample revealed a surface origin which was a classical slip-band extrusion-intrusion mechanism. In the twin-deformation orientation, crack origins were volumetric in nature occurring anywhere internally, and appeared earlier in the fatigue life, similar to that reported for twin-matrix cracks. Frederick[64] has carried out fatigue tests on highly basal textured Ti-6Al-4V sheet and has also found a high endurance limit. His results are shown in Figure 64. The mechanism of crack initiation in Ti-6Al-4V has also been studied[142;143], and both slip and twinning have been evident. Bowen[144] studied the directionality of a Ti-6Al-4V bar forging which apparently had a mild and varying texture. He found a large difference in endurance limit for various directions and much scatter was evident. The results are shown in Figure 65.

It has generally been established[145-148] that a heavily worked α and β structure has superior fatigue properties. This may be due to texturing as previously indicated.

The influence of a notch can be looked upon as enhancing or controlling nucleation. Crack initiation in hexagonal metals such as titanium is very complex when notches are considered. The deformation at the root of a notch is also affected by the thickness of the specimen, that is, whether the material is subjected to plane-strain or plane-stress loading. The results for thin specimens (plane stress) are quite different than those for thick specimens (plane strain). One of the best illustrations of thin-specimen results comes from the SST program.[8] S-N fatigue longitudinal data were generated on two notched .060-inch-thick sheets with different texture. For the highly textured sheet (Figure 66) which had an intense TD peak, the endurance limits are quite high. The longitudinal values are superior to the transverse, probably because of the ineffective nature of the notch when plastic deformation can occur by prism slip in the through-thickness direction. In the case of a transverse specimen, the notch-reduction factor for the endurance limit is about what would be expected for a highly textured material, i.e., 2.5. The lower endurance limits for milder textures or textures which have orthogonal components are also indicated in Figure 66. Here again the damaging effects of grain misalignment are evident.

In thicker specimens the effect of specific deformation mechanisms is more evident, because the constraints imposed by the notch require plane-strain deformation, and the actual mode of deformation which is operative may be

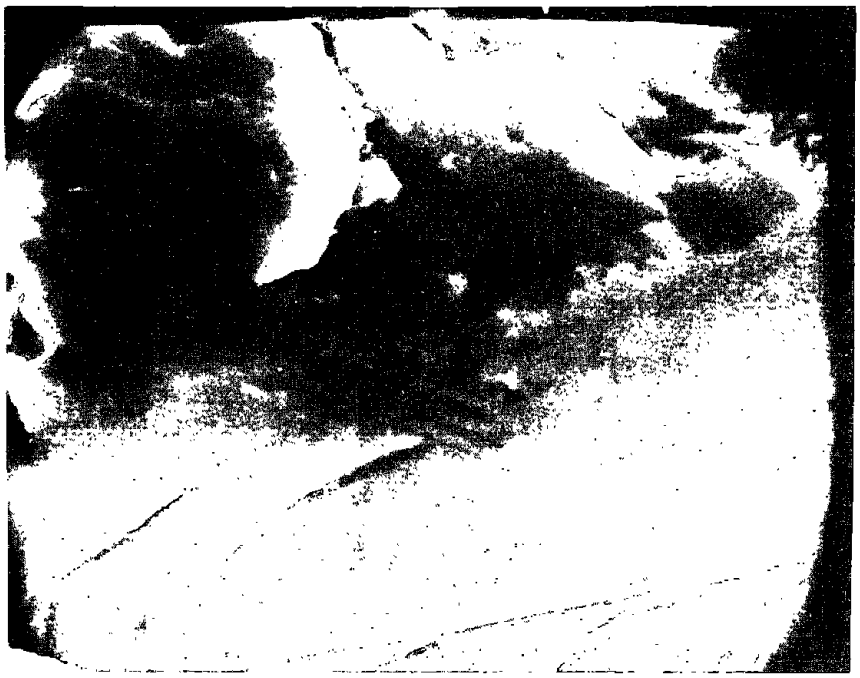

X7000

"a" – Slip Orientation

X1400

"c" – Twin Orientation

FIGURE 63. FRACTURED SURFACES OF SMOOTH (UNNOTCHED) FATIGUE SPECIMENS IN Ti-4Al-4V ALLOY

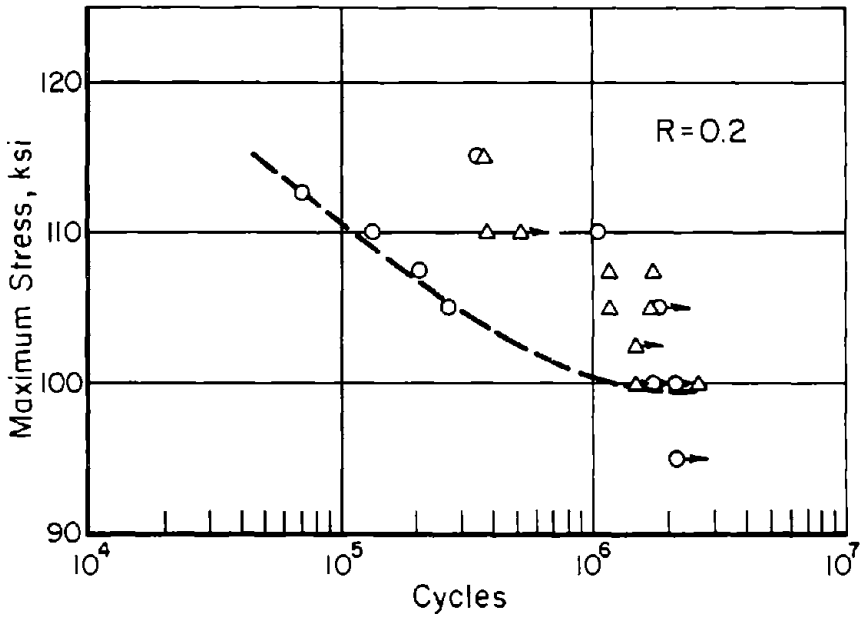

FIGURE 64. FATIGUE TEST RESULTS FOR SMOOTH (UNNOTCHED) SPECIMENS OF HIGHLY BASAL-TEXTURED Ti-6Al-4V SHEET[64]

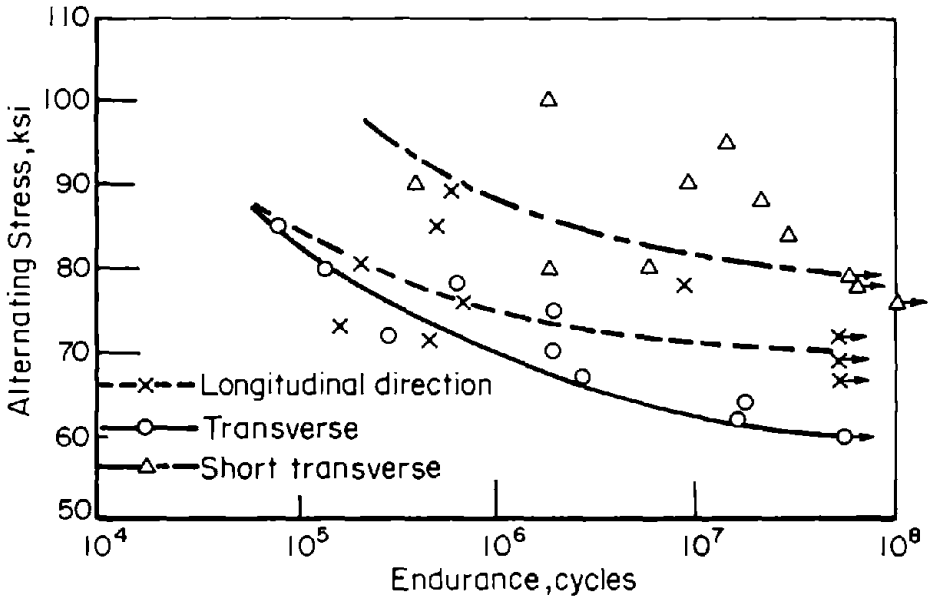

FIGURE 65. THE EFFECT OF TESTING DIRECTION ON THE FATIGUE LIFE OF THE 2.25-INCH THICK FORGED AND ANNEALED Ti-6Al-4V BAR[144]

surmised. In this case, the notch will cause a specific twin mode to activate. Different twin modes cause different degrees of damage to ductility, and the lattice strain is very unique with each mode. Thus, each notch orientation-texture type will have specific behavior characteristics which are related to the damage done by the twin formation. An example of this behavior is shown in Figure 67 where the specimen having the $(10\bar{1}2)$ type twin, which is less damaging to ductility, exhibits a large number of cycles to fatigue initiation. In this case, it was also shown that once the crack starts, the propagation stage is not much affected by notch orientation. Generally speaking, it has been found that propagation is not greatly affected by texture or specimen orientation (see Figure 68).

In opposition to the general case, there are cases where large propagation effects are shown. These, however, can be related to stress-corrosion cracking, as was illustrated in the section on influence of texture on stress-corrosion cracking. Suffice it to say again that stress-corrosion cracking is in some cases crystallographic in nature and occurs near the $(10\bar{1}7)$ or almost on the basal plane. Thus, in an aggressive environment where slow cyclic loading is occurring, an accelerated crack growth can

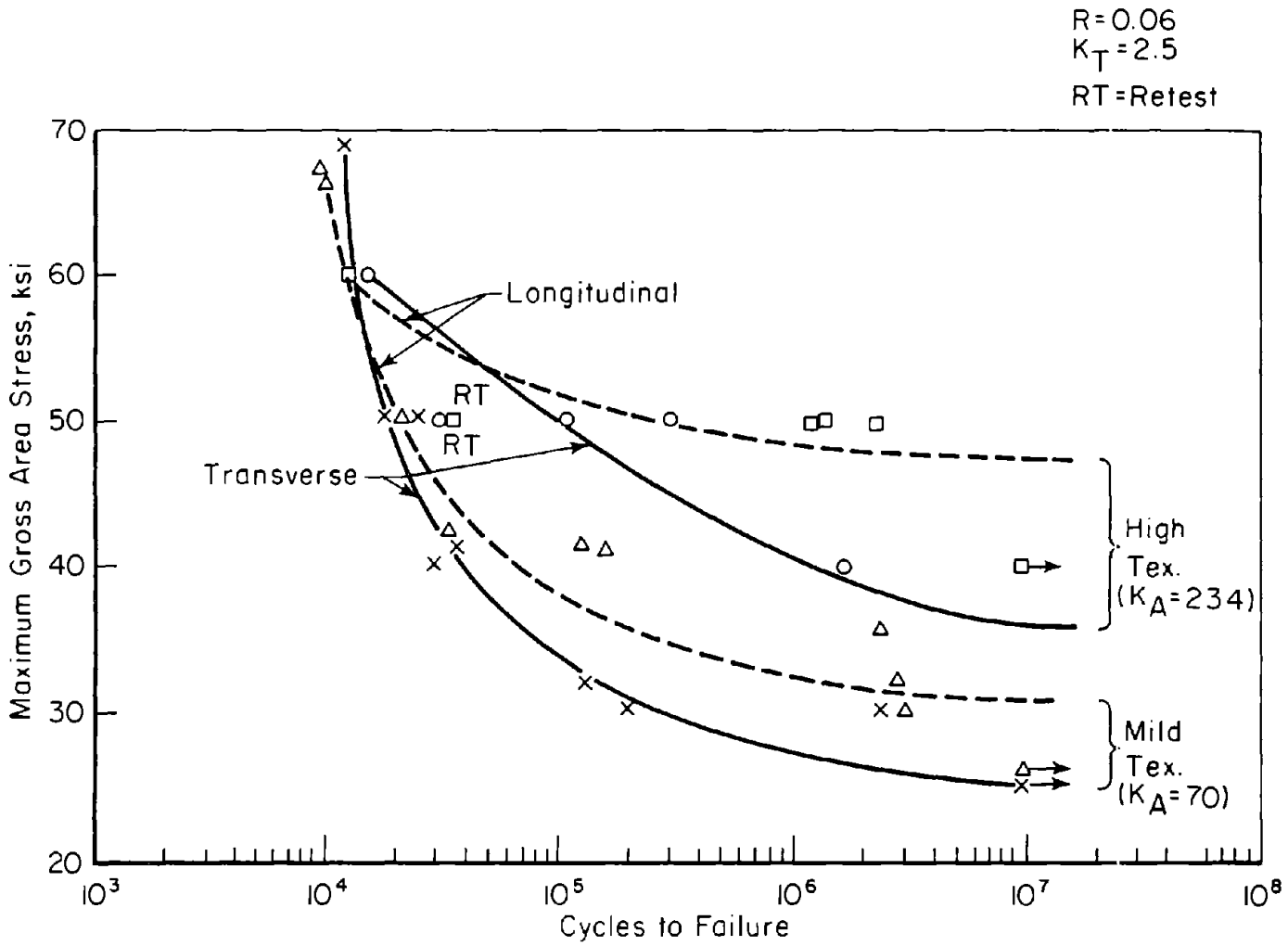

FIGURE 66. FATIGUE PROPERTIES OF CONTINUOUSLY ROLLED, Ti-6Al-4V SHEET, 0.050-INCH THICK [8]

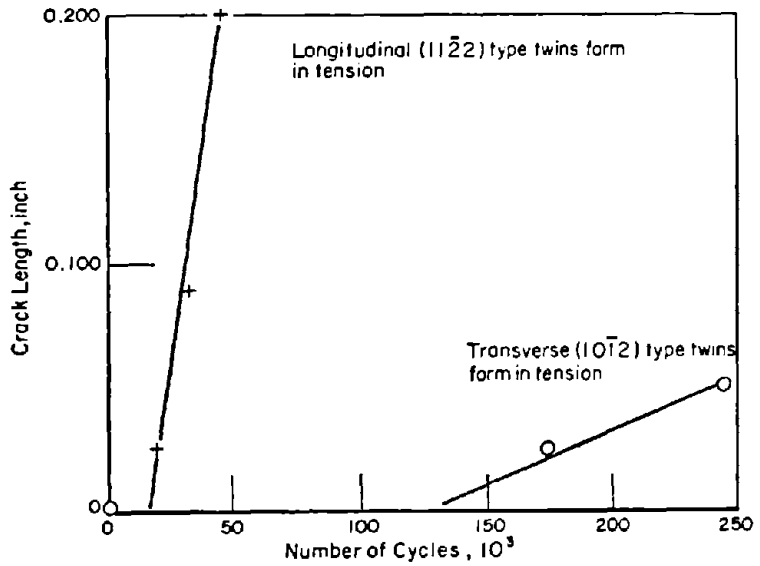

FIGURE 67. EFFECT OF TWIN FORMATION ON CRACK INITIATION

Transverse bend specimens subjected to about 20 percent higher loads.

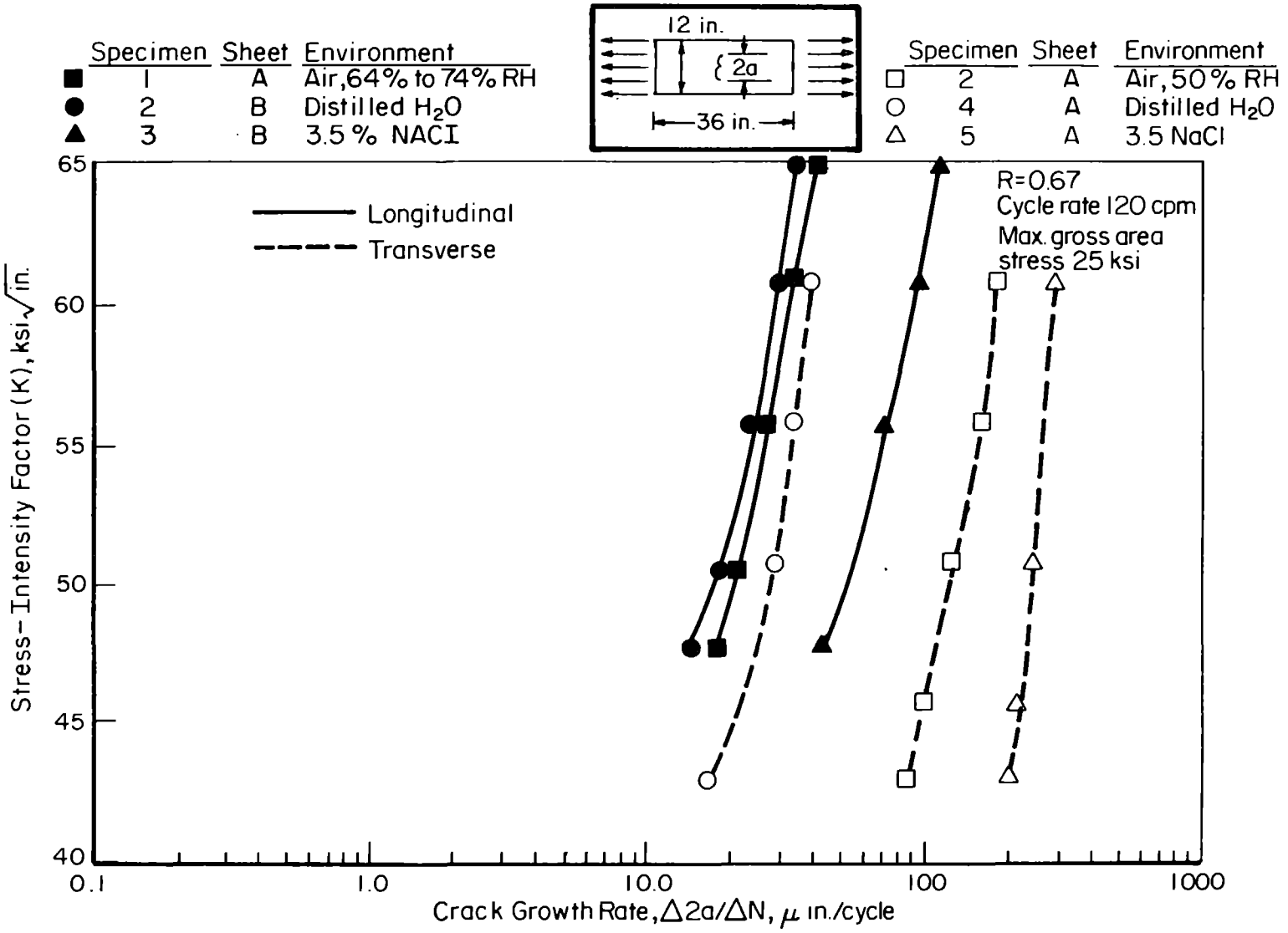

FIGURE 68. EFFECT OF K ON CRACK GROWTH RATE FOR CONTINUOUSLY ROLLED 0.050-INCH SHEET[2]

develop through stress-corrosion assists. This phenomenon is best shown by running longitudinal and transverse tests on textured materials where the basal poles are parallel to the transverse direction. Figure 68 illustrates this. A detailed comparison of various environments and their influence on the fatigue-crack propagation rate of material with a preponderance of basal poles parallel to the transverse direction is shown in Table 15.

TABLE 15. CRACK-GROWTH-RATE SUMMARY FOR CONTINUOUSLY ROLLED TEXTURED Ti-6Al-4V SHEET

K, ksi $\sqrt{in.}$	Environment	Grain Direction	$\Delta 2a/\Delta N$, 10^{-6} in./cycle Range	Avg	Tests
50	Air	L	17-28	20	7
		T	17-29	21	7
50	3.5% NaCl	L	21-56	32	7
		T	64-245	146	8
50	Distilled H_2O	L	20-53	31	7
		T	53-158	105	6
60	Air	L	27-44	33	7
		T	27-44	33	7
60	3.5% NaCl	L	37-84	60	7
		T	142-280	228	8
60	Distilled H_2O	L	33-74	53	7
		T	83-182	125	6

CREEP AND STRESS RUPTURE

Limited results of creep and stress-rupture tests conducted on a textured α-β titanium alloy indicate a significant variation in these properties with relation to specimen orientation.[141,149] Two sets of creep-stress-rupture bars from a highly texture plate of Ti-4Al-4V alloy (see Figure 49 for typical texture and static properties) were tested. The first set was with the c axis of the texture parallel to the loading direction (specimen axis transverse to the rolling direction). This orientation is such that the principal mode of deformation is twinning. The second set was oriented in the a direction (specimen axis longitudinal to the rolling direction) where slip is the principal mode of deformation. These specimens were creep tested at 850 F, in air, in constant-load creep machines. Creep curves at a 50-ksi level as well as stress-rupture curves for each orientation are shown in Figures 69 and 70.

The strain rate for secondary creep in the specimen cut in the longitudinal or a direction is 8.83×10^{-4} in./in./hr and that for the transverse or c direction is 1.38×10^{-4} in./in./hr. This is a 6.4 times greater creep rate in the longitudinal direction than the transverse direction.

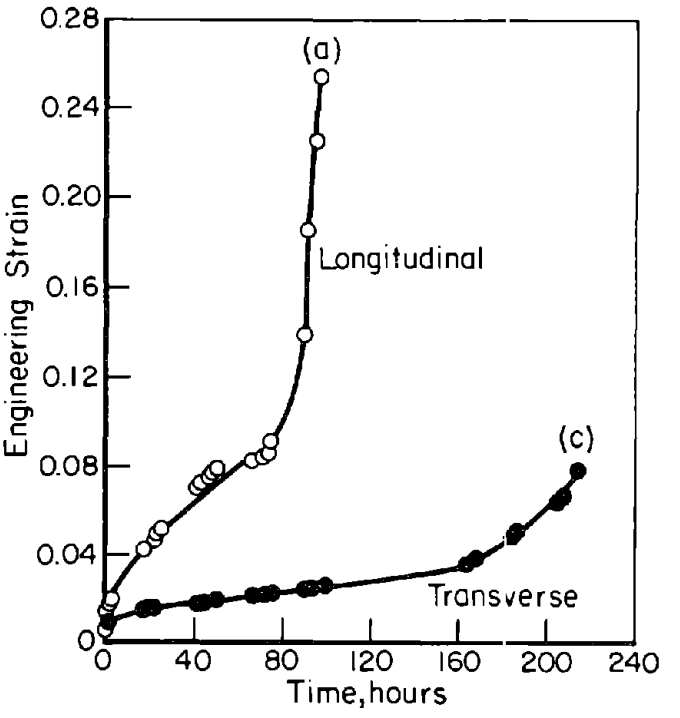

FIGURE 69. CREEP CURVES FOR TEXTURED Ti-4Al-4V IN TRANSVERSE AND LONGITUDINAL ORIENTATIONS AT 850 F AND 50,000 PSI

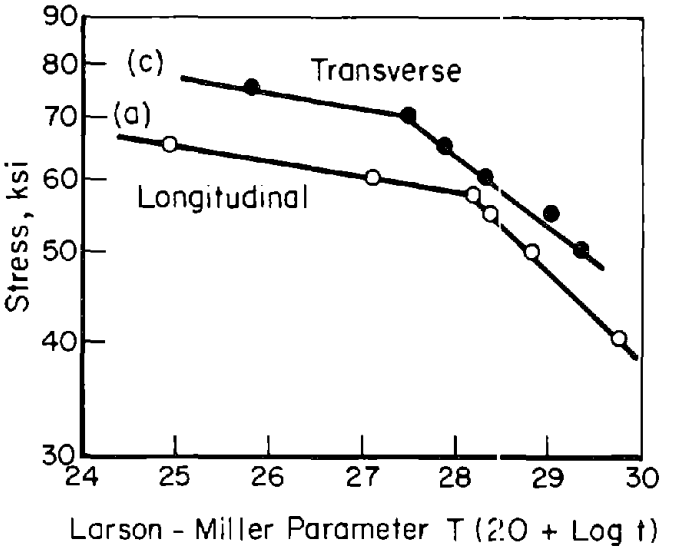

FIGURE 70. LARSON-MILLER PLOT OF STRESS-RUPTURE DATA OBTAINED FOR TEXTURED Ti-4Al-4V IN THE TRANSVERSE AND LONGITUDINAL ORIENTATIONS AT 850 F

The transverse specimens also have a superior stress-rupture life compared with the longitudinal specimens. For a given parameter there is a 5,000-psi increase in stress capability at the low-stress end and approximately a 12,000-psi increase in stress capability at the higher stresses. Thus, these data indicate that texture and orientation significantly affect creep and stress-rupture properties of titanium alloys. Results for zirconium and its alloy have yielded similar conclusions and it is clear that considerable additional work is needed to fully define this important area.

REFERENCES

(1) Parkinson, F. L., "Beta Processed Titanium 6Al-4V Plate", DOT/SST Report No. FAA-SS-72-0, Boeing Co., July 1972.

(2) Parkinson, F. L., "Titanium Alloy 6Al-4V Sheet", DOT/SST Report No. FAA-SS-72-01, Boeing Co., July 1972.

(3) Jensen, G. A., and Eichenberger, T. W., "Titanium Alloy 6Al-4V Mechanical Property Data", DOT/SST Report No. FAA-SS-72-02, Boeing Co., March 1972.

(4) Spurr, W. F., "Titanium Alloy 6Al-4V Bar and Forgings", DOT/SST Report No. FAA-SS-72-04, Boeing Co., May 1972.

(5) Quist, W. E., "Titanium Alloys 6Al-4V and 3Al-2.5V Hydraulic Tubing", DOT/SST Report No. FAA-SS-72-05, Boeing Co., July 1972.

(6) Harruff, G. W., et al, "Titanium 3Al-2.5V CW Hydraulic Tubing Development", DOT/SST Report No. FAA-SS-72-60, Boeing Co., October 1972.

(7) Spurr, W. F., "Titanium Alloy 6Al-4V Extrusions", DOT/SST Report No. FAA-SS-72-06, Boeing Co., July 1972.

(8) Parkinson, F. L., "Mechanical and Metallurgical Characteristics of Titanium Alloy 6Al-4V", DOT/SST Report No. FAA-SS-72-13, Boeing Co., July 1972.

(9) McClintock, F. A., and Argon, A. S., eds. Mechanical Behavior of Materials, Addison-Wesley, 1966.

(10) Whiteley, R. L., "The Importance of Directionality in Drawing Quality Sheet Steel", Trans. ASM, v. 52, 1960, p 154-169.

(11) Klewan, A., and Bernsten, V., "Crystallographic Texture in Ti-5Al-2.5Sn Sheet Material", SAAB-SCANIA AB, Sweden, TR TCM-71-69.

(12) Cullity, B. D., Elements of X-Ray Diffraction, Addison Wesley, 1956.

(13) Lopata, S. L., and Kula, E. B., "A Reflection Method for Pole Figure Determination", Army Materials and Mechanics Research Center, WAL TR 826.52/1, July 1961; also Trans. AIME, J. of Metals, v. 224, August 1962, p 865.

(14) Romero, C. J., "The Effect of Microstructure and Preferred Orientation on the Mechanical Behavior of Titanium Alloy Forgings", Lockheed-California Co., LR 24347, June 1971.

(15) Larson, F. R., "Anisotropy of Titanium Sheet in Uniaxial Tension", Army Materials & Mechanics Research Center, AMRA TR 63-36, December 1963; also Trans. ASM, v. 57, 1964, p 620-631.

(16) Zarkades, A., and Larson, F. R., "Texturing in an Age-Hardened Ti-6Al-4V", Army Materials & Mechanics Research Center, AMMRC TR 69-32, December 1969.

(17) Corn, D. L., and Weiman, S. M., "The Effect of Heat Treatment on Texturing in Ti-4Al", Douglas Missile & Space Systems, Report No. 59538, January 1967.

(18) Tucker, G.E.G., "Texture and Earing in Deep Drawing of Aluminum", Acta Met., v. 9, 1961, p 275-286.

(19) Graham, C. D., Jr., "Textured Magnetic Materials", General Electric TIS 64-RL-3752M.

(20) Chin, G. Y., Hart, R. R., and Wonsiewicz, B. C., "Textured Phosphor Bronze — A Superior Spring Material", Trans. AIME, v. 245, 1969, p 1669-1671.

(21) Backofen, W. A., Hosford, W. F., and Burke, J. J., "Texture Hardening", Trans. ASM, v. 55, 1962, p 264-267.

(22) Babel, H. W., and Frederick, S. F., "A Review of Texture Strengthening of Titanium Alloys", Journal of Metals, v. 20, 1968, p 32-38.

(23) Packer, C. M., "Texturing in Titanium", New York University Titanium Course Lecture 7, September 1969.

(24) Crossley, F. A., "Texture Strengthening of Heat-Treated Alpha-Beta Titanium Alloys", WESTEC Conference, Los Angeles, 1969.

(25) Chin, G. Y., and Mammel, W. L., "Computer Solutions of the Taylor Analysis for Axisymmetric Flow", Trans. AIME, v. 239, 1967, p 1400-1405.

(26) Hosford, W. F., and Backofen, W. A., Fundamentals of Deformation Processing, Syracuse University Press, 1964, p 259.

(27) Rittenhouse, P. L., and Picklesimer, M. L., J. Elect. Tech., v. 4, 1966, p 322.

(28) Barrett, C. S., and Massalski, T. B., Structure of Metals, McGraw-Hill, 1966.

(29) Dillamore, I. L., and Roberts, W. T., "Preferred Orientation — Wrought and Annealed Metals", Met. Rev., v. 10. no. 39, 1965, p 271-380.

(30) Underwood, F. A., Texture in Metal Sheets, McDonald Publishers, London, 1961.

(31) Hu, H., "Textures of Metals", U.S. Steel Corp. Research Lab., Penn., July 1972.

(32) Hall, E. O., Twinning, Butterworths, Scientific Publications, 1954.

(33) McQuillan, A. D., and McQuillan, M. K., Titanium, Butterworths, Academic Press, 1956, p 289.

(34) Paton, N. E., and Backofen, W. A., "Evidence for $\{10\bar{1}1\}$ Deformation Twinning in Titanium", Trans. AIME, v. 245, 1969, p 1369-1370.

(35) Williams, D. N., and Eppelsheimer, D. S., "The Cold Rolled Texture of Titanium", Trans. AIME, v. 197, 1953, p 1378-1382.

(36) Partridge, P. G., "The Crystallography and Deformation Modes of Hexagonal Close-Packed Metals", Met. Rev., v. 12, no. 118, November 1967, p 169-194.

(37) Williams, D. N., and Eppelsheimer, D. S., "A Theoretical Investigation of the Deformation Textures of Titanium", J. Inst. Met., v. 81, 1952-53, p 553-562.

(38) Calnan, E. A., and Clews, C.J.B., "Deformation Textures in Face-Centered Cubic Metals", Phil. Mag., v. 41, 1950 (vii), p 1085-10100.

(39) Calnan, E. A., and Clews, C.J.B., "The Development of Deformation Textures in Metals, Part II — Body Centered Cubic Metals", Phil. Mag., v. 42, 1951 (vii), p 616-635.

(40) Calnan, E. A., and Clews, C.J.B., "The Development of Deformation Features in Metals, Part III — Hexagonal Structures", Phil. Mag., v. 42, 1951 (vii), p 919-932.

(41) Calnan, E. A., and Clews, C.J.B., "The Prediction of Uranium Deformation Textures", Phil. Mag., v. 43, 1952 (vii), p 93-104.

(42) Keeler, J. H., and Geisler, A. H., "Preferred Orientations in Rolled and Annealed Titanium", Trans. AIME, v. 206, 1956, p 80-90.

(43) Hu, H., and Cline, R. S., "Mechanisms of Reorientation During Recrystallization of Polycrystalline Titanium", Trans. AIME, v. 242, June 1968, p 1013-1023.

(44) Roberts, W. T., "Preferred Orientation and Anisotropy in Titanium", J. Less-Common Metals, v. 4, 1962, p 345.

(45) McHargue, C. J., Adair, S. E., Jr., and Hammond, J. P., "Effects of Solid Solution Alloying on the Cold-Rolled Texture of Titanium", Trans. AIME, v. 197, 1953, p 1199-1203.

(46) Sparks, C. J., Jr., McHargue, C. J., and Hammond, J.P., "Effects of Aluminum on the Cold-Rolled Textures of Titanium", Trans. AIME, v. 209, 1957, p 49-50.

(47) Gokyu, I., Suzuki, H., Horucki, R., Nippon Kuizoku Gakkai-Si, v. 18, 1954, p 201.

(48) Larson, F. R., Zarkades, A., and Avery, D. H., "Twinning and Texture Transitions in Titanium Solid Solution Alloys", Army Materials & Mechanics Research Center, AMMRC TR 71-11, June 1971.

(49) Thornburg, D. R., and Puhler, H. R., "Cold Rolling Texture Development in Titanium and Titanium Aluminum Alloys", Titanium Science and Technology, Plenum Press, 1973.

(50) Thornburg, D. R., "Cold Rolling Texture Development in Titanium and Titanium Aluminum Alloys", Thesis, Dept. of Met. and M.S., Carnegie-Mellon University, Pittsburgh, Penn.

(51) Cook, M., and Richards, T. L., "Fundamental Aspects of the Cold Working of Metals", J. Inst. Metals, v. 78, 1950-51, p 463-482.

(52) Tarnovskii, I. Y., et al. Deformation of Metals During Rolling, Pergamon Press, 1965.

(53) Wever, F., "Texture of Metals After Cold Deformation", Trans. AIME Inst. of Metals Division, 1931, p 51-53.

(54) Hobson, O. O., "Textures in Deformed Zirconium Single Crystals", Trans. AIME, v. 242, 1968, p 1105-1110.

(55) Taylor, G. I., "Plastic Strain in Metals", J. Inst. Metals, v. 62, 1938, p 307-324.

(56) McHargue, C. J., Holland, J. R., and Hammond, J. P., "Hot Rolled Textures of Titanium Alloys", Trans. AIME, J. of Metals, v. 205, February 1965, p 113.

(57) Lockheed Missiles & Space Co., Palo Alto, Calif., "Development of Improved Biaxial Strength in Titanium Alloy Rocket Motor Cases Through Texture Hardening", AF Contract No. FO 4611-67-C0074, February 1969.

(58) Newkirk, J. B., and Geisler, A. H., "Crystallographic Aspects of the Beta to Alpha Transformation in Titanium", Act Met., v. 1, 1953, p 370.

(59) Barrett, C. S., Structure of Metals, First Ed., McGraw-Hill Book Co., New York, 1943.

(60) Koh, P. K., "Preferred Orientation in Titanium Alloy Thin Foils", Titanium Science and Technology, Plenum Press, 1972.

(61) Zarkades, A., and Larson, F. R., "A Review of Textures Found in Commercial Titanium Sheet", Army Materials & Mechanics Research Center, AMMRC TR 71-60, December 1971.

(62) Day, D. L., et al, "The Effect of Deformation Processing on the Mechanical Properties Ti-6Al-4V for Armor", Army Materials & Mechanics Research Agency, AMRA CR 66-06F, June 1966.

(63) Dull, D. L., and Amateau, M. F., "The Basal Textures of Ti-6Al-4V Processed by Various Methods", Aerospace Corp., TR 0066(5250-10)-15, February 1970.

(64) Frederick, S. F., "Manufacturing Methods for Production Process for Titanium Sheet with Controlled Texture", McDonnell Douglas Astronautics Co., Interim Tech Report Nos. IR-208-1 (1-V), 1972-1973.

(65) Amateau, M. F., et al, "The Effect of Processing on Plastic Strain Anisotropy of Ti-6Al-4V", Aerospace Corp., TR-0059 (6250-10)-5, September 1970.

(66) Zarkades, A., and Larson, F. R., "Elasticity of Titanium Sheet Alloys", The Science Technology and Application of Titanium, Pergamon Press, 1970 and Army Materials & Mechanics Research Center, AMMRC TR 68-10, May 1968.

(67) Flowers, J. W., Jr., O'Brien, K. C., and McEleney, P. C., "Elastic Constants of Alpha Titanium Single Crystals of 25 C", J. Less-Common Metals, 1964, p 393-5.

(68) Fisher, E. S., and Renken, D. J., "Single-Crystal Elastic Moduli and the HCP-BBC Transformations in Ti, Zi, and Hf", Physical Review, 135 (2A) 1964, p 482-94.

(69) Schmid, E., and Boas, W., Plasticity of Crystals, F. A. Hues, London, 1950.

(70) Wang, C. T., Applied Elasticity, McGraw-Hill, 1953.

(71) Alers, G. A., and Liu, Y. C., "Calculation of Elastic Anisotropy in Rolled Sheet", Trans. AIME 236, 1966, p 482.

(72) Liu, Y. C., and Alers, G. A., "The Anisotropy of Young's Modulus in Cold-Rolled Sheets of Binary Cu-Zn Alloys", Trans. AIME 236, 1966, p 489.

(73) Martin, A. G., "Calculations of Elastic Properties of Anisotropic Sheets and Rods of Cubic and Hexagonal Crystals", Army Materials & Mechanics Research Center, AMMRC TR 71-15, July 1971.

(74) Pursey, H., and Cox, H. L., "The Correction of Elasticity Measurements on Slightly Anisotropic Materials", Phil. Mag. 45, 1954, p 295-302.

(75) Harrigan, M. J., et al, "The Effect of Texture on the Mechanical Properties of Titanium Alloys", North American Rockwell Corp., NA-69-909, December 1969.

(76) Harrigan, M. J., et al, "The Effect of Rolling Texture on the Fracture Properties of Ti-6Al-2Sn-4Zr-6Mo Alloy", Titanium Science and Technology, Plenum Press, 1973.

(77) Olsen, R. H., and Moreen, H. A., "Calculation of the Elastic Anisotropy of Ti-6Al-4V Alloy Sheet from Pole Figure Data", Met. Trans. AIME, v. 4, March 1973.

(78) Feng, C., "A Study of the Elastic and Plastic Anisotropy of Ti-8Al-1Mo-1V", Lockheed-Georgia Co., RM-308, June 1968.

(79) Larson, F. R., "Textures in Titanium Sheet and Its Effect on Elastic and Platic Flow Properties, Army Materials Research Agency, AMRA TR 65-24, October 1965.

(80) Zarkades, A., and Larson, F. R., "Experimental Determination of Texture and Mechanical Anisotropy of Tensile Properties in Commercial Pure Titanium Sheet", Army Materials & Mechanics Research Center, AMMRC TR 67-05, December 1967.

(81) Zarkades, A., and Larson, F. R., "Sheet Tensile Properties of Ti Alloys as Effected by Textures", Army Materials & Mechanics Research Center, AMMRC TR 68-03, January 1968.

(82) Reed-Hill, R. E., Conference on Deformation of Twinning, University of Rorida.

(83) Rogers, D. H., and Roberts, W. T., "Plastic Anisotropy of Titanium and Zinc Sheet I & II", Inst. J. Mech. Sci., v. 10, 1968, p 211-229.

(84) "Fundamentals of Deformation Processing", Ninth Sagamore Ordnance Materials Research Conference, Requette Lake, New York, 28-31 August 1962. Sponsored by U.S. Army Materials Research Agency. Syracuse University Press, 1964.

(85) Keeler, S. P., "Ductility of Anisotropic Sheet Metal", Chapter 8, Ductility ASM Seminar, October 1967.

(86) von Mises, R., Gottinger Nachrichten, Math.-Phys. Klasse, 1913, 582.

(87) Tresca, H., Compt Rend. Acad. Sci., Paris, v. 59, 1864, p 754 and v. 64, 1867, p 809.

(88) Hill, R. A., "Theory of Yielding and Plastic Flow in Anisotropic Metals", Proceedings of the Royal Society, London, v. 193, 1948, p 281.

(89) Hosford, W. F., Jr., and Backofen, W. A., "Strength and Plasticity of Textured Metals Deformation Processing", Sagamore Conference, Syracuse University Press, 1964.

(90) Hosford, W. F., "Texture Strengthening ASM Metals", Eng. Quant., November 1966, p 13.

(91) Lee, P., and Backofen, W. A., "One Experimental Determination of the Yield Locus for Ti and Ti Alloy Sheet", Trans. AIME, July 1966, p 1077.

(92) Sliney, J. L., "Biaxial Tensile Behavior of Ti-5Al-2.5Sn", Army Materials Research Agency, AMRC TR-62-22, June 1967.

(93) Sliney, J. L., et al, "Preliminary Report on the Biaxial Tensile Behavior of Anisotropic Sheet Materials", Army Materials Research Agency, AMRA TR 63-11, August 1963.

(94) Sullivan, T. L., "Texture Strengthening and Fracture Toughness of Titanium Alloy Sheet at Room and Cryogenic Temperatures", Lewis Research Center, NASA TN D-4444, May 1968.

(95) Sullivan, T. L., "Texture Strengthening and Fracture Toughness of 4Al-0.20 and 5Al-2.5Sn ELI Ti Sheet in Biaxial Stress Fields at Room and Cryogenic Temperatures", Lewis Research Center, NASA TM X-52272, April 1967.

(96) Babel, H. W., Eitman, D. A., and McIver, R. W., "The Biaxial Strengthening of Textured Titanium", Douglas Missile and Space Systems Division, No. 3471, June 1965.

(97) Frederick, S. F., and Corn, D. L., "The Biaxial Properties of Titanium Alloys at Cryogenic Temperatures", Douglas Missile and Space Division, No. 4257, April 1967.

(98) Babel, H. W., and Kam, C. Y., "Textured Titanium in Design", Douglas Missile and Space Division, No. 3679, April 1966.

(99) Fatzpatrick, J. M., et al, "Development of Improved Biaxial Strength in Titanium Alloy Rocket Motor Cases Through Texturing", Lockheed Missile and Space Co., Final Report AFRPL - TR 69-59.

(100) Fitzpatrick, J. M., "Texture Strengthening of Ti-6Al-4V", Metals Eng. Quaterly, February 1972.

(101) Hosegawa, A., et al, "The Texture Hardening of Titanium and Its Alloy Sheets", Titanium Science and Technology, Plenum Press, 1973.

(102) Hatch, A. J., "Testing of Ti-5Al-2.5Sn, ELI and Ti-6Al-4V Miniature Pressure Vessels", TMCA Report No. 6, October 1965.

(103) Rees, T. W., "The Development and Control of Crystallographic Texture in 3Al-2.5V Titanium Alloy Tubing", Mil. Spec. for Ti-3Al-2.5V Alloy Hydraulic Tubing, SAE Melting, Orlando, Florida, January 1973.

(104) Spurr, W. F., and Quist, W. E., "The Effects of Crystallographic Texture on the Mechanical and Fracture Properties of Ti-3Al-2.5V Hydraulic Tubing", Mil. Spec. for Ti-3Al-2.5V Alloy Hydraulic Tubing, SAE Meeting, Orlando, Florida, January 1973.

(105) Gissy, J. L., et al, "Hardness of Single Crystals of High-Purity Alpha Titanium", Trans. AIME, June 1958.

(106) Daniels, F. W., and Dunn, C. G., "The Effect of Orientation on Knoop Hardness of Single Crystals on Zinc and Silicon Ferrite", Trans. ASM, v. 41, 1949.

(107) Feng, C., and Elbaum, C., "Effect of Crystallographic Orientation and Oxygen Content on Knoop Hardness Values of Iodide Titanium", Trans. AIME, February 1958.

(108) Zarkades, A., "The Anisotropy of Knoop Hardness in Unalloyed Titanium Sheet", Army Materials Research Agency, AMNA TR 67-04, January 1967.

(109) Wheeler, R. G., and Ireland, D. R., "Multiaxial Plastic Flow of Zircaloy-2 Determined from Hardness Data", Electrochemical Technology, July-August 1966, p 313-317.

(110) Lee, D., and Backofen, W. A., "Yielding and Plastic Deformation in Textured Sheet of Titanium and Its Alloys", Trans. AIME, v. 236, December 1966, p 1696-1704.

(111) Wonsiewicz, B. C., and Wilkening, W. W., "A Comparison of Conventional and Knoop-Hardness Yield Loci for Magnesium and Magnesium Alloys", TMS-AIME, 1969, v. 245, p 1313-1319.

(112) Fishburn, R. A., and Roberts, W. T., "Evaluation of Anisotropy in Titanium Sheet by Knoop Hardness Measurements", Titanium Science and Technology, Plenum Press, 1973.

(113) Amateau, M. F., and Raymond, L., "The Use of Knoop Hardness to Determine the Yield Loci of Ti-6Al-4V", Aerospace Corp., Report #TR-0066 (5250-10)-14, February 1970.

(114) Douglas, D. L., "Hardness Anisotropy of Columbium", Trans. ASM, v. 54, 1961.

(115) Garfunkle, M., and Garlick, R. G., "A Stereographic Representation of Knoop Hardness Anisotropy", Lewis Research Center, NASA TN D4226, November 1967.

(116) Zarkades, A., and Larson, F. R., "Effect of Texture on the Charpy Impact Energy of Some Titanium Alloy Plate", Army Materials & Mechanics Research Center, AMMRC TR 72-21, June 1972.

(117) English, A. T., "Influence of Mechanical Fibering on Anisotropy of Strength and Ductility", Journal of Metals, April 1965, p 395.

(118) Hatch, A. J., "Mechanical Metallurgy and Fracture Toughness of Titanium Alloys", Titanium Technical Conference, Air Force Materials Laboratory and Research Institute, Dayton, Ohio, November 1967.

(119) Backofen, W. A., and Hosford, W. F., Jr., "The Strength and Plasticity of Anisotropic Metals", Watertown Arsenal Laboratories, TR 834.12/2-3, September 1963.

(120) Rittenhouse, P. L., and Picklesimer, M. L., "The Effects of Fabrication Variables on the Anisotropy of Mechanical Properties, Part I", Oak Ridge National Laboratory, ORNL-2944, November 1960.

(121) Rittenhouse, P. L., and Picklesimer, M. L., "The Effects of Fabrication Variables on the Anisotropy of Mechanical Properties, Part II", Oak Ridge National Laboratory, ORNL-2498, February 1961.

(122) Burrier, H. I., Jr., Amateau, M. F., and Steigerwald, E. A., "The Relationship Between Plastic Deformation and Fracture in Alpha Titanium", Technical Report AFML-TR-62-239, July 1965.

(123) Amateau, M. F., and Steigerwald, E. A., "The Relationship Between Plastic Deformation and Fracture in Alpha Titanium", Technical Report AFML-TR-66-263, June 1966.

(124) Judy, R. W., et al, "Fracture Resistance Characteristics of Ti-6Al-2Mo and Ti-6Al-4V in 3 inch Thick Sections", Naval Research Laboratory, NRL 2156, August 1970.

(125) Frederick, S. F., and Hanna, W. D., "Fracture Toughness and Deformation of Titanium Alloys at Low Temperatures", Met. Trans., v. 1, February 1970, p 347-352.

(126) Brown, B. F., et., "Stress Corrosion Cracking in High Strength Steels and in Titanium and Aluminum Alloys", Naval Research Laboratory, Supt. of Documents, Washington, D.C., 1972.

(127) Meyer, D. A., and Sandoz, G., "Fractography and Crystallography of Subcritical Crack Propagation in High Strength Titanium Alloys", Trans. AIME, v. 245, June 1969, p 1263.

(128) Meyer, D. A., "A Study of the Crystallographic Orientation of Cleavage Facets Produced by Stress-Corrosion Cracking of Ti-7Al-2Nb-1Ta in Water", Report of NRL Progress, August 1965, p 21-23.

(129) Unpublished Work, Czyrklis, W. F., Army Materials & Mechanics Research Center.

(130) Fager, D. N., and Spurr, W. F., "Some Characteristics of Aqueous Stress-Corrosion in Titanium Alloys", Trans. ASM, v. 61, 1968, p 283.

(131) Chandrathil, N., "The Fatigue of Textured Face Center Cubic Sheet Metals", University of Saskatchewan, Ph. D. Thesis, 1968.

(132) Hempel, M., "The Fatigue Properties of Titanium and Titanium Alloys, Part VII: Addendum and Appendix to Parts I to VI", Royal Aircraft Establishment Library, Translation No. 1596, July 1971.

(133) Partridge, P. G., "Cyclic Twinning in Fatigued Close-Packed Hexagonal Metals", Phil. Mag., v. 12, 1965, p 1043.

(134) Beevers, C. J., and Halliday, M. D., "On the Formation of Internal Fatigue Damage in Association with Twins in α-Titanium", Metal Science Journal, v. 2, 1969, p 74.

(135) Beevers, C. J., "Fatigue Behavior of α-Titanium and α-Titanium-Hydrogen Alloys", The Science, Technology, and Application of Titanium Book, Pergamon Press, Oxford, 1970, p 535.

(136) Gollard, D. I., and Beevers, C. J., "The Effect of Temperature on the Fatigue Response of Alpha-Titanium", Metal Science Journal, v. 5, 1971, p 174.

(137) Partridge, P. G., "Effect of Cyclic Stresses on the Microstructures of Hexagonal Close-Packed Metals", Czech J. Phys. B19 (1969), p 323.

(138) Armstrong, R. W., and Horne, G. T., "Fatigue Behavior in Shear of Oriented Magnesium Single Crystals", Journal Inst. of Metals, v. 91, 1962-63, p 311.

(139) Beevers, C. J., and Robinson, J. L., "Some Observation on the Influence of Oxygen Content on the Fatigue Behavior of α-Titanium", J. Less-Common Metals, 17, 1969, p 345-325.

(140) Partridge, P. G., and Peel, C. J., "Effect of Cyclic Stresses on Unalloyed Polycrystalline Titanium", The Science, Technology, and Application of Titanium Book, Pergamon Press, Oxford, 1970.

(141) Zarkades, A., and Larson, F. R., "Effect of Texture on Some Properties of Titanium", Army Materials & Mechanics Research Center, AMMRC TN, 1973.

(142) Benson, D. K., Grosskreutz, J. C., and Shaw, G. G., "Mechanisms of Fatigue in Mill-Annealed Ti-6Al-4V at Room Temperature and 600 F", Met. Trans., v. 3, May 1972, p 1239.

(143) Wells, C. H., and Sullivan, C. P., "Low-Cycle Fatigue Crack Initiation in Ti-6Al-4V", Trans. ASM, v. 62, 1969, p 263.

(144) Bowen, A. W., "The Effect of Testing Direction on the Fatigue and Tensile Properties of a Ti-6Al-4V Bar", Second International Conference on Titanium, to be published.

(145) McAllister, R. C., "The Effect of Microstructure on the Fatigue Behavior of Ti-6Al-4V Bar", TNCA Report Project BM-12-3, 30 August 1967.

(146) Guffanti, J. A., "Fatigue Properties of Specially Processed Ti-6Al-4V Plates", TIMET Case Studies M-136, January 1969.

(147) Hatch, A. J., "An Investigation of Factors Affecting Fatigue Life of Ti-6Al-4V", TMCA, Project 48-30, Tech Report No. 2, November 1968.

(148) Lucas, J. J., "Fatigue Improvements in Ti-6Al-4V Forgings", Presented American Helicopter Society, Washington, D.C., May 1971.

(149) Hodi, F. S., "Effect of Texture on the Creep and Stress Rupture Properties of Ti-4Al-4V", Army Materials & Mechanics Research Center, unpublished.

INDEX

(133) Partridge, P. G., "Cyclic Twinning in Fatigued Close-Packed Hexagonal Metals", Phil. Mag., v. 12, 1965, p 1043.

(134) Beevers, C. J., and Halliday, M. D., "On the Formation of Internal Fatigue Damage in Association with Twins in α-Titanium", Metal Science Journal, v. 2, 1969, p 74.

(135) Beevers, C. J., "Fatigue Behavior of α-Titanium and α-Titanium-Hydrogen Alloys", The Science, Technology, and Application of Titanium Book, Pergamon Press, Oxford, 1970, p 535.

(136) Gollard, D. I., and Beevers, C. J., "The Effect of Temperature on the Fatigue Response of Alpha-Titanium", Metal Science Journal, v. 5, 1971, p 174.

(137) Partridge, P. G., "Effect of Cyclic Stresses on the Microstructures of Hexagonal Close-Packed Metals", Czech J. Phys. B19 (1969), p 323.

(138) Armstrong, R. W., and Horne, G. T., "Fatigue Behavior in Shear of Oriented Magnesium Single Crystals", Journal Inst. of Metals, v. 91, 1962-63, p 311.

(139) Beevers, C. J., and Robinson, J. L., "Some Observation on the Influence of Oxygen Content on the Fatigue Behavior of α-Titanium", J. Less-Common Metals, 17, 1969, p 345-325.

(140) Partridge, P. G., and Peel, C. J. "Effect of Cyclic Stresses on Unalloyed Polycrystalline Titanium", The Science, Technology, and Application of Titanium Book, Pergamon Press, Oxford, 1970.

(141) Zarkades, A., and Larson, F. R., "Effect of Texture on Some Properties of Titanium", Army Materials & Mechanics Research Center, AMMRC TN, 1973.

(142) Benson, D. K., Grosskreutz, J. C., and Shaw, G. G., "Mechanisms of Fatigue in Mill-Annealed Ti-6Al-4V at Room Temperature and 600 F", Met. Trans., v. 3, May 1972, p 1239.

(143) Wells, C. H., and Sullivan, C. P., "Low-Cycle Fatigue Crack Initiation in Ti-6Al-4V", Trans. ASM, v. 62, 1969, p 263.

(144) Bowen, A. W., "The Effect of Testing Direction on the Fatigue and Tensile Properties of a Ti-6Al-4V Bar", Second International Conference on Titanium, to be published.

(145) McAllister, R. C., "The Effect of Microstructure on the Fatigue Behavior of Ti-6Al-4V Bar", TNCA Report Project BM-12-3, 30 August 1967.

(146) Guffanti, C. A., "Fatigue Properties of Specially Processed Ti-6Al-4V Plates", TIMET Case Studies M-136, January 1969.

(147) Hatch, A. J., "An Investigation of Factors Affecting Fatigue Life of Ti-6Al-4V", TMCA, Project 48-30, Tech Report No. 2, November 1968.

(148) Lucas, J. J., "Fatigue Improvements in Ti-6Al-4V Forgings", Presented American Helicopter Society, Washington, D.C., May 1971.

(149) Hodi, F. S., "Effect of Texture on the Creep and Stress Rupture Properties of Ti-4Al-4V", Army Materials & Mechanics Research Center, unpublished.

INDEX

78

METALS AND CERAMICS INFOF MATION CENTER
Battelle
Columbus Laboratories
505 King Avenue
Columbus, Ohio 43201

SELECTED LIST OF RECENT TECHNICAL PUBLICATIONS

Copies of the publications listed below may be purchased from the National Technical Information Service (NTIS), U.S. Department of Commerce, Springfield, Virginia 22151 at the prices listed. Orders should include the MCIC Publication Number. Specify the AD number, if one is given. Checks or money orders should be made payable to the National Technical Information Service. NTIS prepaid coupons may be used or orders may be charged to an NTIS Deposit Account. A complete list of MCIC publications is available on request to MCIC.

MCIC-71-01 **Effects of Surface Condition on the Mechanical Properties of Titanium and Its Alloys** [68 pages, 88 references, 57 figures, 34 tables] (August 1971) $7.50. AD 732 248.

MCIC-71-02 **Shot Peening for Improved Fatigue Properties and Stress-Corrosion Resistance** [49 pages, 40 references, 39 figures, 10 tables] (December 1971) $7.50. AD 735 409.

MCIC-72-11 **Beta Titanium Alloys** [215 pages plus index, 115 references, 121 figures, 97 tables] (September 1972) $19.95. AD 753 439.

MCIC-73-13 **Advances in Joining Technology — The 60's and Beyond** [62 pages, 93 references, 25 figures, 42 tables] (January 1973) $12.05. AD 754 262.

MCIC-73-14 **Current and Future Materials Usage in Aircraft Gas Turbine Engines** [79 pages plus index, 80 references, 52 figures, 41 tables] (June 1973) $13.50. AD 766 334.

MCIC-73-15 **Metallurgy of Fusion-Weld Repair** [59 pages, 44 references, 18 figures, 38 tables, index] (August 1973) $15.00. AD 768 210.

MCIC-73-16 **Titanium Castings Today** [111 pages, 35 references, 33 figures, 41 tables] (December 1973) $16.00. AD 772 725.

MCIC-74-18 **Metal Implants for Orthopedic and Dental Surgery** [55 pages, 195 references, 39 figures, 8 tables, index] (February 1974) $9.95. AD 775 913.

MCIC-73-19 **The Proceedings of the 1972 Tri-Service Conference on Corrosion** [396 pages, 304 figures, 40 tables] (December 1973) $24.00. AD 771 345.

MCIC-HB-01 **Damage Tolerant Design Handbook** [419 pages, 11 major sections, 206 references, 138 figures, 208 tables, in loose leaf] (December 1972) $37.50. AD 753 774.

MCIC-HB-02 **Titanium Alloys Handbook** [688 pages, 728 references, 483 figures, 239 tables, in loose leaf] (December 1972) $35.00. AD 758 335

MCIC-HB-03 **Forging — Equipment, Materials, and Practices** [496 pages, 253 references, 398 figures, 1 tables] (December 1973) $25.00. AD 771 344.